National Institute for Public Health
and the Environment
Ministry of Health, Welfare and Sport

Ammonia exchange measured over a corn field in 2010

Ammonia exchange measured over a corn field in 2010

National Institute for Public Health
and the Environment
Ministry of Health, Welfare and Sport

Ammonia exchange measured over a corn field in 2010

RIVM Report 680180003/2012

Colophon

H. Volten, RIVM
M. Haaima, RIVM
D.P.J. Swart, RIVM
M.C. van Zanten, RIVM
W.A.J. van Pul, RIVM

Contact:
H. Volten
Centre for Environmental Monitoring (CMM)
hester.volten@rivm.nl

This investigation has been performed by order and for the account of VROM, within the framework of Project Ammonia

Abstract

Ammonia deposition and emission measured over a corn field in 2010

Ammonia in the air in the Netherlands is primarily (90 per cent) due to agricultural activities, such as cattle breeding. These emissions are described and reported by the Emission Inventory of the RIVM. They are employed for international reports and model calculations pertaining to ammonia in the environment. Previous research revealed that there are missing emission sources. One of these sources is the emission from agricultural crops. The contribution of these emissions is unknown. Further research is required.

Results over corn field
To obtain insight into emissions from agricultural crops the RIVM has performed measurements over a corn field in Lelystad. Corn was selected since one third of all agricultural crops in the Netherlands consist of corn. It was found that the corn both emits and takes up ammonia. Net ammonia is emitted, on average 2.6 kilograms per hectare (with an uncertainty interval of 0.15 to 5.1 kilograms per hectare). The gross emission by the crop is estimated at between 3.5 and 6.4 kilograms per hectare. Due to issues with the calibration of the measurement equipment the uncertainty in the results is large.

Method
The measurements of ammonia over the corn field took place during the growing season of 2010 (June to October). Using an optical measurement method (DOAS: Differential Optical Absorption Spectroscopy) ammonia concentrations were measured at two altitudes. Subsequently the concentration differences were combined with measurements of turbulence in the air. This yields the emission or deposition of ammonia. Because the measured concentration differences are small, the emissions and depositions are extremely sensitive to the calibration of the measurement equipment.

Keywords:
ammonia, emissions, DOAS, corn

Rapport in het kort

Gemeten opname en uitstoot van ammoniak boven een maïsveld in 2010

Ammoniak in de buitenlucht is in Nederland voor het merendeel (90 procent) afkomstig van agrarische activiteiten, zoals de veehouderij. Deze emissies worden in beeld gebracht en gerapporteerd door de EmissieRegistratie van het RIVM. Ze worden gebruikt voor internationale rapportages en voor modelberekeningen over ammoniak in het milieu. Uit eerder onderzoek blijkt dat er emissieposten ontbreken. Een van die posten is de emissie uit landbouwgewassen. Het is onduidelijk hoe groot deze emissies zijn. Nader onderzoek is daarom geboden.

Bevindingen boven maïsveld
Om enig zich te krijgen op de emissie uit landbouwgewassen heeft het RIVM metingen verricht boven een veld met maïsplanten in Lelystad. Hierbij is voor maïs gekozen aangezien een derde van de landbouwgewassen in Nederland uit dit gewas bestaat. Het blijkt dat het maïs zowel ammoniak uitstoot als opneemt. Netto wordt ammoniak uitgestoten, gemiddeld 2,6 kilogram per hectare (tussen de onzekerheidsmarges van 0,15 en 5,1 kilogram per hectare). De bruto-uitstoot door het gewas wordt geschat op tussen 3,5 en 6,4 kilogram ammoniak per hectare. Door problemen met de ijking van de meetapparatuur is de onzekerheid in de resultaten groot.

Werkwijze
De metingen van ammoniak boven het maïsveld vonden plaats tijdens het groeiseizoen in 2010 (juni tot en met oktober). Met een optische meetmethode (DOAS: Differentiële Optische Absorptie Spectroscopie) zijn op twee hoogten ammoniakconcentraties gemeten. Vervolgens wordt het verschil tussen deze concentraties gecombineerd met metingen van de turbulentie van de lucht. Hieruit wordt de uitstoot of opname van ammoniak vastgesteld. Doordat het gemeten concentratieverschil klein is, is de uitstoot of opname extreem gevoelig voor de ijking van de meetinstrumenten.

Trefwoorden:
ammoniak, emissies, DOAS, maïs

Contents

Management samenvatting

Achtergrond
Ammoniak in de buitenlucht is in Nederland voor het merendeel (90%) afkomstig van agrarische activiteiten. Ammoniak komt vrij bij verdamping uit de mest in stallen, bij beweiding en bij het uitrijden van mest op gras- en bouwland. Ook uit kunstmest verdampt nog een deel ammoniak. Al deze emissies worden in beeld gebracht en gerapporteerd als de officiële Nederlandse emissiecijfers onder regie van de EmissieRegistratie. Uit de analyse en duiding van het ammoniakgat is naar voren gekomen dat er nog ontbrekende emissieposten bestaan (Van Pul et al., 2008). Een van die posten is de emissie van landbouwgewassen die voornamelijk plaatsvindt bij hogere temperaturen en tijdens het afrijpen (afsterven) van het gewas. Op basis van literatuurgegevens is een schatting van deze emissies gemaakt, die nationaal uitkomt op 5 kton per jaar. Dit bedraagt ongeveer 4% van de huidige ammoniakemissies. De onzekerheid in dit cijfer is echter vrij groot. De ammoniakemissies worden voor 2010 geraamd op 122 kton en liggen daarmee onder het afgesproken EU-doel van 128 kton vanuit de National Emission Ceiling Directive (NECD). De relevantie van de extra emissieposten is dat ze a) tezamen met de andere onzekerheden in emissieposten het halen van de emissiedoelen uit de NECD kunnen bemoeilijken en b) een rol spelen in de vergelijking tussen de berekende en gemeten ammoniakconcentraties. Vandaar dat een goede kwantificering van deze posten belangrijk is. In dit rapport wordt verslag gedaan van ammoniakemissie- en depositiemetingen die door RIVM verricht zijn boven een snijmaïsveld.

Doel van het onderzoek en rapport
In de zomer van 2010 zijn metingen verricht boven een snijmaïsveld in Lelystad. Deze metingen worden gebruikt om te bepalen of snijmaïs ammoniak aan de lucht afgeeft tijdens warme, droge periodes en aan het einde van het groeiseizoen ten gevolge van de afrijping (of afsterving) van het gewas, ook wel afrijpingsemissie genoemd. Het doel van dit onderzoek was in de eerste plaats om inzicht te krijgen in de ammoniakuitwisseling tussen het maïsveld en de lucht door gericht onderzoek te doen naar de uitstoot door het maïsveld. Ons tweede doel was het uit deze metingen afleiden van planteigenschappen die gebruikt worden voor het modelleren van ammoniakemissies. Ten slotte hebben we een poging gedaan om tot een seizoensgemiddelde ammoniakemissie of emissiefactor te komen gebaseerd op deze planteigenschappen.

Werkwijze
Om de emissie van ammoniak van landbouwgewassen te meten is een meetsysteem ontwikkeld dat gebaseerd is op twee DOAS-systemen (Differentiële Optische Absorptie Spectroscopie). Deze systemen meten de ammoniakconcentraties in de lucht op twee hoogtes door middel van lichtabsorptie in een specifiek golflengtebereik over een pad van ongeveer 50 m. De concentratieverschillen tussen beide hoogtes werden gecombineerd met turbulentiemetingen (door middel van de aerodynamische gradiënt methode; AGM) om de uitwisseling van ammoniak met het oppervlak te bepalen. Behalve turbulentie- en concentratiemetingen zijn aanvullende meteorologische gegevens verzameld voor de interpretatie van de metingen, zoals kort- en langgolvige straling, temperatuur, relatieve luchtvochtigheid, bladnatheid en druk. De meetperiode duurde 111 dagen in de maanden juni tot oktober 2010 en bestreek de periode van groei van de maïs waarbij het gewas de bodem niet geheel bedekte tot en met de oogst van de maïs. Na afloop van de

meetcampagne is er een probleem geconstateerd met de stabiliteit van de onderlinge kalibratie van de DOAS instrumenten wat resulteerde in een onzekerheidsinterval voor de uitwisselingsmetingen. Er zal verder onderzoek uitgevoerd moeten worden om dit verschil in ijkingen te verhelpen en daarmee de nauwkeurigheid van de uitwisselingsmetingen te vergroten.

Resultaten
De resultaten laten zien dat zowel emissie als depositie van ammoniak optreedt, afhankelijk van het tijdstip op de dag, maar ook van de weersomstandigheden.

De fluxmetingen boven het snijmaïsveld in Lelystad in 2010 laten zien dat zowel uitstoot (906 halfuurswaarden) en opname (596 halfuurswaarden) optrad. De snijmaïsplanten stoten overdag over het algemeen de meeste ammoniak uit vooral op warme en zonnige dagen tijdens de groeiperiode. Bij regenachtig weer en 's nachts ligt de uitwisseling dicht bij nul. Aan de andere kant laten bladnatheidsgegevens samen met uitwisselingsgegevens zien dat, af en toe, op warme nachten uitstoot van ammoniak kan plaatsvinden. De metingen laten een netto emissie van ammoniak zien van 2,6 (0,15-5,1) kg per ha, gedurende de periode dat de maisplanten de bodem helemaal bedekten. Het verschil tussen de gewasemissie en de netto emissie wordt veroorzaakt door de opname (depositie) van ammoniak die plaatsvindt.

Een van de gevonden planteigenschappen was het gemiddelde stomatale compensatiepunt χ_s van 10,0 (± 0,6) µg m^{-3} met een onzekerheidsinterval van 7,6 tot 10,6 µg m^{-3}, en een gemiddelde gamma Γ_s van 3200 (± 230) met een onzekerheidsinterval van 2400 tot 4200. Deze compensatiepunten en gamma's werden uit de gemeten data afgeleid met de methode beschreven door Wichink Kruit et al. (2010a). De standaard fouten in de gemiddelden staan tussen haakjes. Daarnaast geven we een onzekerheidsinterval aan als gevolg van bovengenoemd probleem bij de onderlinge kalibratie van de DOAS instrumenten. Als we deze waarden toepassen in modelberekeningen (Wichink Kruit et al., 2010a) levert dat een gemiddelde stomatale emissie genomen over de periode dat het gewas de grond bedekte (88 dagen in de periode van juli tot oktober) van 61,0 ng m^{-2} s^{-1}. Dit betekent dat het gewas 3,5-6,4 kg ammoniak per ha uitstootte, waar de spreiding het gevolg is van de onzekerheid in de afleiding van de gamma waarden uit de metingen.
De emissiewaarden zijn van dezelfde orde van grootte als de waarde afgeleid uit metingen in Denemarken boven koolzaad, tarwe, gerst en erwten (Schjoerring and Mattsson, 2001).

Summary

Context
In the Netherlands**,** ammonia is present in the atmosphere mainly (90%) due to agricultural emission. Ammonia is released during the storage of slurry and manure in or near livestock houses and during the land spreading of slurries. Also artificial fertilizers may release ammonia. The emissions are registered and reported as the official Dutch emission numbers in the Emission Inventory. From the analysis and interpretation of the so-called ammonia gap (Van Pul et al., 2008) it appeared that more emission sources exist. One of these sources is the emission by agricultural crops that primarily takes place at higher temperatures and during senescence (ripening) of the crop. Based on literature data an estimate has been made of these emissions. On a national scale this amounts to 5 kton per year, about 4% of the current ammonia emissions. The uncertainty in this number is, however, rather large. The ammonia emissions in 2010 are estimated at 122 kton (CBS et al., 2011a) which is just below the EU-target of 128 kton in the National Emission Ceiling Directive (NECD). The relevance of the extra emission sources is that they complicate reaching the emission targets of the NECD but also play a role in understanding the difference between the modelled and measured ammonia concentrations. Therefore, a good quantification of the emission sources is important. Here, we report ammonia exchange values (fluxes) that were measured over a green (fodder) corn field.

Goal of the research and report
In the summer of 2010 we have performed ammonia exchange measurements over a corn field in Lelystad, the Netherlands. These measurements are used to determine whether corn emits ammonia, e.g. during warm and dry episodes or at the end of the crop growing season due to senescence of the plants. The objectives of this research were, first, to obtain insight into the ammonia exchange between the corn canopy and the atmosphere by focusing on the emissions by the corn canopy. Second, we aimed to derive from these measurements plant parameters such as compensation point and gamma that are used in modelling of the ammonia emissions. Last, we attempted to estimate the seasonal ammonia emission or emission factor of the crop based on these plant parameters.

Method
In order to be able to perform ammonia exchange measurements, we used a measurement system based on two DOAS (Differential Optical Absorption Spectroscopy) systems. These systems measure ammonia concentrations in air at two altitudes, using light absorption in a specific wavelength range over a path length of about 50 m. The concentration differences between both altitudes combined with turbulence measurements (using the aerodynamic gradient method (AGM)) determine the exchange of ammonia with the surface. In addition to turbulence and concentration measurements, ancillary meteorological data were recorded in order to be able to interpret the exchange measurements, such as short-wave and long-wave radiation, temperature, relative humidity, leaf wetness, and pressure. The measurement campaign lasted 111 days in the period June-October 2010 and covered the growth period of the corn, with the plants not completely covering the canopy until the harvest of the corn. An issue with the stability of the mutual calibration of the DOAS instrument was discovered after the measurement campaign which resulted in a rather large uncertainty interval for the flux results.

Results

The flux measurements over corn have shown that both emission and deposition events occur, depending on time of day but also on meteorological conditions. The flux measurements over corn at the measurement site in Lelystad in 2010 have shown that both emission (906 half hour values) and deposition (596 half hour values) events occur. The corn canopy generally emits most ammonia during daytime, especially during warm and sunny days during the growth period. In rainy periods and during nights the average flux tends to remains close to zero. On the other hand, leaf wetness data combined with flux data show that occasionally, during warm dry nights, significant emission events may occur. The measurements show a net emission of ammonia of 2.6 (0.15-5.1) kg ammonia per ha, when the crop was covering the soil. The difference between the crop emission and the net emission is caused by the uptake (deposition) of ammonia that occurs.

An average stomatal compensation point, χ_s of 10.0 (± 0.6) µg m^{-3} with an uncertainty interval of 7.6 to 10.6 µg m^{-3} and average gamma Γ_s of 3,200 (± 230) with an uncertainty interval of 2,400 to 4,200, were derived from the measured data following Wichink Kruit et al. (2010a). Standard errors in the averages are given in parentheses. In addition, we give an uncertainty interval due to the mutual calibration issue of the DOAS instruments mentioned above. Using these values in model calculations (Wichink Kruit et al., 2010a), yields an average stomatal flux over the period when the crop was full grown and covering the soil entirely (88 days in the period July-October 2010) of 61.0 ng m^{-2} s^{-1}. This means that the crop emitted 3.5-6.4 kg ammonia per ha, where the range is due to the uncertainty in the derivation of the gamma values from the measurements. The emission values are in the same range, i.e. in the order as yielded by measurements over oilseed rape, wheat, barley and pea carried out in Denmark (Schjoerring and Mattsson, 2001).

1 Introduction

In the Netherlands ammonia is present in the atmosphere mainly due to anthropogenic ammonia emissions, of which the agricultural emissions cover approximately 90%. Agricultural emission primarily occurs during the storage of slurry and manure in or near livestock houses (over 50%) and during the land spreading of slurries (approximately 40%). About 10% of the emission comes from artificial fertilizer application and during grazing of cattle (CBS et al., 2011b) All these emissions are included in the official emission inventory in the Netherlands (e.g. http://www.emissieregistratie.nl). However, additional sources of ammonia do exist. From the discussions about the so-called ammonia gap[1] (van Pul et al., 2008) it was suggested that emissions from agricultural crops could contribute to a certain extent to the national emissions. Background to these emissions is that crops during the crop growing season and particularly during senescence can emit ammonia. Based on the work by (Schjoerring and Mattsson, 2001) it was estimated that this would amount up to approximately 5 million kg of ammonia on a national basis (van Pul et al., 2008). Also after harvesting, ammonia emissions may occur from decomposition of plant material that is left on the field. It was estimated based on literature survey and experiments in the Netherlands that this could amount up to 3 million kg of ammonia in the Netherlands (de Ruijter et al., 2010).

Some experimental information on the emission of ammonia from crops is available (Loubet et al., 2002, Husted and Schjoerring, 1996, Mattsson et al., 1997, Wichink Kruit et al., 2007, Burkhardt et al., 2009) but measurements over crops other than grass in the Netherlands and during the senescence of plants are lacking. Therefore, measurements were carried out to obtain experimental data on these emissions. Since about 30% of crops grown in the Netherlands consist of corn, measurements over a corn field (at a location close to Lelystad) were carried out. In 2009 a novel ammonia flux measurement system with the gradient technique, was used based on the Differential Optical Absorption Spectroscopy (DOAS) technique. The measured results were reported in Wichink Kruit et al. (2010b) and showed that the ammonia flux measurement system based on the DOAS technique is in principle accurate and sufficiently stable to measure NH_3 exchange in an operational way. However, due to theft of equipment a considerable amount of crucial data was lost. Therefore, the measurement campaign over the whole growth season of the corn had to be repeated in 2010.

Measuring the emissions of a crop with these techniques is in fact a study on the exchange or flux of ammonia to and from the crop. In other words the emission as well as the deposition from ammonia to the crops is measured. In general the flux of ammonia to and from a crop is a function of the nitrogen availability in the plant itself, the meteorological conditions and the ambient ammonia concentration. In interpreting the measurements the same theories and techniques are used as in deposition studies performed over the last decades. One of the important plant parameters in these studies is the compensation point of the plants (Farquhar et al., 1980). The compensation point denotes the ambient ammonia concentration at which no exchange of ammonia is present.

[1] The ammonia gap indicated an underestimation of the calculated ammonia concentrations based on the national emissions in comparison with measurements of the ammonia concentration.

The compensation point can therefore be considered as the internal plant concentration. The compensation point, in turn, is dependent on leaf temperature and the ratio of the ammonium and hydrogen concentration, also called gamma. By evaluating the measurements in terms of compensation points and gammas a more 'objective' parameter is obtained which is less dependent on meteorology conditions than the measured fluxes. These more objective parameters along with the ambient ammonia concentration subsequently can be used to estimate or model the ammonia fluxes under different meteorological conditions.

The objectives of this research were:
- to get insight into the ammonia exchange between the corn canopy and the atmosphere focusing on the emissions by the corn canopy;
- to evaluate from the measurements plant parameters such as compensation point and gamma that are used in modelling of the ammonia emissions;
- to estimate the seasonal ammonia emission or emission factor of the crop based on these plant parameters.

In this report first the measurement site, instrumentation and the methodology to derive fluxes from the measurements are given (section 2). Subsequently, an overview of the results and a characterization of the meteorological conditions during the measurement campaign are shown (section 3). The derivation of compensation points, gammas and emission factors from the measurements is discussed in section 4. The results of this study are discussed and concluded in sections 5 and 6.

2 Site description, instrumentation and methodology

2.1 Site description

The reported NH_3 flux measurements are calculated from concentration profiles measured over a corn field in Lelystad opposite Runderweg 5, in the Netherlands. The exact location of the site is 52°30'52''N and 5°32'2''E. Figure 1 shows an aerial overview of the site and its surroundings. The locations during the campaign in 2010 are indicated in white. A previous campaign took place in 2009 (Wichink Kruit et al., 2010b), very near the present location (indicated by black symbols). The squares show the locations of the DOAS instruments, the small circles show the locations of the retroreflector masts. The meteorological observations are performed half way the DOAS instruments and the masts. The semi circles indicate the allowed wind directions for valid exchange measurements. The ground level of the measurement site is 5 m below mean sea level.

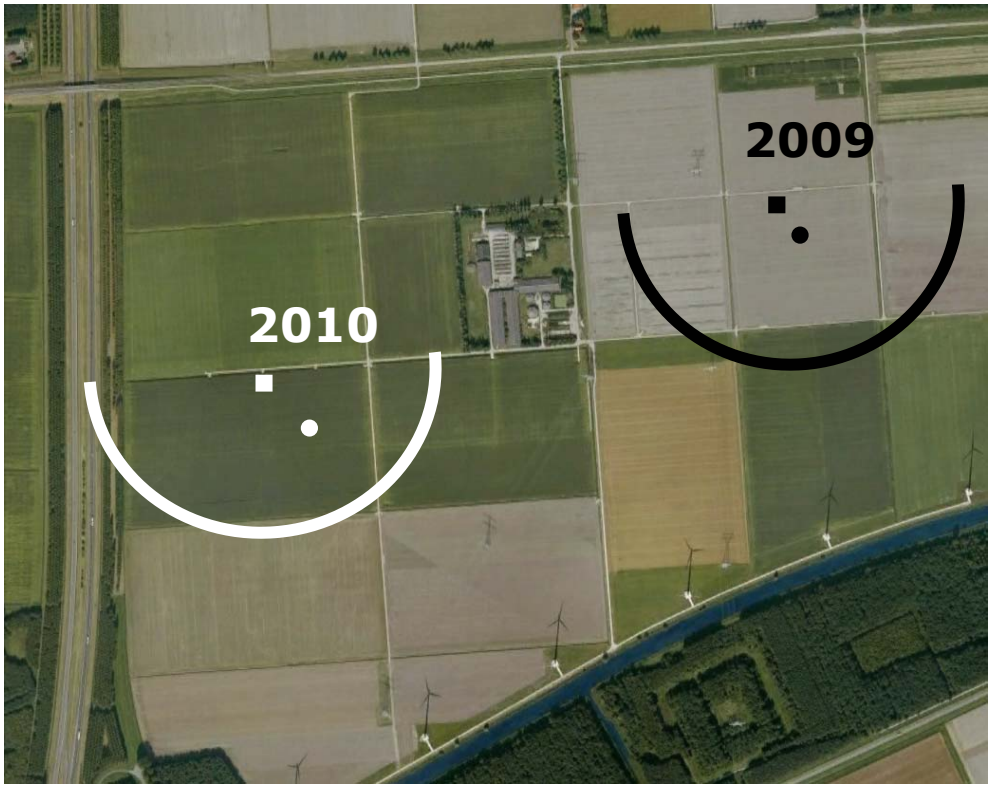

Figure 1. Aerial overview of the measurement site in 2010 and its direct surroundings
The white symbols show the location of the ammonia flux instrumentation 2010. A very similar campaign took place in 2009. The location of instrumentation during this campaign is shown in black. The farm shown in between the two sites was removed previous to the two campaigns, except for the (closed) manure storage containers.

The selected measurement site had to fulfil a number of requirements apart from being a corn field with large enough proportions. The 2010 site has dimensions of about 300 x 500 m. Another requirement is the absence of other

ammonia sources. In this site in the near surroundings few animals were kept, but there is a farm located 585 m to the north-northeast. The farm in the centre on Figure 1 was removed previously, except for the (closed) manure storage containers. The measurements performed in the direction of the farm to the north-northeast were excluded from the final results. The orientation of the instrumentation was chosen such that for the most prevailing winds, from the southwest, the fetch was clear from obstacles and ammonia sources. A typical ratio between measurement height and fetch was used of 1:100 (for short vegetation) (Monteith and Unsworth, 1990). In neutral conditions, the fetch for a measurement height of 5 m should then be at least 500 m. In stable conditions the required fetch, in principle, should be larger, and in unstable conditions it reduces to smaller distances. In general, the fetch over the corn field in the wind directions between 85 (roughly east) and 265 (roughly west) degrees north are large enough to let the measured fluxes be representative for corn. During the measurement campaign manure was applied twice to fields in the vicinity, causing large peaks in the measured ammonia concentrations. For this reason the data between 14 to 19 July, and 18 to 23 August 2010 were excluded.

2.2 Ammonia flux instrumentation

In order to be able to determine the amount of ammonia deposited on or emitted by corn, ammonia concentrations in air need to be determined at a minimum of two heights with high precision and a good stability. The measurements discussed in this report were performed at a height of about 5 m above ground level (see section 2.1) and at a height of roughly 50 cm above the corn. The ammonia concentrations were measured with two DOAS systems developed at the RIVM (see for a more detailed description Volten et al., 2012). The Differential Optical Absorption Spectroscopy (DOAS) principle is based on open path measurements. Ammonia concentrations are determined over an open path of about 50 m between a telescope and a retroreflector. The telescope directs the UV and visual light produced by a Xe-lamp towards the retroreflector that reflects the light back to the telescope (see Figure 2). Thus, the total path length over which is measured is 100 m.

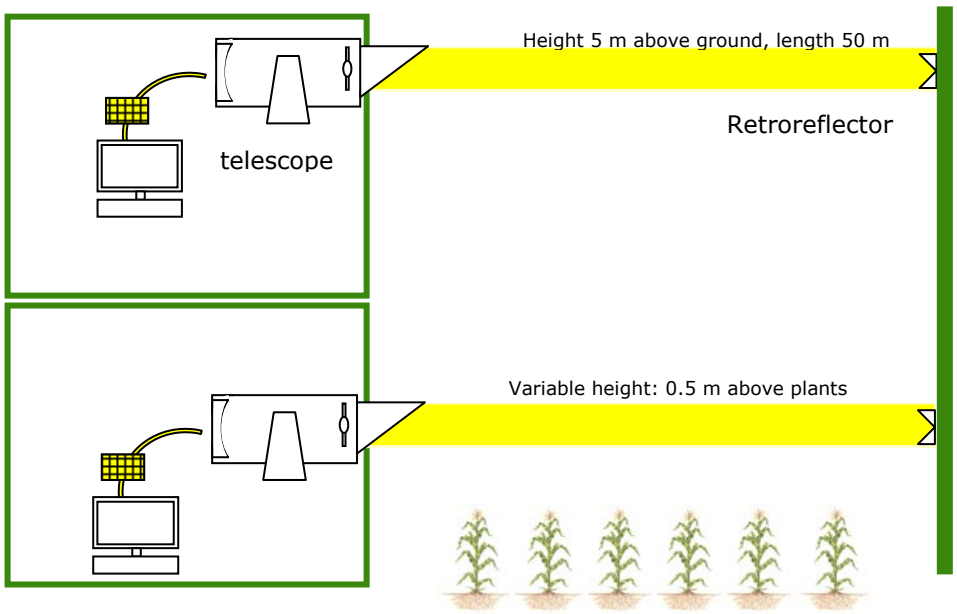

Figure 2. Schematic overview of a DOAS deposition system

Figure 3. The DOAS systems placed in the field. The DOAS systems are placed in two office containers placed on top of each other. As the corn grows, the height of the lowest system is adapted to the corn height. Halfway between the containers and the retroreflector mast, meteorological instruments are placed.

Figure 4. The retroreflectors of the DOAS systems
On the left, the mast with the retroreflectors of the DOAS systems is visible. Atmospheric turbulence is measured with a sonic anemometer on top of the mast on the right. In addition, meteorological variables like temperature, relative humidity, pressure and radiation are measured with a meteorological weather station in the right mast.

Subsequently, the known spectrum of the Xe-lamp, i.e. the lamp spectrum, is compared with the spectrum of the light that travelled over the open path. By relating the differences between the two normalized spectra to the known absorption lines of ammonia, the ammonia concentration in the air can be retrieved. The DOAS systems are placed in the field in two containers placed on top of each other (see Figure 3). Each container has a number of windows and has been equipped with a movable optical table in order to easily adjust the height of the DOAS system. As the corn grows, the height of the lowest systems is adapted to the height of the corn; the height of the lowest retroreflector (see Figure 4) is adapted accordingly.
Concentration measurements are obtained by averaging spectra over 5-minute intervals. These 5-minute values typically have a standard deviation of 0.15 µg/m^3. The clocks of both DOAS systems are synchronized by a DCF77 clock. Each half hour the DOAS instruments enter an automatic alignment mode in order to optimize the signal.

The height of the corn canopy was measured several times during the measurement campaign (see Appendix A) and is represented by the blue dots in Figure 5. The figure also shows the fitted height of the corn canopy (green line) and the two measurement heights (red and black line). The low measurement path is adapted to the height of the canopy. The altitude of the high measurement path is chosen to fit the required fetch (see section 2.1). In general the lower measurement level was approximately 0.5 m above the corn canopy and roughly 1-1.5 m above the displacement height (see section 2.4). On 13 October the equipment was removed from the field for the harvest of the corn and the subsequent tillage of the field.

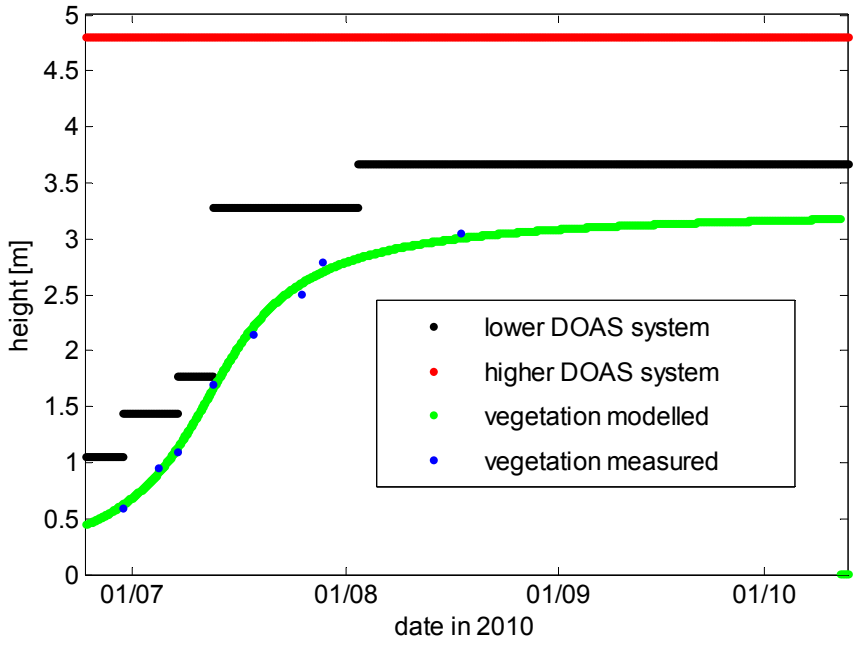

Figure 5. Height of the corn canopy in 2010
At a vegetation height of about 2 m and up the corn was covering the ground completely.

2.3 Meteorological instrumentation

A micrometeorological weather station was placed in the corn field approximately halfway between the DOAS flat and the retroreflector tower mast (see Figure 3 and Figure 4). The weather station mast was equipped with a 3-D sonic anemometer (Gill Windmaster) that measured turbulence with a frequency of 10 Hz at a height of 4.4 m. From the turbulence measurements 30-minute averages of the friction velocity, sensible heat flux and Obukhov length were calculated. These variables are needed in the flux calculation (see section 2.4). Wind speed and wind direction were also derived from the turbulence measurements and were logged once every minute.
In addition, other meteorological variables were measured to support the interpretation of the flux measurements:

- temperature and relative humidity (Campbell Scientific Model CS215 in a 41303-5A radiation shield);
- barometric pressure (Campbell Scientific Model CS100);
- short wave (Q_s), long wave (Q_l), and net (Q_{net}) radiation (Campbell Scientific/Kipp & Zonen CNR1);
- leaf wetness (Campbell Scientific Model 237);
- CO_2/H_2O concentration (LI-COR Biosciences, LI-7500).

These meteorological variables are logged as 1-minute averages. All meteorological variables are finally converted to 30-minute averages to support the evaluation of the ammonia flux.

2.4 Flux calculations

At present, no operational fast response sensor for ammonia exists. As a consequence, the ammonia fluctuations, χ', cannot be measured and the ammonia flux, $F_\chi = -\left(\overline{w'\chi'}\right)$, cannot be derived directly with the eddy covariance method.
Therefore, we have to rely on a commonly used method to derive the ammonia flux: the gradient or flux-profile technique (see Wichink Kruit et al., 2007, for a detailed description). In brief, this method relates the flux of ammonia to the vertical gradient of ammonia analogous to the description of molecular diffusion by Fick's law:

$$F_\chi = -\mathrm{K}_\chi \frac{\partial \chi}{\partial z} \qquad (1)$$

where ∂χ/∂z is the concentration gradient, i.e. the concentration difference, ∂χ, over a height difference, ∂z, and K_χ is the eddy diffusion coefficient for ammonia. K_χ is a property of the flow and depends largely on turbulence in that flow. The eddy diffusion coefficient for ammonia can be written as:

$$K_\chi = \frac{k u_* z}{\Phi_\chi(\zeta)} \qquad (2)$$

where *k* is the von Karman's constant (= 0.4), u_* is the friction velocity, *z* is the height above the displacement height d (defined by 2/3 of the canopy height) and $\Phi_\chi(\zeta)$ is the flux-profile relationship (or stability function) for ammonia (Dyer and Hicks, 1970, Businger et al., 1971, Webb et al., 1980). The dimensionless flux-profile relationship Φ_χ is a function of the atmospheric stability parameter ζ = z/L, where *L* is the Obukhov length scale defined by:

$$L = -\frac{T}{kg}\frac{u_*^3}{\overline{w'T'}} \quad (3)$$

where T is the air temperature, g is the gravitational acceleration and $\overline{w'T'}$ is the sensible heat flux.
By integrating equation (1), the following formulation for the ammonia flux is obtained:

$$F_\chi = -ku_* \frac{\left[\chi(z_2) - \chi(z_1)\right]}{\left[\ln\left(\frac{z_2}{z_1}\right) - \Psi_\chi\left(\frac{z_2}{L}\right) + \Psi_\chi\left(\frac{z_1}{L}\right)\right]} \quad (4)$$

where $\psi_\chi(\zeta)$ is the integrated stability function for ammonia; z_1 and z_2 are the measurement heights. In this report we use the integrated stability functions of (Paulson, 1970, Dyer, 1974.) for unstable conditions (i.e. L < 0) and the integrated stability functions for stable conditions (i.e. L > 0) (Beljaars and Holtslag, 1991).
We obtained u_* (and L) directly from eddy covariance measurements using a sonic anemometer. The vertical concentration gradients are measured by the DOAS gradient system.

Deposition velocities can be derived from the measured fluxes by dividing the measured ammonia flux by the (calculated) ammonia concentration at reference height (z-d = 1 m):

$$v_{d,ref} = -\frac{F_\chi}{\chi_{ref}} \quad (5)$$

where $v_{d,ref}$ is the deposition velocity at reference height, F_χ is the ammonia flux and χ_{ref} is the concentration at reference height.
This deposition velocity is restricted by the maximum deposition velocity that is determined by the amount of turbulence in the atmosphere. The maximum deposition velocity at reference height can be calculated from the friction velocity (squared) and the wind speed at reference height:

$$v_{d,max} = \frac{u_*^2}{u_{ref}} \quad (6)$$

The derivation of the fluxes from gradients is valid if the measurements are taken well above the roughness elements of the surface or above the roughness layer (Cellier and Brunet, 1992, Garratt, 1980). These authors have formulated corrections to be applied to derived fluxes if measurements are taken too close to the surface. Following the approach of Cellier and Brunet, we estimated the roughness layer for our crop to be about 3 m, i.e., about 3-4 times the row spacing of 0.8 m. This implied that most of the crop growing season the lowest measurement path was in the roughness layer. Based on a) their new derived flux profile relationships applicable to the roughness layer (Figure 11 in Cellier and Brunet, 1992) and b) on the relation for the ratio between the dimensionless gradients above and in the roughness layer by Garratt, 1980, we concluded that we underestimate the fluxes[2] with typically about 20%. However, the uncertainty in this estimate is quite large caused by the uncertainty in a number of field input parameters. Therefore a correction factor should only be used as an overall correction on the data. For that reason we did not correct the individual fluxes, however, a correction of 1.3 was applied on the

[2] Fluxes were taken at a geometrical height of approximately 2 m.

average fluxes and used in the calculation for the derivation of compensation points and gammas (see section 4).

2.5 Calibration of the individual and combined DOAS systems

The calibration procedure for an individual DOAS system to measure ammonia concentrations is described extensively by Volten et al. (2012). In short, the procedure consists of two main steps. First, for each lamp, the emitted spectrum, unaffected by absorption from gases in the atmosphere, is measured, using a short light path of 1 m by placing the retroreflector at a distance of 50 cm. This determines the calibration of the zero level. Second, the reference spectrum, i.e. an absorption spectrum of ammonia, is measured by supplying a known amount of ammonia gas in a flow cell placed in a short light path of about 1 m in total. This provides the span value. These calibration measurements are performed in the laboratory for each DOAS system individually, thereby accounting for specific instrument features.

After the initial calibration procedure in the laboratory for the individual DOAS instruments, the instruments have to be calibrated relative to one another. In order to be able to determine ammonia fluxes, systematic differences between the high and low DOAS systems have to be taken into account. Such systematic differences may e.g. occur due to small differences in the hardware or in the alignment of the optics in the instrument. The mutual calibration is done by placing both DOAS instruments at the same height next to each other in the laboratory in Bilthoven. These parallel measurements are carried out over an open path of about 50 m.

Systematic differences may also occur due to small inaccuracies in the calibration procedures described above. In particular, during the determination of the zero concentrations the light path of in total 1 m may still contain some ammonia or the placement of the retroreflector at such a small distance slightly changes the path of the light through the DOAS instrument. Therefore, a zero concentration level was determined in the field (see section 2.5.1). The field zero level was used in the final analysis of the measured data.

Also the mutual calibration of the two DOAS systems has been repeated at the actual measurement site. In section 2.5.2 we explain the procedure to calibrate the combined DOAS systems in the field using cross calibration measurements, and we show how this compared to the parallel measurements in the laboratory before and after the campaign. The procedure in the field has been repeated twice to monitor whether systematic differences between instruments remained constant.

2.5.1 Determining zero concentrations in the field

The idea to determine clean spectra without ammonia signature in the field was triggered by the significant amount of negative values for ammonia concentrations observed on the Lelystad site. We therefore suspected that the lab reference spectra had not completely been without ammonia spectral features as is necessary for a correct determination of the zero level. If ammonia concentrations in the surrounding area are significant, reducing the path length from 100 m to 1 m by placing the retroreflector from 50 m to 50 cm will result in a small residual ammonia signature of ~1% of the actual ambient concentration. This causes slightly too low values in the actual measured concentrations.

Assuming that in Lelystad ambient ammonia concentrations were occasionally very low (< 0,1 µg/m^3), we selected the 60 spectra measured in the field representing the lowest ammonia concentrations, to obtain a clean field lamp spectrum. We selected those spectra for which there were relatively high intensities of detected light (no fog), and small standard deviations in the ammonia concentrations (σ < 0.30 µg/m^3). In addition, the spectra were selected based on the absence of potentially interfering SO_2 and NO lines. Averaging these 60 spectra resulted in a new field reference spectrum used in the data processing of all ammonia measurements presented in this report. Compared to using the laboratory zero reference, this increased the ammonia concentrations on average by 0.67 µg/m^3 for the lower DOAS system and by 0.58 µg/m^3 for the upper DOAS system.

2.5.2 *Calibration of the combined DOAS systems*

As a first step, the DOAS systems were mutually calibrated by placing them at the same height next to each other in the laboratory in Bilthoven. These parallel measurements were carried out over an open path of about 50 m through the windows in the laboratory wall. The measurements took place before the measurement campaign from 28 May until 17 June 2010 and were repeated after the measurement campaign from 18 until 24 October 2010. The laboratory regressions, shown in Figure 6, are similar although we see a difference in the offset of both regressions curves. Before the campaign we found y = 0.983 (± 0.002) x -0.133 (± 0.017) and after the campaign y = 0.973 (± 0.004)x + 0.049(± 0.009) with one-sigma uncertainties given in parentheses. Taking into account that both systems were moved from the laboratory to the field and back, and the considerable amount of elapsed time between both measurement episodes, the similarity between both regression curves is rather good. Also, the correlation between the measurements of both DOAS systems was high, R^2 = 0.994 and 0.984 respectively for the first and second episode.

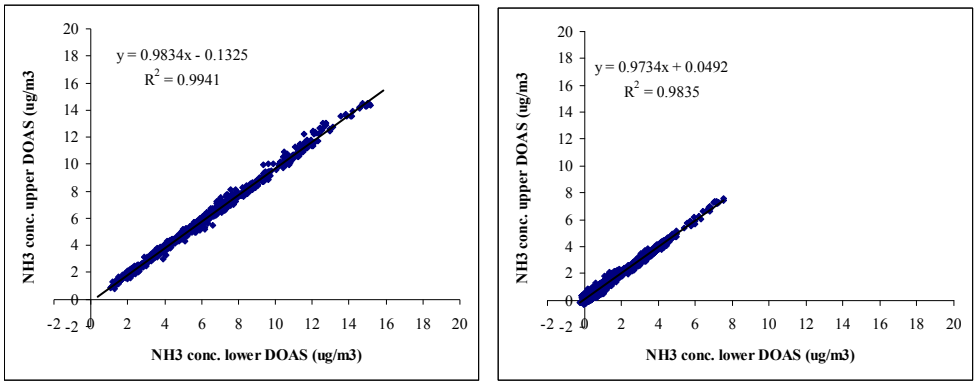

Figure 6. Regression plots of the parallel calibration measurements that took place in the laboratory before the campaign from 28 May until 17 June 2010 (left panel) and after the campaign from 18 until 24 October 2010 (right panel)

Since putting the DOAS instruments in the field involves taking the systems apart and realigning them on site, which may affect their optical properties slightly, we also calibrated the systems in the field using a new method. We performed these field calibration measurements, so called 'cross calibration measurements', on site twice during the campaign. During a cross calibration

measurement the two DOAS systems are checked relative to each other by directing their light beams towards the retroreflector of the other system; i.e. the upper DOAS uses the lower retroreflector and vice versa, thus crossing the light paths. Assuming that the ammonia concentration fields are homogeneous in the horizontal direction, the two DOAS systems should produce the same concentration values, and systematic differences may be detected and corrected for.

Two episodes of approximately three days of cross calibration measurements took place on 26 to 29 July and 23 to 26 Augustus 2010, i.e. during the measurement campaign. The cross calibration regressions curves shown in Figure 7 were y = 1.0028 (± 0.0092)x + 0.3453 (± 0.0164) in July and y = 0.9911 (± 0.0036) x + 0.5059 (± 0.0099) in August. One-sigma uncertainties are given in parentheses. The correlation between the measurements of both DOAS systems was high, R^2 = 0.9864 and 0.9939, respectively for the cross calibration measurement in July and August. The high correlations in the measurements are a good indication that both instruments were observing a homogeneous concentration field and that the cross calibration method is indeed valid.

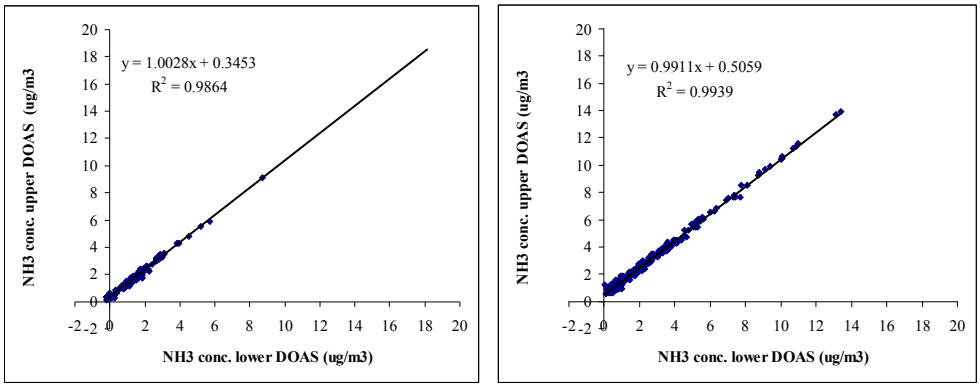

Figure 7. Regression plots of the cross calibration measurements that took place in the field from 26 to 29 July 2010 (left panel) and from 23 to 26 August 2010 (right panel)

The linear fits for the cross calibration regression lie close together; again they differ mainly in offset. In principle, an offset between the two DOAS instruments is accounted for in the analysis, but only on the condition that the offset is constant. It is therefore essential to understand more about the nature of the difference in offset between the regression curves. If the difference varies in the order of 0.1-0.2 µg m^{-3} as is suggested by the offset difference between the regression curves of 0.16, this is significant for flux determinations. In order to investigate the origin and the behaviour of the variations in the offsets between the different regression plots, we plotted in Figure 8 and Figure 9 the difference between the NH_3 concentration measurements during the cross calibration measurements. We see that the difference between the measurements of the two instruments is indeed not constant. Apart from rapid variations (noise) on 5-minute scale that very likely on longer time scales will average out, we see a more slow variation on the scale of several hours up to days. This variation on a longer time scales is much less probable to average out. The standard deviation in the average offset during the cross calibration measurements was 0.17 µg m^{-3}. The laboratory parallel measurements yielded similar results (not

shown), indicating that this is a feature that did not solely occurred for the cross calibration configuration.

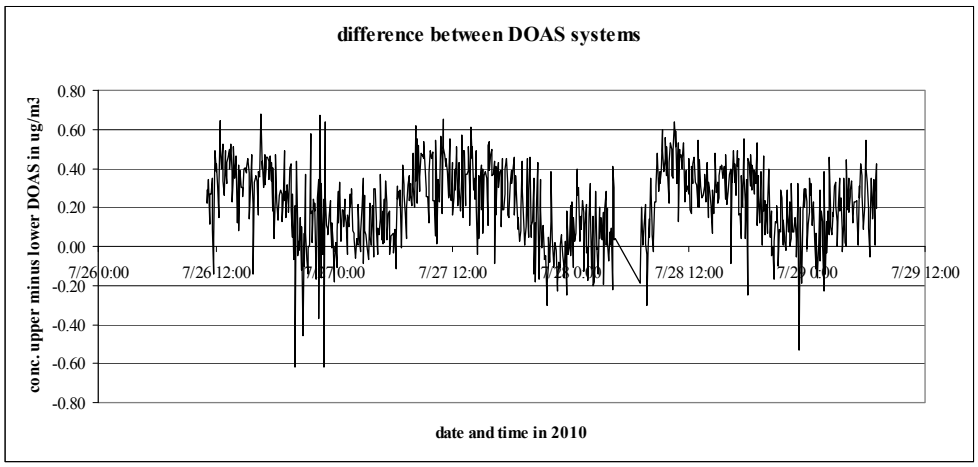

Figure 8. The difference between the NH_3 concentration measurements of the upper and the lower DOAS (five minute values) during the cross calibration measurement performed from 26 to 29 July 2010

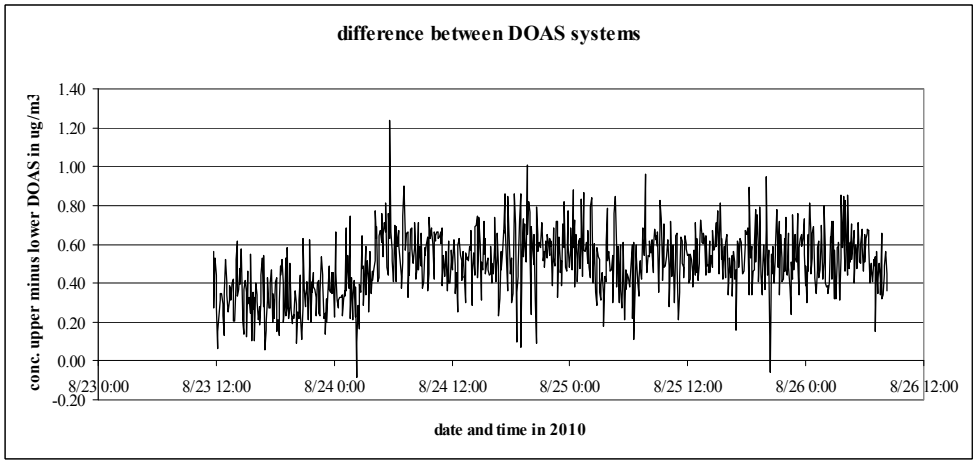

Figure 9. Difference between the NH_3 concentration measurements of the upper and the lower DOAS (five minute values) during the cross calibration measurement performed from 23 to 26 August 2010

Preferably, for flux determinations such longer time scale variations would need to be eliminated or, in case that is not possible, be monitored and corrected for. Since the campaign took place in 2010, this is not feasible for the data discussed in this report. Therefore, we have taken the variable offset between the two instruments into account in the following manner. We assume that the behaviour of the offset during the field measurements closely resembled that during the two cross calibration measurements. Therefore, we constructed an average field regression line using both cross calibration measurement series. The resulting linear fit, $y = 0.9948 \text{ x } (\pm 0.0036) \text{ x} + 0.461 (\pm 0.009)$, with an $R^2 = 0.9921$, has been used to correct the data of the upper DOAS system (see Figure 10). In order to obtain an estimate of the effect of the variable offset on the end results presented in this paper we used the standard deviation of 0.17 µg m^{-3} to augment and reduce the offset in this linear regressions curve,

i.e., in addition, we analysed all data using y = 0.9948 x + 0.63 and y = 0.9948 x + 0.29. The results obtained in this manner yielded upper and lower limits to our results. These limits have been used to calculate an uncertainty interval for a number of derived quantities presented in sections 3 and 4, including the fluxes averaged over the entire measurement period (see section 4).

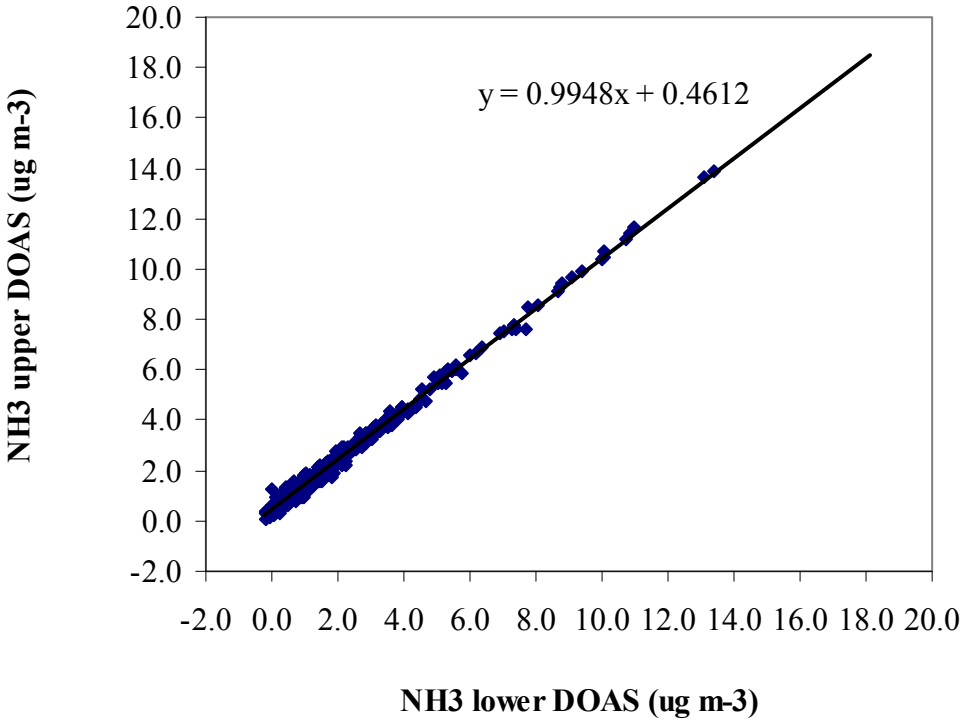

Figure 10. Regression plot for both field cross calibration measurements The slope and the offset have been used to correct the data of the upper DOAS system.

For the final calibration of the instruments we assumed that the cross calibration measurements yield a more relevant calibration for the flux measurements than the laboratory calibration measurements, since the latter were performed at a different location. This implies moving and realigning the equipment which may result in slightly different optical properties of the instruments. Using the laboratory parallel calibration measurements instead of the cross calibration measurement, the results are very different. In Appendix B a summary of these results are presented; they are discussed in section 5.

3 Overview of the NH_3 flux measurements

3.1 General overview measurement campaign

In this section, an overview of the available concentration and flux measurements is given. Table 1 shows the different periods in the measurement campaign. Before and after the field campaign, calibration measurements were performed in the laboratory. The flux measurements started on June 25, 2010. Cross calibration measurements were performed during three days in July and August. The flux measurements continued until 13 October when the retroreflector mast and the meteomast had to be removed from the field for the harvesting of the corn.

Table 1. Overview of the total measurement period

	Start	End
Calibration measurements in the laboratory	27-05-2010	17-06-2010
Flux measurements over corn in Lelystad	25-06-2010	26-07-2010
Cross calibration measurements in Lelystad	26-07-2010	29-07-2010
Flux measurements over corn in Lelystad	29-07-2010	23-08-2010
Cross calibration measurements in Lelystad	23-08-2010	26-08-2010
Flux measurements over corn in Lelystad	26-08-2010	12-10-2010
Harvest and turnover of the soil	13-10-2010	
Calibration measurements in the laboratory	18-10-2010	24-10-2010

The overall data coverage during the flux measurement periods mentioned in Table 1 amounts to a theoretical maximum of 5328 half-hourly measurements in the period between 25 June and 13 October 2010, including the cross calibration measurements. The uptimes for the lower and upper DOAS were 81.8% and 98.4%, respectively. The data loss of the upper DOAS was caused by some minor hardware problems and fog. The larger data loss of the lower DOAS was caused by fog and a software problem which took some time to be properly diagnosed and fixed. The total effective uptime for the flux measurements was 79.9%, i.e. 4259 half-hourly measurements calculated based on the available concentration gradients and the turbulence measurements.

In order to select reliable ammonia fluxes, a selection from the half-hourly data was made based on several quality and selection criteria (see also Wichink Kruit et al., 2010b). The percentage of cumulative rejected data (in parenthesis) of these 4259 half-hourly measurements is given per additional criteria.

- Standard deviation errors in the concentration measurements should be smaller than 0.3 µg m^{-3} for concentrations ≤ 20 µg m^{-3} and smaller than 1.5% for concentrations > 20 µg m^{-3} (8.5%). This selection criterion is used to remove data with a weak signal of the DOAS systems due to fog, a condensed retroreflector or other reasons, that result in large standard deviation errors.
- The wind direction should be roughly from the south (see Figure 1), i.e. between 85 (roughly east) and 265 (roughly west) degrees north in order to measure fluxes over the corn canopy with a fetch larger than 100 m (48.6%).
- The NH_3 concentrations should be larger than 0.1 µg m^{-3} (52.3%). At these low concentrations, the derived flux values are necessarily

negligible, whereas at the same time they often have relatively large standard errors.
- The deposition velocity must be smaller than the transfer velocity (defined as the deposition velocity without a surface resistance for ammonia, see section 4.2) (57.9%).

In addition, the NH_3 concentration should not be influenced by manure application events in the surrounding area. This occurred twice. Data until five days after the manure applications were excluded before processing the data. The final number of half-hourly measurements after applying these criteria is 1502 (or 35.3% of the available fluxes). Summarizing, 40% of all data were rejected because of wrong wind directions. Out of the available 4259 half-hourly measurements, 1502 are used for further analysis.

In Figure 11, ammonia concentration measurements, ammonia fluxes and deposition velocities are shown for the entire field campaign demonstrating the high uptime of the two DOAS instruments. The small dots represent observations that satisfy the first criterion (small enough errors in the concentration, i.e., 4259 half-hourly measurements). The large dots represent observations that satisfy all criteria, i.e., 1502 half-hourly measurements. Two significant gaps in the filtered data set are due to manuring events in an adjacent field between 14 July and 19 July 2010 and between 18 August and 23 August 2010, respectively. In Figure 12 the main corresponding meteorological parameters, temperature, relative humidity, radiation, and wind speed are shown.

The concentrations are generally below 20 µg m^{-3} and occasionally become larger than 20 µg m^{-3}. The individual fluxes, not corrected for surface roughness effects, are generally between 0.3 and -0.2 µg m^{-2} s^{-1}. The mean standard error in the individual NH_3 flux half hour values is 0.027 µg m^{-2} s^{-1}.
Both episodes of positive (emission) and negative (deposition) fluxes occur during the campaign. In total, 906 half hour values are positive and 596 half hour values are negative.

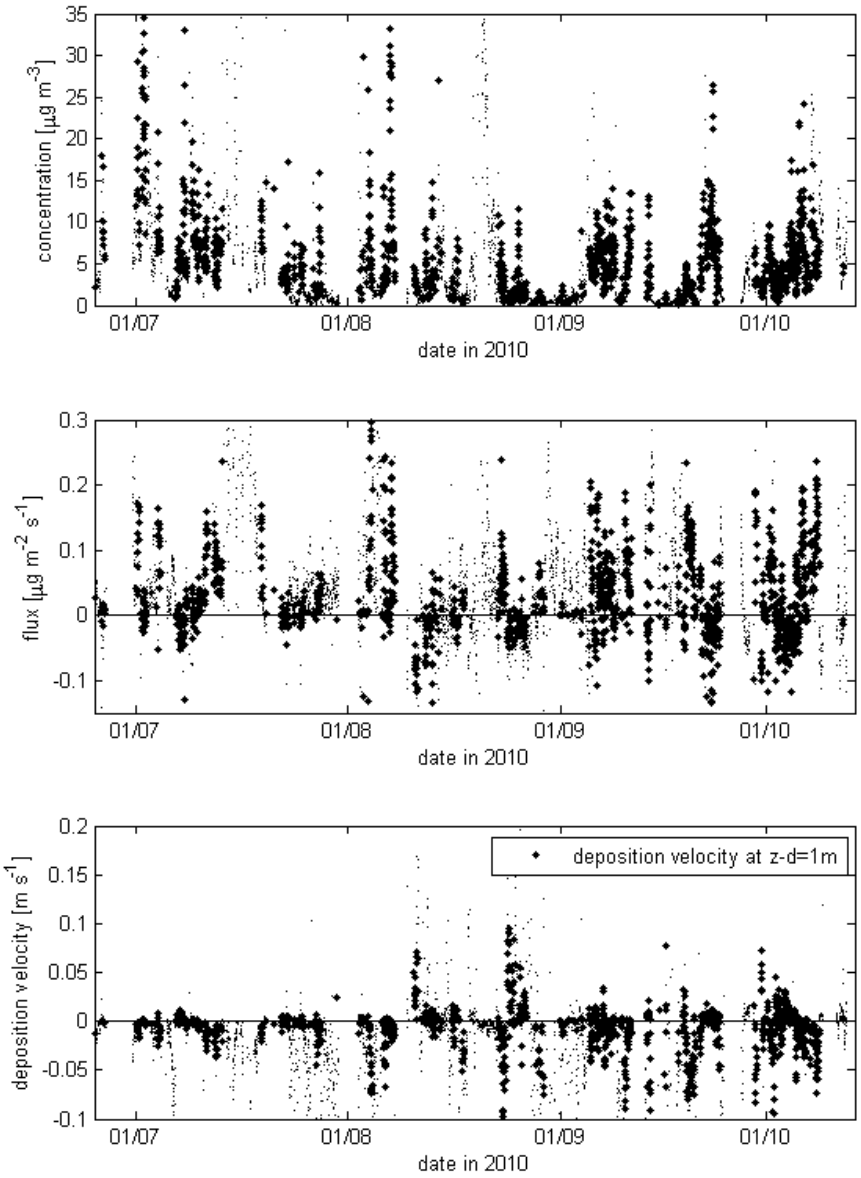

Figure 11. Ammonia concentrations (upper panel), ammonia fluxes (middle panel), and deposition velocities (lower panel) during the field campaign in 2010 The small dots represent observations that satisfy the first criterion (small enough errors in the concentrations). The large dots represent observations that satisfy all criteria. The data between 14 to 19 July, and 18 to 23 August 2010 were excluded because of manuring events in an adjacent field.

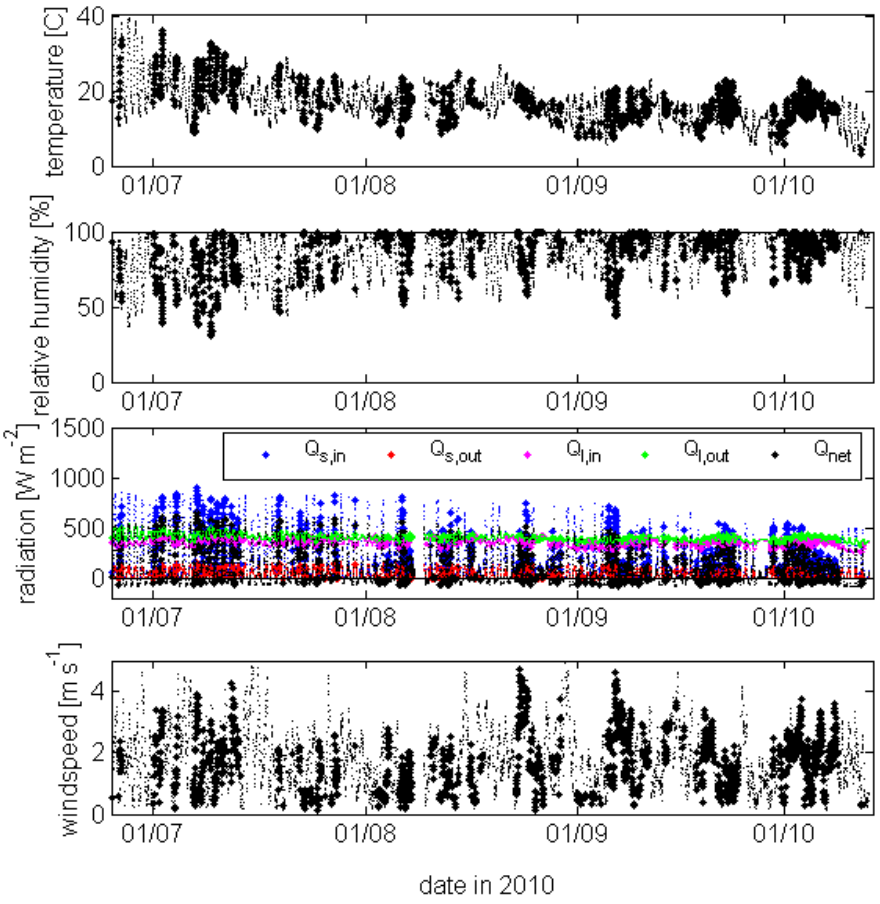

Figure 12. Temperature, relative humidity, radiation, and wind speed during the Lelystad 2010 campaign
The small dots represent observations corresponding to ammonia measurements which satisfy the criterion of small enough errors in the concentrations. The large dots correspond to observations which satisfy all criteria. The data between 14 to 19 July, and 18 to 23 August 2010 were excluded because of manuring events in an adjacent field.

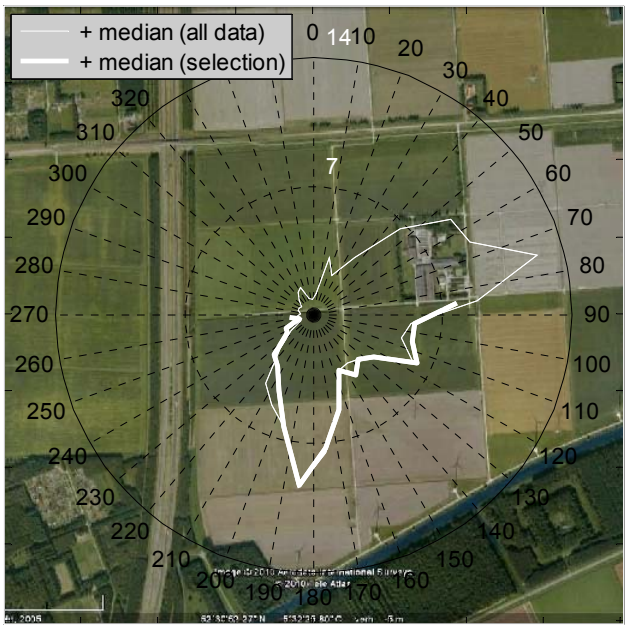

Figure 13. Wind rose of the median ammonia concentration measurements as a function of wind direction during the field campaign
The black dotted and solid circles indicate ammonia concentrations of 7 and 14 µg m^{-3}, respectively.

Figure 13 shows a wind rose of the ammonia concentrations before (thin white lines) and after (thick white lines) applying the selection criteria. A farm in the north-northeast is clearly visible in this wind rose, but these data are not considered in the final data evaluation because in that wind direction we do not measure over the corn canopy. Especially the low concentrations to the northwest are remarkable. These low concentrations are likely due to the very clean upwind conditions, i.e. due to the IJsselmeer, and the absence of any intensive agricultural activities in this wind direction. We did not find indications that the highway (running north-south) at about 370 m distance to the west of the measurement site influenced the ammonia concentration significantly. The higher concentrations to the south might partly be caused by agricultural activities on the fields to the south of our measurement site.

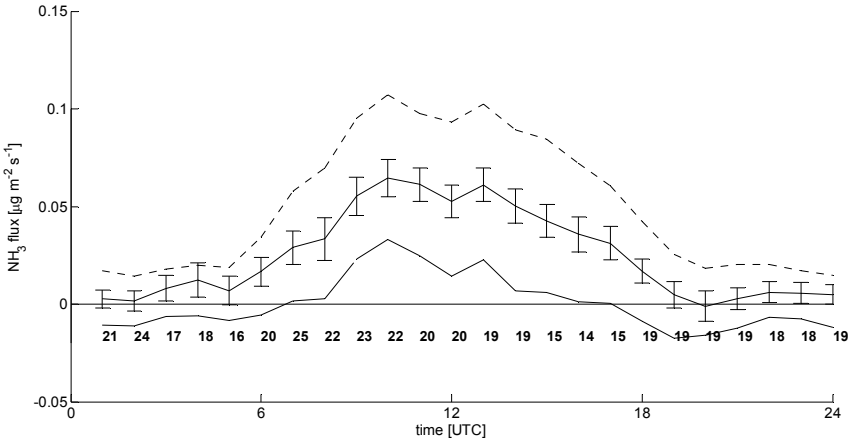

Figure 14. Diurnal cycle of the selected mean ammonia fluxes at 1 m above zero-displacement height during the 2010 measurement campaign
The bars represent the standard deviation of the mean for each hour. The numbers at the bottom of the figure are the number of measurements on which the mean is calculated. The dotted and dashed lines indicate respectively the upper and lower limits of the uncertainty interval discussed in section 2.5.2.

In Figure 14 we show the diurnal cycle of the selected mean ammonia fluxes at 1 m above zero-displacement height during the measurement campaign. The uncertainty interval discussed in section 2.5.2 is also plotted. Figure 14 indicates that on average emission prevailed, even though during the campaign both emission and deposition episodes occurred (see Figure 11).

Figure 15 shows the frequency distribution of the ammonia flux at 1 m above the zero-displacement height including the uncertainty interval discussed in section 2.5.2. The figure shows the highest frequency of fluxes around zero with more emission than deposition events. The mean NH_3 flux with the standard error in parentheses is 0.035 (± 0.002) µg m^{-2} s^{-1} for the data selection (after corrections due to deviations from the flux-profile with 1.3; see section 2.4).

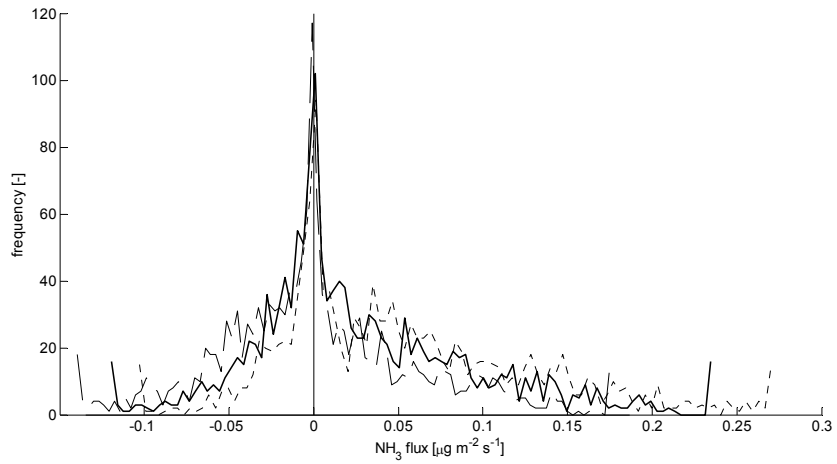

Figure 15. Frequency distribution of the selected ammonia fluxes at 1 m above zero-displacement height during the growth period
The dotted and dashed lines indicate respectively the upper and lower limits of the uncertainty interval discussed in section 2.5.2.

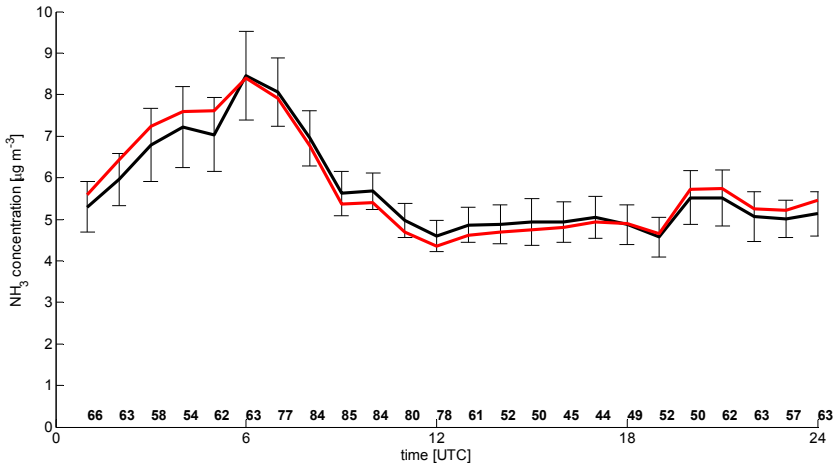

Figure 16. Diurnal cycle of the selected ammonia concentrations at the upper (red line) and lower (black line) measurement heights during the campaign The bars represent the standard deviation of the mean for each full hour (only given for the concentration at the lower level). The numbers at the bottom of the figure are the number of measurements on which the mean is calculated.

Figure 16 shows the diurnal cycle of the selected measured ammonia concentrations at the two measuring heights (red and black lines) during the growth period. The bars represent the standard deviation of the mean for each hour for the concentration at the lower level; the standard deviation values for the upper level are similar. The numbers at the bottom of the figure are the number of measurements on which the mean is based. The concentrations tend to be higher in the early hours of the day and lower in the afternoon. This effect is mainly caused by the increased atmospheric mixing during daytime. On average, the air concentration is 5.77 (± 0.13) µg m^{-3} for the data selection, with the standard error in parentheses. The average concentration at the upper measurement height at night is higher than for the lower measurement height, indicating on average more probability for deposition at night time. During daytime we see the reverse.

3.2 Ammonia exchange and the weather

The weather in the Netherlands is –even in summer- usually rather variable. Sunny and warm periods are alternated with unstable showery spells, and cooler periods. Although really homogeneous weather conditions are hard to find, the meteorological institute (KNMI) provides a characterisation of the weather conditions in episodes[3]. For the period of our measurement campaign these episodes are indicated in
Figure 17. We have investigated whether these episodes produced differences in the deposition and emission behaviour of ammonia in the air. Also a number of illustrative events will be presented. A weekly overview of all collected data is given in Appendix C.

[3] see http://www.knmi.nl/klimatologie/maand_en_seizoensoverzichten/weerbeschrijvingen

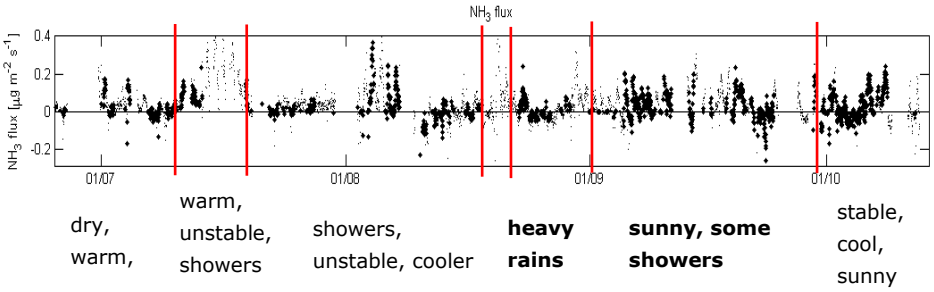

Figure 17 Weather conditions during the campaign split up in different episodes From around 15 July the corn covered the soil completely. The periods indicated in bold are discussed in more detail below.

There is no clear trend in the ammonia fluxes during the growing season of the corn. An expected increase in the ammonia emission due to senescence of the crop is not noticeable. As already can be inferred from
Figure 17, there is a higher probability for emission events of ammonia during warm, dry, and sunny weather conditions, whereas during rainy or showery conditions ammonia deposition becomes average more likely. Apparently, the influence of such weather conditions is larger than a possible senescence effect. We illustrate this further by showing the daily average ammonia fluxes for a period with heavy rains (see Figure 18) and a predominantly sunny period with occasional showers (see Figure 19).

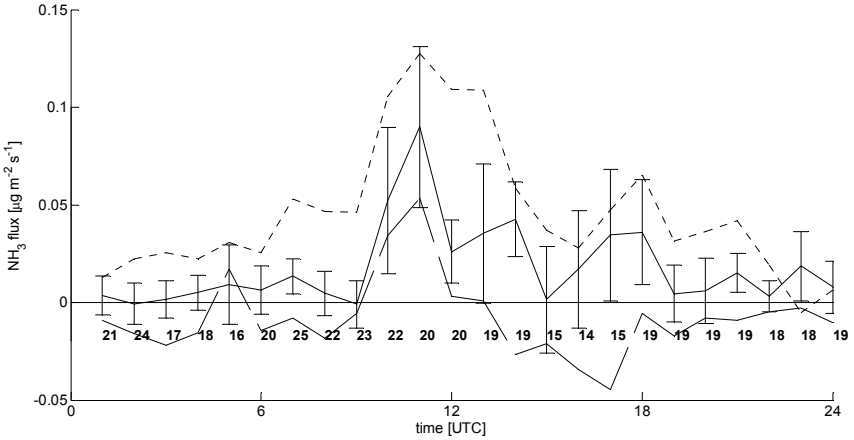

Figure 18. Daily average ammonia flux for a period of heavy rain from 23 August to 1 September 2010
The bars represent the standard deviation of the mean for each full hour. The dotted and dashed lines indicate respectively the upper and lower limits of the uncertainty interval discussed in section 2.5.2.

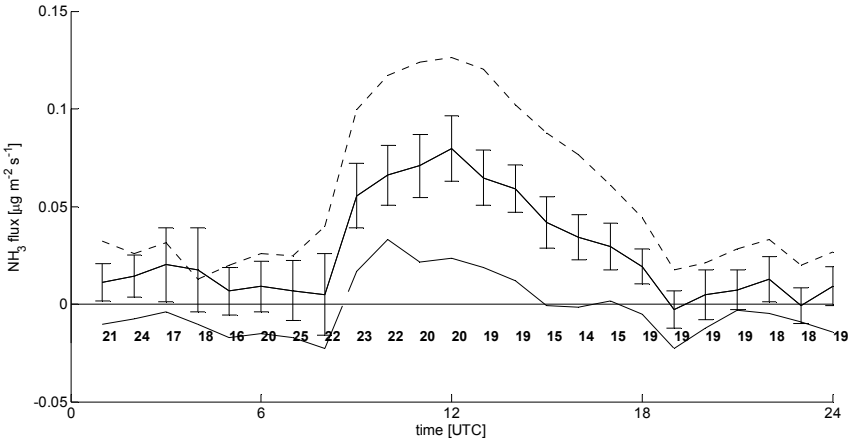

Figure 19. Daily average ammonia flux for a primarily sunny period with occasional showers from 1 to 28 September 2010
The bars represent the standard deviation of the mean for each full hour. The dotted and dashed lines indicate respectively the upper and lower limits of the uncertainty interval discussed in section 2.5.2.

The daily average ammonia flux for the episode of heavy rains shows a flux fluctuating close to zero with large standard deviations indicating a large variability in observed diurnal fluxes. The average flux over this period is 0.020 (±0.005) µg m^{-2} s^{-1}. The daily average ammonia flux for the sunny and warm episode shows a behaviour that is more similar to the average over the total campaign, i.e. a bell-shape indicating on average predominantly ammonia emissions during daytime. The average flux over that period is also close to the average over the entire period, i.e. 0.035 (±0.004) µg m^{-2} s^{-1}.

3.3 Ammonia emissions and leaf wetness

In the previous section we saw that weather conditions play an important role in the occurrence of emission or deposition events. It is probable that the leading mechanism determining this effect is the presence of moisture on surfaces. In this section we look into this subject by studying leaf wetness measurements in relation to the flux measurements.

Although on several occasions a less clear picture occurs, a rather general pattern we often observe is illustrated in Figure 20 for 6 September 2010. During night time (0:00 to 8:00 UTC) the leaves are wet; ammonia deposition is dominant for all values within the uncertainty interval (see section 2.5.2). Starting around 8:00 UTC the leaves become dry, coinciding with the occurrence of positive ammonia fluxes also for all values within the uncertainty interval.

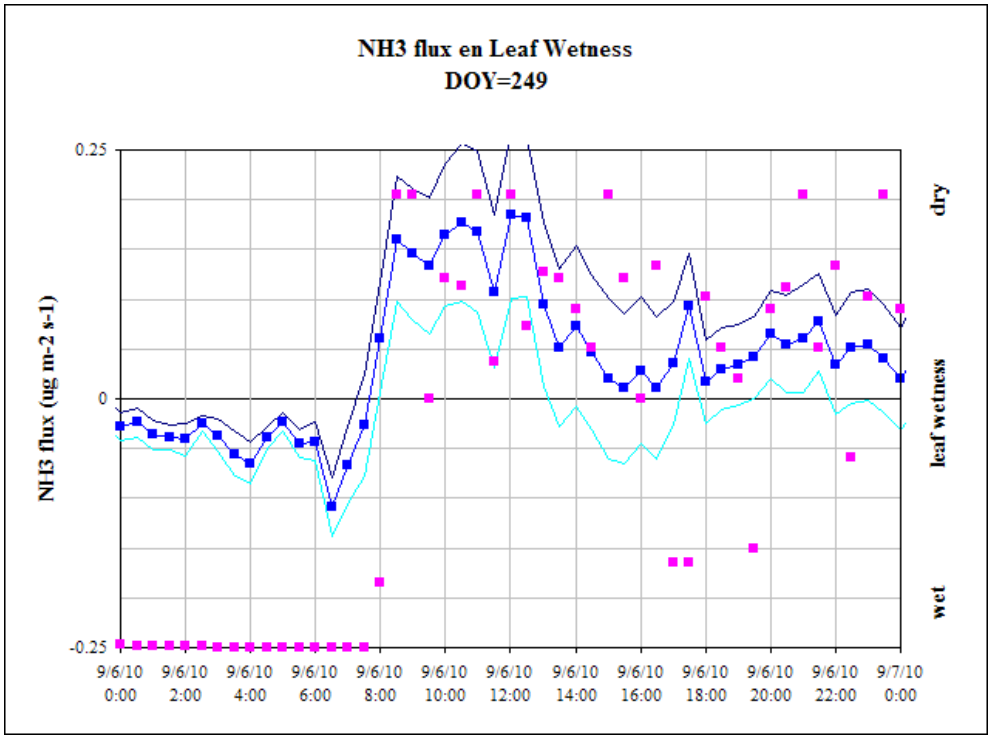

Figure 20. Ammonia flux (sky blue squares and line, left vertical axis) and leaf wetness (pink squares, right vertical axis) on 6 September 2010
Filled symbols indicate values that met the selection criteria explained in section 3.1. The navy and turquoise blue lines indicate respectively the upper and lower limit of the uncertainty interval discussed in section 2.5.2.

The following nights of 6 to 7 September (see Figure 20 and Figure 21) and of 7 to 8 September (see Figure 21) we observe that dry leaves, relatively high wind speeds (see Appendix C), and subsequent ammonia emissions occur also in the nightly hours for a considerable fraction of the values in the uncertainty interval indicated by the blue lines. This may explain why on average the daily fluxes tend towards emissions even during night times (see Figure 14).

Figure 21 shows another interesting feature. Assuming that emissions occur predominantly under dry conditions and wet conditions most often equal deposition, we see that the expected behaviour is shown quite consistently by the sky blue squares of the average. The navy blue line, indicating the upper limit to the uncertainty interval, shows emission during wet conditions, and the turquoise line, indicating the lower limit, shows deposition during dry conditions. Since it is not an ironclad rule that dry conditions imply emission and vice versa, we cannot draw hard conclusions, but this may indicate a too generous uncertainty interval.

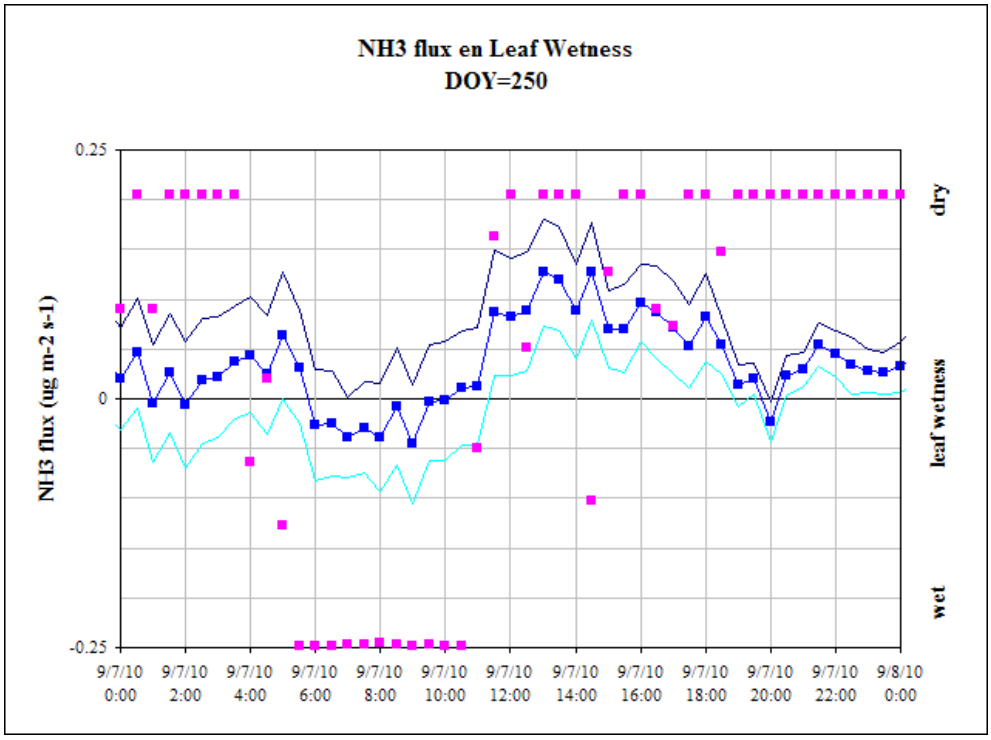

Figure 21. Ammonia flux (sky blue squares and line, left vertical axis) and leaf wetness (pink squares, right vertical axis) at the end of the campaign on 7 September 2010.
Filled symbols indicate values that met the selection criteria explained in section 3.1. The navy and turquoise blue lines indicate respectively the upper and lower limit of the uncertainty interval discussed in section 2.5.2.

4 Derivation of emission factors, compensation points and gamma

In this chapter the measurements of the ammonia fluxes will be used to derive emission factors for ammonia from corn. This will be done in two ways: 1) by using the measurement data itself and the selection of episodes therein and 2) by evaluating the measurement data in terms of parameters with which emission and deposition are modelled, e.g. compensation points and gammas. Throughout section 4 we incorporated the correction due to deviations from the flux-profile (see section 2.4) by multiplying with 1.3.

4.1 Emission factors from measurements

The measurements of the ammonia fluxes consist of periods with emissions and deposition. We will present two ways to interpret the data with respect to emission factors.

4.1.1 Flux of 2. kg NH_3/ha based on net emission and deposition averaged

The net average flux over the season for the selected data is 35 (± 2) ng m^{-2} s^{-1} (with the standard error given in parentheses as in the rest of the section) with an uncertainty interval (see section 2.5.2) of 2 to 68 ng m^{-2} s^{-1}. That is: a net ammonia emission on the corn and underlying soil is measured. If we use this number for the entire crop growing season (111 days in the period June-October) this yields an emission of 3.4 (± 0.2) kg NH_3/ha with an uncertainty interval (see section 2.5.2) of 0.2 to 6.5 kg NH_3/ha. If we only consider the period when the corn covered the soil completely (crop height greater than 2 m) so that a negligible emission from soil is expected the emission amounts up to 2.6 (± 0.15) kg NH_3/ha with an uncertainty interval (see section 2.5.2) of 0.15 to 5.1 kg NH_3/ha. This is of course only valid if the measurements are representative for the entire crop growing season. The number might be an underestimate since measurement events from northerly wind directions were excluded. As was already indicated the ammonia concentrations from that direction are quite low and would favour emission events. Different weather conditions might also lead to another flux. However, it is not expected that this is a major effect if we look at the meteorological data from the entire season and the selection (Figure 12).

4.1.2 Emission averaged flux

If we want to consider the gross emission of ammonia we have to average solely over the emission events during the season. For the season this was 83 (± 3) ng m^{-2} s^{-1} (with an uncertainty interval of 64 to 104 ng m^{-2} s^{-1}; see section 2.5.2). This value was based on 906 half hour flux values. If we repeat this for all deposition events, this yields -38 (± 2) ng m^{-2} s^{-1} (with an uncertainty interval of -32 to -51 ng m^{-2} s^{-1}; see section 2.5.2), based on 596 half hour flux values. The same considerations as in section 4.1.1 about representativeness holds for these numbers. However, part of the observed emissions is re-emission of previous deposited ammonia. Particularly during morning hours emission fluxes are measured that coincide with the evaporation of the water layer and ammonia therein (see section 3.3). If we want to consider the emission from the plants themselves via the stomata than only dry conditions should be taken into account in averaging. As a switch we took the RH < 80%

as an indicator for dry leave surface. The flux over the season under dry conditions for the selected data is then 55 (± 6) ng m^{-2} s^{-1} (with an uncertainty interval of 3 to 103 ng m^{-2} s^{-1}; see section 2.5.2). If we consider the selected data of the dry flux from 19 July to 12 October when the crops are covering the soil completely, the number remains similar 58 (± 6) ng m^{-2} s^{-1} (with an uncertainty interval of 10 to 117 ng m^{-2} s^{-1}; see section 2.5.2).

4.2 Compensation point and Γ

The exchange process of ammonia can be parameterized using a resistance scheme in which plant characteristics are incorporated (see section 4.2.1 for a description of the scheme).

A derived temperature-dependent compensation point χ_s and Γ, the ratio of $[NH_4^+]/[H^+]$ in the leaf apoplast, can be used to make an estimate of the stomatal emissions of ammonia during the entire crop growing season taking into account the variation in meteorological conditions and different ammonia concentrations. In this way we overcome the drawbacks that might be associated by converting the emission factor estimates in section 4.1.1.

Moreover, exchange estimates can be made for different locations in the Netherlands (or even abroad) and other years.

4.2.1 Derivation of the compensation point and gamma from the measured data

Dry deposition may be parameterized using a well-known resistance approach (e.g., Van Zanten et al. 2010) where the deposition flux is the result of a concentration difference between atmosphere and earth surface and the resistance between them. Several pathways exist for the deposition flux, each with its own resistance and concentration. Two pathways are taken into account:

- through the stomata (subscript *s*);
- through the external leaf surface (water layer or cuticular waxes, subscript *w*).

By considering only data for the period from 19 July onward, when the vegetation height is over 2 m and the leaves are assumed to cover the soil completely the influence of the soil is eliminated. The concentration in the stomata, or at the external leaf surface is often called a *compensation point*. This name stems from the fact that the compensation point concentration indicates the concentration level in the air above the leaf surface at which no exchange is measured (since the concentration difference is zero). Dry deposition schemes including compensation point parameterisations are able to model emission as well.

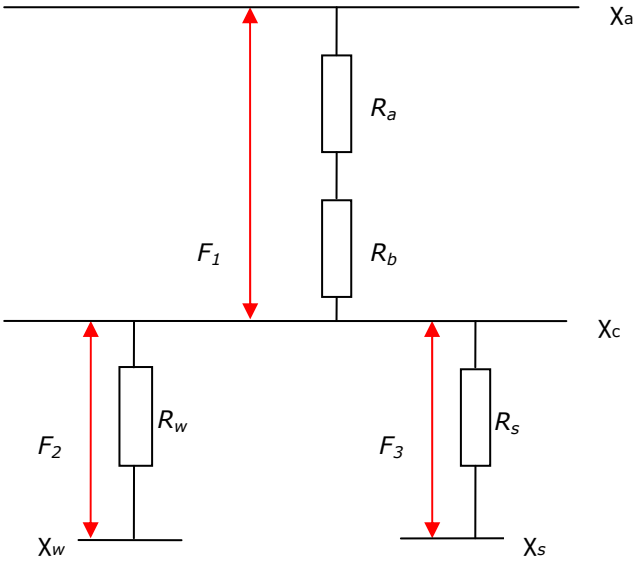

Figure 22. Schematic representation of resistance approach with compensation points

A schematic representation of concentrations χ, resistances *R* and fluxes *F* is given in Figure 22.

In this Figure 22:
- χ_a is the concentration in air
- χ_c is the concentration at the canopy top
- χ_w is the concentration at the external leaf surface
- χ_s is the concentration in the stomata
- R_a is the aerodynamic resistance
- R_b is the quasi-laminar layer resistance
- R_w is the external leaf surface or water layer resistance
- R_s is the stomatal resistance

The fluxes *F* over the different pathways in Figure 22 are:

$$F_1 = -\frac{(\chi_a - \chi_c)}{R_a + R_b}, F_2 = -\frac{(\chi_c - \chi_w)}{R_w}, F_3 = -\frac{(\chi_c - \chi_s)}{R_s}. \quad (1)$$

By selecting data under dry conditions the path through R_w may be neglected, and total flux then equals

$$F = F_1 + F_3 = -\frac{(\chi_a - \chi_s)}{R_a + R_b + R_s}. \quad (2)$$

The resistances R_a, R_b, R_s are determined using the measured meteorological data and plant characteristics (see Van Zanten et al. 2010) for the parameterisations of the resistances). Since we have measured the total flux *F* and the concentration in the air χ_a, we can derive the compensation point χ_s.

In Figure 23 we have plotted the derived compensation points χ_s for the period after 19 July. The data used for the derivation were the selected data obtained

under non-stable dry daytime conditions (Wichink Kruit et al., 2007). Daytime data were selected to ensure that the stomata of the plants are open. We imposed dry conditions, i.e. a relative humidity smaller than 80%, and $R_w > 2 \times R_s$ to be able to neglect the term F_2 in the total flux, and we selected positive χ_s values only. The depicted error bars are the result of a propagation of the standard deviations in the measured fluxes.

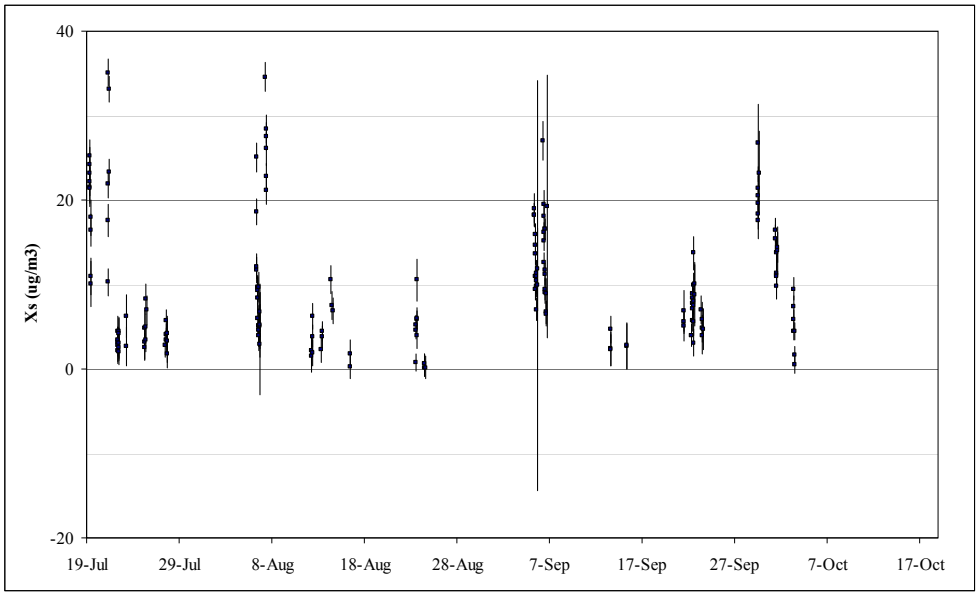

Figure 23. Compensation points as a function of time for the period after 19 July The error bars result from the standard deviations in the underlying flux measurements.

We see in Figure 23 that the compensation points vary considerably over time. This variability may be expected since compensation points, amongst other things, depend on temperature and meteorological conditions as is found also in other studies (Wichink Kruit et al., 2007).
The average χ_s is 10.0 µg m^{-3} (with an uncertainty interval between 7.6 and 10.6 µg m^{-3}, see section 2.5.2). The standard error in the average χ_s is 0.6 µg m^{-3}.

The Γ values are calculated using the χ_s values using the following formula (Wichink Kruit et al., 2010a)

$$\chi_s = \frac{2.75 \cdot 10^{15}}{T_s + 273.15} \exp\left(\frac{-1.04 \cdot 10^4}{T_s + 273.15}\right) \cdot \Gamma_s \ . \qquad (3)$$

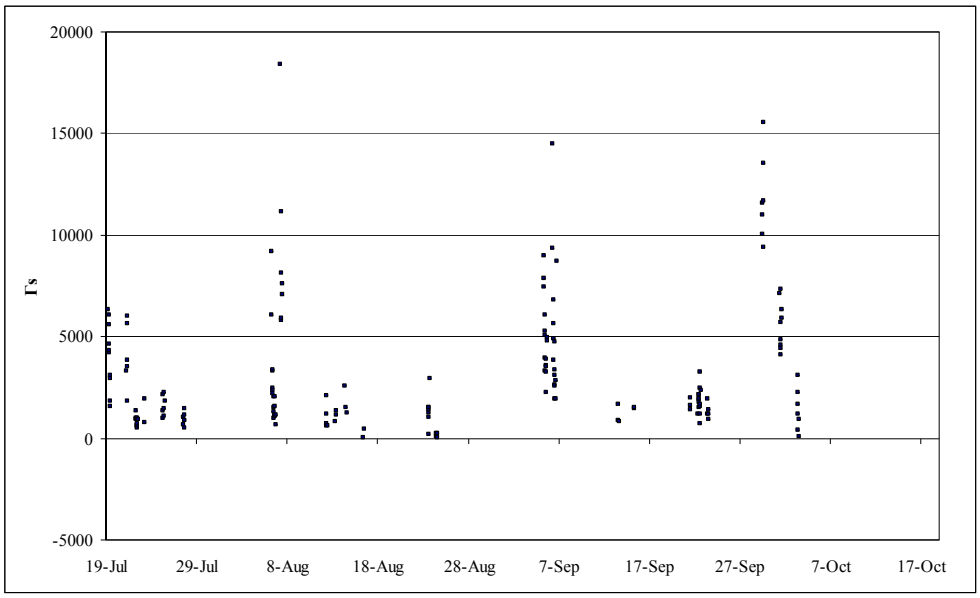

Figure 24. Γ_s as a function of time in the period after 19 July

Figure 24 shows the Γ_s corresponding to the χ_s in Figure 23. Again the variation in time is large. The average Γ_s is 3,200 with an uncertainty interval (see section 2.5.2) of 2,400 to 4,200. The spread in the data result in a standard error in the average Γ_s of 230.

4.3 Emission factor for the crop growing season

With the use of Γ_s, the measured concentration and the meteorological conditions an estimate of the net (stomatal) emission during the entire crop growing season can be made. With this method also a value for the flux is obtained on hours when flux measurements are not available. It is somewhat uncertain whether the derived Γ_s values are also valid for the period before 17 July when the crop was in its strongest growing stage. Therefore we split the analyses in a part in which the crop is fully grown and the entire crop growing season.
A model calculation using the parameterization proposed by Wichink Kruit at al. (2010a) which has been implemented in the DEPAC module (van Zanten et al., 2010), yields an average stomatal flux over the period when the crop was fully grown of F_s = 53.0 ng m^{-2} s^{-1}., using the measured mean Γ_s = 3,200. This is a net flux of ammonia and includes also deposition events. The gross emission is 61.0 ng m^{-2} s^{-1}. This is equivalent to about 4.8 kg NH_3/ha with an uncertainty range of 3.5-6.4 kg NH_3/ha due to the uncertainty in the gamma values (of 2400-4200).

5 Discussion

Essential in the interpretation of the fluxes of ammonia is the calibration of the DOAS-systems. The final results and the conclusions that can be drawn from the experiments heavily depend on this. Therefore, we firstly discuss two issues on the calibration and subsequently what it means for the results.

5.1 Effect of DOAS calibration on measured fluxes

5.1.1 Variable offset

For the 2010 data we have found that the offset between the two DOAS systems is not constant but varies on the time scales of hours to days with a standard deviation of 0.17 µg m^{-3}. For future flux determinations we will aim to eliminate the variations or, in case that is not feasible, a method to monitor the variations will need to be devised so they can be corrected for.
For the current 2010 data we have constructed an uncertainty interval for our results based on the afore mentioned standard deviation of 0.17 µg m^{-3}.

5.1.2 Calibration with laboratory regression curve

For the calibration of the two DOAS instruments relative to each other we assumed that the cross calibration measurements yield a more relevant calibration for the flux measurements than the laboratory calibration measurements. This assumption was based on the facts that the cross calibrations in the field were performed during the actual measurement campaign and at the same location with the same configuration and alignment. In Appendix B we show some of the results we would have obtained if we had used the average of the two laboratory parallel calibration regressions. On average the measurements then show deposition of ammonia of about 8 kg NH_3/ha during the crop growing season. This is quite different from the net-emission of about 3.4 kg NH_3/ha obtained using the field calibration. Remarkable is that deposition events dominate, even under circumstances when emissions would be expected to occur, i.e, under dry and sunny weather conditions. Although these unlikely results were not the reason why we disregarded the laboratory regression curves, they do support our choice for using the field cross calibration regression curves.

5.1.3 Ammonia flux results in 2009

In 2009 similar flux measurements were performed over a corn field as reported here (Wichink Kruit et al., 2010b). In 2009 the cross calibration measurements were lost due to a break-in in the measurement cabin during the campaign. We therefore were forced to use the laboratory calibrations. On average the measurements from 2009 showed deposition of ammonia of about 11 kg NH_3/ha during the crop growing season, which is in line with the results obtained in 2010 when using the laboratory calibration data. Since we do not have the cross calibration measurements from 2009 we cannot tell whether this similarity in the results is a coincidence or whether it is indicative of the same problem that occurred in 2010. We can only caution that the exchange results from 2009 should be used only with the utmost care.

5.2 Results of the experiments using field calibrations

Overall the results of the experiment are largely dependent on what calibration is chosen. As was pointed out in section 3 it is considered that the field calibrations are considered to be more relevant. We pursued the interpretation of the experiments by using this in-field calibration. Below the results using the field calibrations are discussed taking into account the variable offset (see section 5.1.1) which results in a range given for each ammonia exchange result.

5.2.1 Overall fluxes

The ammonia fluxes measured using DOAS systems over a corn field in Lelystad in 2010 show in great detail the occurrence of both emission and deposition events during the crop growing season. In follow-up studies the extensive dataset of flux and meteorological values may be used for detailed studies of processes influencing the ammonia exchange in a corn field. In this report, we made a brief beginning by looking at the effects of general weather patterns and leaf wetness of the flux measurements, but the main focus is on documenting the data and giving an estimate on the ammonia emission factor of the crop. One of the main findings is that crops may be net sources of ammonia rather than sinks. No clear seasonal pattern in the ammonia flux could be seen, i.e. no significant larger flux could be seen when the crop was senescencing. The net-emission when the crop was covering the soil based on the measurements alone was 2.6 kg NH_3/ha and lies in the same range as yielded by measurements over oilseed rape, wheat, barley and pea carried out in Denmark (Schjoerring and Mattsson, 2001), i.e. in the order of 1-5 kg NH_3/ha. The average emission of the crop itself was 3.5-6.4 kg NH_3/ha based on the gamma-values derived from the measurements. The range of 3.5-6.4 kg NH_3/ha indicates the uncertainty due to the uncertainty in the derived gamma values from the measurements. The net emission that is measured is the result of the crop emission and the deposition of ammonia. Therefore the crop emission factor is larger than the net emission factor derived from measurements alone. According to the Danish Emission Inventory (Mikkelsen et al., 2011), the calculated emission may be overestimated and the emission factor has therefore been adjusted to 2 kg N/ha (= 2.43 kg NH_3/ha) for crops in rotation such as corn. However, (Mikkelsen et al., 2011) also state that it is uncertain how much NH_3 is emitted from crops under different soil, geographic, and climatic conditions, so it is not certain how the Danish situation relates to the expected emission factor in the Netherlands.

5.3 Compensation points and Γ values

Measured fluxes and compensation points are dependent on the type of corn, nitrogen (N) status of the soil and air, temperature, growth stage, and meteorological conditions (Zhang et al., 2010). For this reason it is very hard to directly compare the different flux measurements for corn published in the literature. Here we confine ourselves to a comparison of reported measured average compensation points and Γ values. An excellent database of stomatal (and canopy) compensation points derived from measurements was published by Zhang et al. (2010). In summary, they find that typical summer daytime χ_s values over agricultural crops are between 5 and 10 µg m^{-3}. Our measurements yield a χ_s of 10.0 µg m^{-3}, (with an uncertainty interval between 7.6 and 10.6 µg m^{-3}, see section 2.5.2) which lies more or less within this range. More

specifically, they report field values for χ_s of 6.9 and 6 µg m^{-3} using micrometeorological methods, respectively, for a irrigated corn field (Harper and Sharpe, 1995) and a fully developed corn canopy (Meyers et al., 2006), which is of the same order as our findings. With the Modified Bowen-ratio method a lower value of χ_s = 2.31 µg m^{-3} was found for a developed corn canopy in summer (Bash et al., 2010), resulting also in a lower mean Γ_s of 221, compared to what we found, i.e. an average Γ_s of 3,200 with an uncertainty interval (see section 2.5.2) of 2,400 to 4,200. (Loubet et al., 2006) reported an average Γ_s of 3,000. This value was modelled based on experimental results in a corn field, and is much closer to our findings.

6 Conclusions

In this study, we report ammonia fluxes measured over a corn canopy in Lelystad, the Netherlands, during the crop growing season of 2010. A measurement technique based on Differential Optical Absorption Spectroscopy (DOAS) was applied. The DOAS systems (Volten et al., 2012) used in this measurement campaign were able to measure small concentration differences. The concentration measurements were combined with turbulence measurements from a sonic anemometer to obtain fluxes. The up times for the lower and upper DOAS were 81.8% and 98.4%, respectively. The data reduction due to the wind direction selection is the main limiting factor in obtaining flux values (40%). After applying all selection criteria 35.3% of the available fluxes remain.

In order to calibrate the DOAS systems, we applied a new calibration procedure. During this cross calibration measurement in the field the two DOAS systems are checked relative to each other by directing their light beams towards the retroreflector of the other system. Under the assumption that the ammonia concentration fields are homogeneous in the horizontal direction, the two DOAS systems should produce the same concentration values. Thus, small systematic differences between the two systems are detected and accounted for. Unfortunately, we found a problem with a small variability on a times scale from hours to days in the offset between the two instruments. This instability causes an uncertainty interval in our final flux results, which we aim to reduce or eliminate for future flux measurements.
Apart from this variability between the instruments it was found that the calibration between the instruments differ between these cross calibration in the field and the calibration in the laboratory. Since the concentration differences that have to be measured are very small, the difference in the calibrations lead to a totally different results. It is assumed, however, that the cross calibration measurements are more relevant for the field situation than the laboratory calibration. The results in this report are based on that assumption.

The flux measurements over corn at the measurement site in Lelystad in 2010 have shown that both emission (906 half hour values) and deposition (596 half hour values) events occur. The corn canopy generally emits most ammonia during daytime, especially during warm and sunny days during the growth period. At night times and during rainy periods the average flux tends to remain close to zero. On the other hand, leaf wetness data combined with flux data show that occasionally, during warm dry nights, significant emission events may occur. No clear seasonal pattern in the ammonia flux could be seen, i.e. no significant larger flux could be seen when the crop was senescing. A net emission of ammonia was measured of 2.6 (0.15-5.1) kg NH_3/ha. This includes the emission and deposition events.

Average stomatal emission fluxes were calculated using a model incorporating the parameterization proposed by Wichink Kruit et al. (2010a) which has been implemented in the DEPAC module (van Zanten et al., 2010). When using the measured Γ_s = 3,200, the measured concentrations and a crop growing season pattern adapted to corn, this yields an average stomatal emission flux for the period when the crop was fully grown of 61.0 ng m^{-2} s^{-1}. This means that the crop emitted in that period about 4.8 (3.5-6.4) kg NH_3/ha, where the range indicates the uncertainty due to the derived gamma values. The average

emissions are in the same range, i.e. in the order of 1-5 kg NH_3 ha^{-1}, as yielded by measurements over oilseed rape, wheat, barley and pea carried out in Denmark (Schjoerring and Mattsson, 2001).

References

BASH, J. O., WALKER, J. T., KATUL, G. G., IONES, M. R., NEMITZ, E. & ROBARGE, W. P. 2010. Estimation of in-canopy ammonia sources and sinks in a fertilized zea mays field. *Environ. Sci. Technol.,* 44**,** 1683-1689.

BELJAARS, A. C. M. & HOLTSLAG, A. A. M. 1991. Flux parameterization over land surfaces for atmospheric models. *Journal of Applied Meteorology,* 30**,** 327-341.

BURKHARDT, J., FLECHARD, C. R., GRESENS, F., MATTSSON, M., JONGEJAN, P. A. C., ERISMAN, J. W., WEIDINGER, T., MESZAROS, R., NEMITZ, E. & SUTTON, M. A. 2009. Modelling the dynamic chemical interactions of atmospheric ammonia with leaf surface wetness in a managed grassland canopy. *Biogeosciences,* 6**,** 67-84.

BUSINGER, J. A., WYNGAARD, J. C., IZUMI, Y. & BRADLEY, E. F. 1971. Flux-profile relationships in the atmospheric surface layer. *J Atmos Sci,* 28**,** 181-189.

CBS, PBL & WAGENINGEN UR. 2011a. *Emissies naar lucht, 1990-2010 (indicator 0079, versie 18, 11 oktober 2011).* [Online].

CBS, PBL & WAGENINGEN UR 2011b. www.compendiumvoordeleefomgeving.nl. *CBS, Den Haag PBL, Den Haag/Bilthoven en Wageningen UR, Wageningen.*

CELLIER, P. & BRUNET, Y. 1992. Flux-gradient relationships above tall plant canopies. *Agric. For. Meterol.,* 58**,** 93-117.

DE RUIJTER, F. J., HUIJSMANS, J. F. M. & RUTGERS, B. 2010. Ammonia volatilization from crop residues and frozen green manure crops. *Atmos. Environ.,* 44**,** 3362-3368.

DYER, A. J. 1974. A review of flux-profile relationships. *Boundary-Layer Meteorology,* 7**,** 363-372.

DYER, A. J. & HICKS, B. B. 1970. Flux-gradient relationships in the constant flux layer. *Quarterly Journal of the Royal Meteorological Society,* 96**,** 715-721.

FARQUHAR, G. D., FIRTH, P. M., WETSELAAR, R. & WEIR, B. 1980. On the gaseous exchange of ammonia between leaves and the environment: Determination of the ammonia compensation point. *Plant Physiology* 66**,** 710-714.

GARRATT, J. R. 1980. Surface influence upon vertical profiles in the atmospheric near- surface layer. *Quarterly Journal of the Royal Meteorological Society,* 106**,** 803-819.

HARPER, L. A. & SHARPE, R. R. 1995. Nitrogen dynamics in irrigated corn: Soil-plant nitrogen and atmospheric ammonia transport. *AGRON. J.,* 87**,** 669-675.

HUSTED, S. & SCHJOERRING, J. K. 1996. Ammonia flux between oilseed rape plants and the atmosphere in response to changes in leaf temperature, light intensity, and air humidity. Interactions with leaf conductance and apoplastic $NH4^+$ and H^+ concentrations. *PLANT PHYSIOL.,* 112**,** 67-74.

LOUBET, B., CELLIER, P., MILFORD, C. & SUTTON, M. A. 2006. A coupled dispersion and exchange model for short-range dry deposition of atmospheric ammonia. *Q. J. R. Meteorol. Soc.,* 132**,** 1733-1763.

LOUBET, B., MILFORD, C., HILL, P. W., SIM TANG, Y., CELLIER, P. & SUTTON, M. A. 2002. Seasonal variability of apoplastic NH_4^+ and pH in an intensively managed grassland. *Plant Soil,* 238**,** 97-110.

MATTSSON, M., HÄUSLER, R. E., LEEGOOD, R. C., LEA, P. J. & SCHJOERRING, J. K. 1997. Leaf-atmosphere NH_3 exchange in barley mutants with reduced activities of glutamine synthetase. *PLANT PHYSIOL.,* 114**,** 1307-1312.

MEYERS, T. P., LUKE, W. T. & MEISINGER, J. J. 2006. Fluxes of ammonia and sulfate over maize using relaxed eddy accumulation. *Agric. For. Meteorol.,* 136**,** 203-213.

MIKKELSEN, M. H., ALBREKTSEN, R. & GYLDENKÆRNE, S. 2011. Danish emission inventories for agriculture. Inventories 1985 - 2009. *NERI Technical Report* 810**,** 136.

MONTEITH, J. L. & UNSWORTH, M. H. 1990. *Principles of environmental physics 2nd edn,* London

PAULSON, C. A. 1970. Mathematical Representation of Wind Speed and Temperature Profiles in the Unstable Atmospheric Surface Layer. *J. Appl. Meteorol.,* 9**,** 857-861.

SCHJOERRING, J. K. & MATTSSON, M. 2001. Quantification of ammonia exchange between agricultural cropland and the atmosphere: Measurements over two complete growth cycles of oilseed rape, wheat, barley and pea. *Plant Soil,* 228**,** 105-115.

VAN PUL, W. A. J., VAN DEN BROEK, M. M. P., VOLTEN, H., VAN DER MEULEN, A., BERKHOUT, A. J. C., VAN DER HOEK, K. W., WICHINK KRUIT, R. J., HUIJSMANS, J. F. M., VAN JAARSVELD, J. A., DE HAAN, B. J. & KOELEMEIJER, R. B. A. 2008. Het ammoniakgat: onderzoek en duiding [The ammonia gap: research and interpretation]. *RIVM rapport 680150002***,** 95.

VAN ZANTEN, M. C., SAUTER, F. J., WICHINK KRUIT, R. J., VAN JAARSVELD, J. A. & VAN PUL, W. A. J. 2010. Description of the DEPAC module [Beschrijving van de DEPAC module]. *RIVM rapport 680180001***,** 74.

VOLTEN, H., BERGWERFF, J. B., HAAIMA, M., LOLKEMA, D. E., BERKHOUT, A. J. C., VAN DER HOFF, G. R., POTMA, C. J. M., WICHINK KRUIT, R. J., VAN PUL, W. A. J. & SWART, D. P. J. 2012. Two instruments based on differential optical absorption spectroscopy (DOAS) to measure accurate ammonia concentrations in the atmosphere. *Atmos. Meas. Tech.,* 5**,** 413-427.

WEBB, E. K., PEARMAN, G. I. & LEUNING, R. 1980. Correction of flux measurements for density effects due to heat and water vapour transfer. *Quarterly Journal of the Royal Meteorological Society,* 106**,** 85-100.

WICHINK KRUIT, R. J., VAN PUL, W. A. J., OTJES, R. P., HOFSCHREUDER, P., JACOBS, A. F. G. & HOLTSLAG, A. A. M. 2007. Ammonia fluxes and derived canopy compensation points over non-fertilized agricultural grassland in The Netherlands using the new gradient ammonia - high accuracy - monitor (GRAHAM). *Atmos Environ 2007; 41(6):1275-87*.

WICHINK KRUIT, R. J., VAN PUL, W. A. J., SAUTER, F. J., VAN DEN BROEK, M., NEMITZ, E., SUTTON, M. A., KROL, M. & HOLTSLAG, A. A. M. 2010a. Modeling the surface-atmosphere exchange of ammonia. *Atmos Environ 2010; 44(7):945-57*.

WICHINK KRUIT, R. J., VOLTEN, H., HAAIMA, M., SWART, D. P. J., VAN ZANTEN, M. C. & VAN PUL, W. A. J. 2010b. Ammonia exchange measurements over a corn field in Lelystad, the Netherlands in 2009 [Ammoniakuitwisselingsmetingen boven een smijmaisveld in Lelystad, Nederland in 2009]. *RIVM report 680180002***,** 63.

ZHANG, L., WRIGHT, L. P. & ASMAN, W. A. H. 2010. Bi-directional air-surface exchange of atmospheric ammonia: A review of measurements and a development of a big-leaf model for applications in regional-scale air-quality models. *J. Geophys. Res. D Atmos.,* 115**,** D20310, doi:10.1029/2009JD013589.

Acknowledgement

We would like to thank the people from the Waiboerhoeve, Runderweg 8, 8219 PK, Lelystad for letting us use their corn field. In particular, we are grateful to Jan Bloemert and Sjoerd de Vries for their frequent assistance during the campaign. We would like to thank Klaas van der Hoek for advise, encouragement and constructive comments on this report.

Appendix A. Photographs of the Corn Canopy

During the campaign the height of the canopy was measured and photographs were taken of the plants that give an indication of the growing stage and of the extent the leaves are covering the soil.

Figure 25. Corn canopy at the beginning of the campaign at 30 June 2010
The height of the canopy was 60 cm.

Figure 26. Corn canopy at 5 July 2010
The height of the canopy was 95 cm.

Figure 27. Corn canopy at 8 July 2010
The height of the canopy was 105 cm.

Figure 28. Corn canopy at 19 July 2010
The height of the canopy was 200 cm.

Figure 29. Corn canopy at 26 July 2010
The height of the canopy was 260 cm.

Figure 30. Corn canopy at the end of the campaign on 13 October 2010
The height of the canopy was 310 cm.

Appendix B. Laboratory regression results

For the final calibration of the two DOAS instruments we explicitly assumed that the cross calibration measurements yield a more relevant calibration for the flux measurements than the laboratory calibration measurements, since the latter were performed at a different time and in a different location involving moving and realigning the equipment. In this appendix we show some of the results we did not use, but that we would have obtained if we had used the average of the two laboratory parallel calibration regressions curves shown in Figure 6, i.e. $y = 0.9784 (\pm 0.003)\ x - 0.4165 (\pm 0.014)$, with one-sigma uncertainties given in parentheses.

In Figure 31 the diurnal cycle of the selected mean ammonia fluxes is shown at 1 m above zero-displacement height using average lab regression. We see that on average deposition occurs during the whole day. The frequency plot in Figure 32 shows that more deposition events (1103) occur than emission events (236).

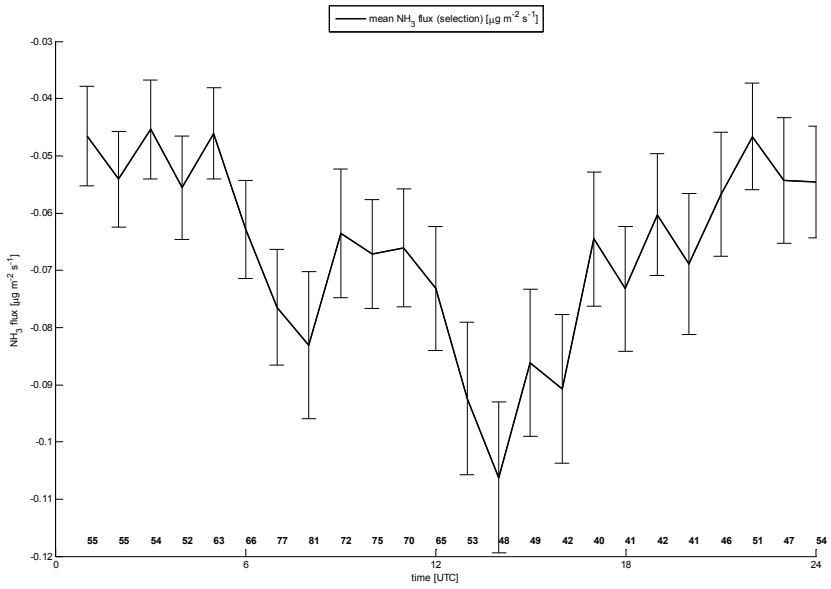

Figure 31. Diurnal cycle of the selected mean ammonia fluxes at 1 m above zero-displacement height during the 2010 measurement campaign using average lab regression
The bars represent the standard deviation of the mean for each hour. The numbers at the bottom of the figure are the number of measurements on which the mean is calculated.

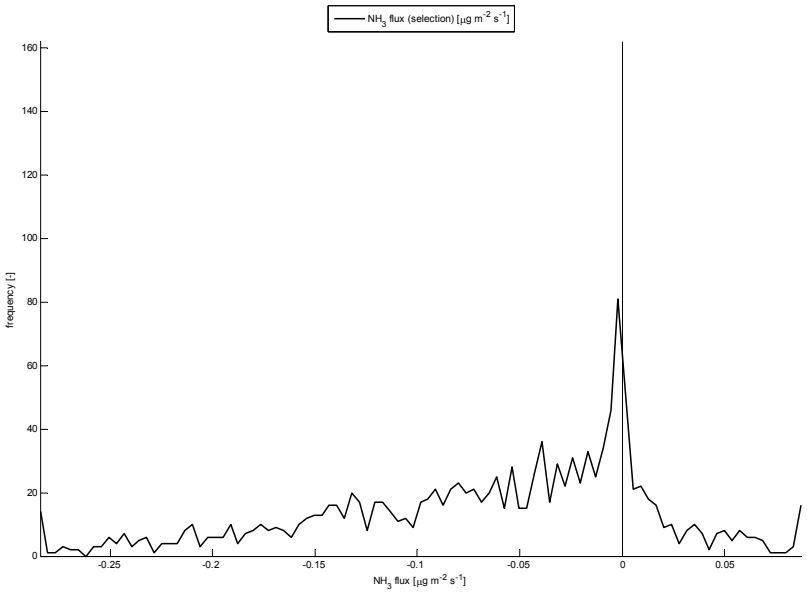

Figure 32. Frequency distribution of the selected ammonia fluxes at 1 m above zero-displacement height during the growth period using average lab regression The dotted and dashed lines indicate respectively the upper and lower limits of the uncertainty interval discussed in section 2.5.2.

In section 3.3 ammonia emissions were illustrated in Figure 20 and Figure 21 showing a rather generally observed pattern of wet leaves occurring together with ammonia deposition. As the leaves become dry more positive ammonia fluxes occur. This behaviour disappears when we apply the calibration using laboratory regression curves. In Figure 33 and Figure 34 we see that deposition occurs even when the leaves are dry.

Using the lab regression curve the net average flux over the season for the selected data is -86 (± 3) ng m^{-2} s^{-1} (with the standard error given in parentheses as in the rest of the section). That is: a net ammonia deposition on the corn and underlying soil is measured. If we use this number for the entire crop growing season (111 days in the period June-October) this yields a deposition of 8.2 (± 0.3) kg NH_3/ha.

If we want to consider the gross emission of ammonia we have to average solely over the emission events during the season. For the season this was 39 (± 3) ng m^{-2} s^{-1}. This value was based on 236 half hour flux values. If we repeat this for all deposition events, this yields -113 (± 3) ng m^{-2} s^{-1}, based on 1103 half hour flux values.

If we want to consider the emission from the plants themselves via the stomata than only dry conditions should be taken into account in averaging. As a switch we took the RH < 80% as an indicator for dry leave surface. The flux over the season under dry conditions for the selected data is then negative, i.e. we have a deposition of -121 (± 6) ng m^{-2} s^{-1}.

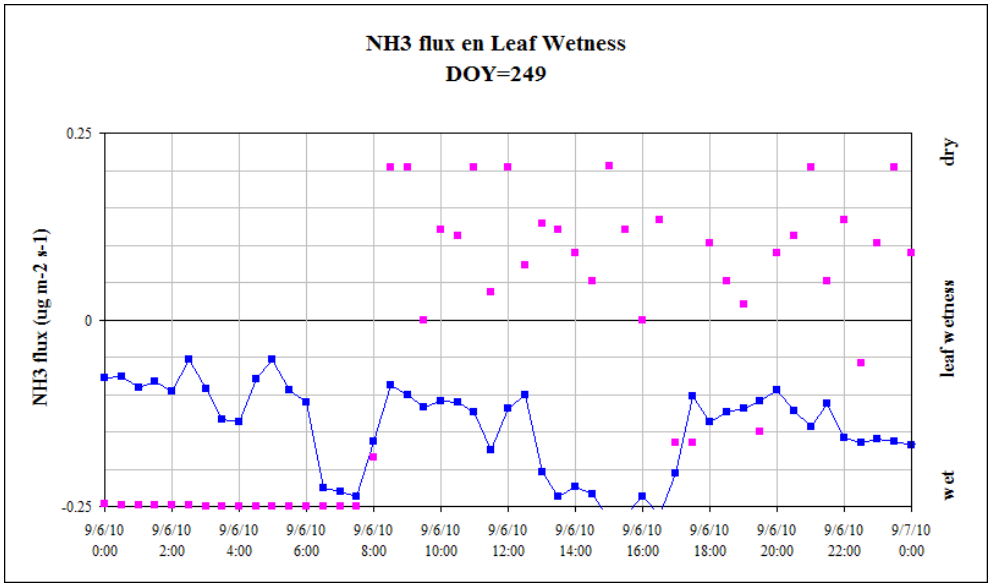

Figure 33. Ammonia flux (sky blue squares and line, left vertical axis) and leaf wetness (pink squares, right vertical axis) on 6 September 2010
Filled symbols indicate values that met the selection criteria explained in section 3.1. for average lab regression.

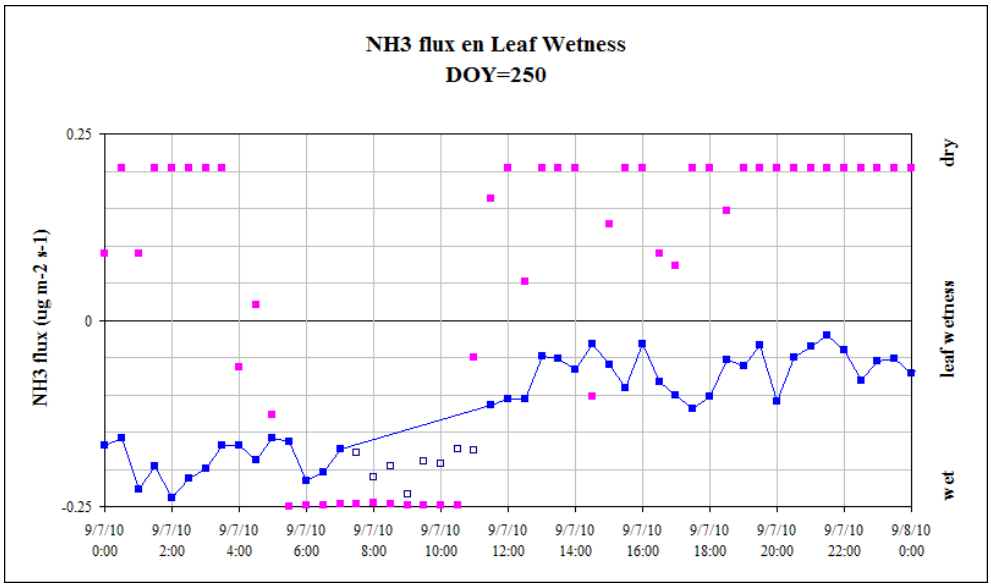

Figure 34. Ammonia flux (sky blue squares and line, left vertical axis) and leaf wetness (pink squares, right vertical axis) at the end of the campaign on 7 September 2010
Filled symbols indicate values that met the selection criteria explained in section 3.1. for average lab regression.

In Figure 35 we have plotted the derived compensation points χ_s for the period after 19 July using the average lab regression. The data used for the derivation were the selected data obtained under non-stable dry daytime conditions (Wichink Kruit et al., 2007). Daytime data were selected to ensure that the stomata of the plants are open. We imposed dry conditions, i.e. a relative humidity smaller than 80%, and $R_w > 2 \times R_s$ to be able to neglect the term F_2 in

the total flux. The depicted error bars are the result of a propagation of the standard deviations in the measured fluxes. Despite imposing dry conditions, we see that only four values are left larger than zero. The average of these four positive values yields χ_s is 5.8 µg m^{-3}. The average Γ_s is 1,730

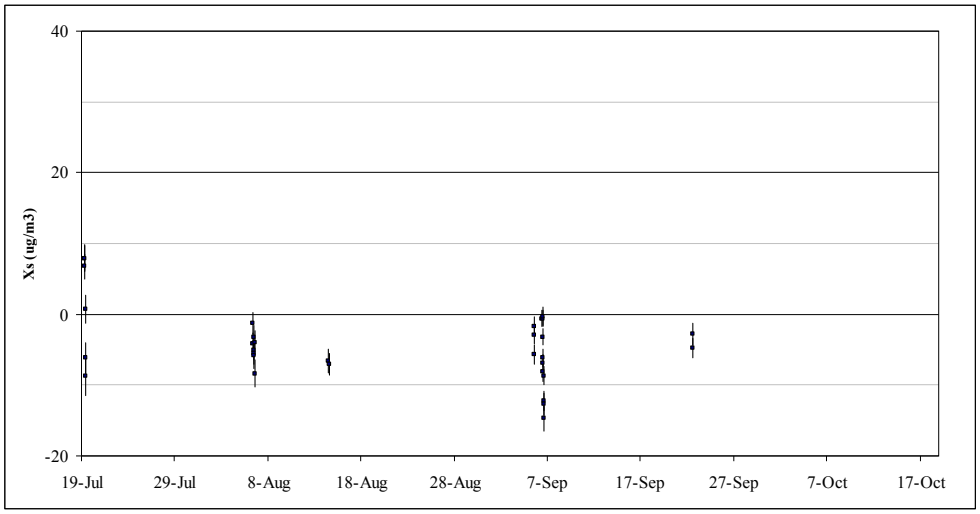

Figure 35. Compensation points using average lab regression as a function of time for the period after 19 July
The error bars result from the standard deviations in the underlying flux measurements. Four values are left larger than zero. The average χ_s *is 5.8 µg* m^{-3}*. The average* Γ_s *is 1,730*

Appendix C. Overview of the campaign week by week

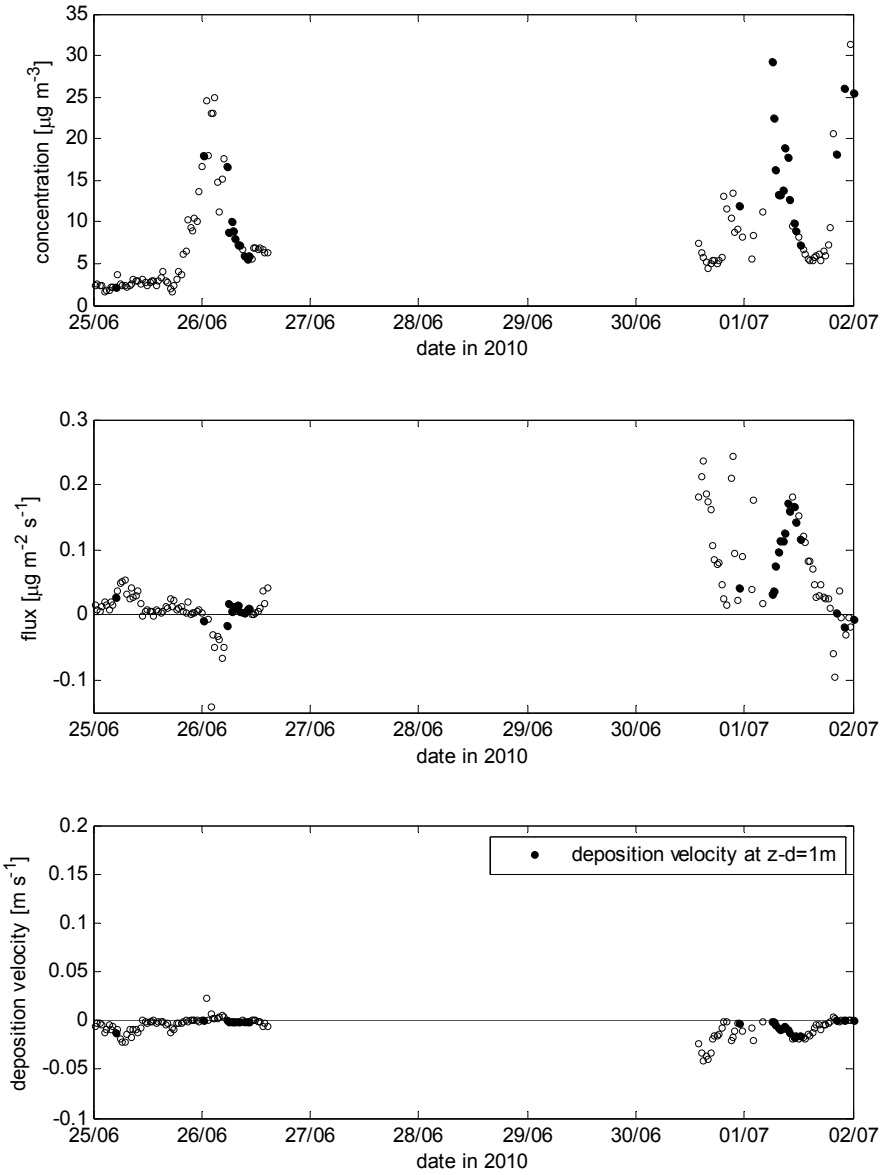

Figure 36. Ammonia concentrations (upper panel), ammonia fluxes (middle panel) and deposition velocities measured between 25 June 2010 and 2 July 2010 in the field in Lelystad measured over an open path of 50 m (one way)
Filled dots represent data used for valid flux determinations; open dots represent all available data. The flux data have not been corrected for surface roughness effects.

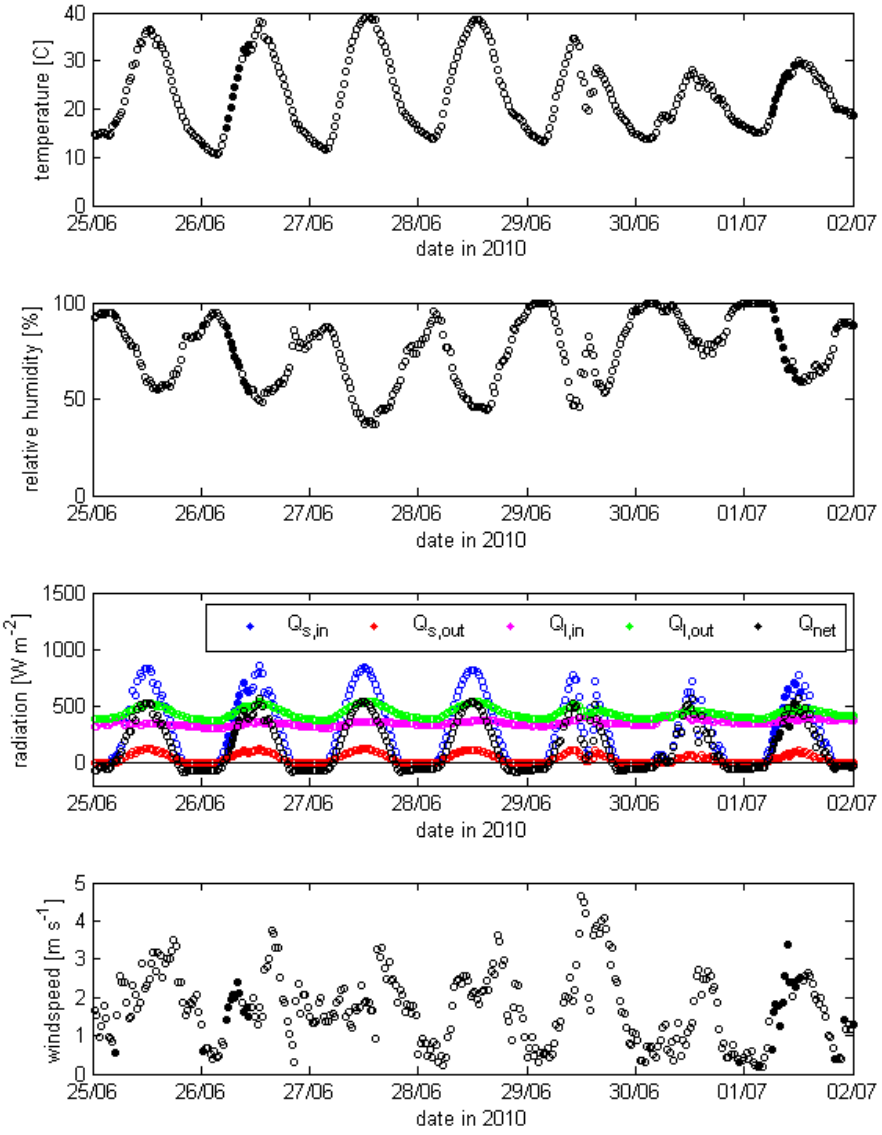

Figure 37. Temperature, relative humidity, radiation, and wind speed measured between 25 June 2010 and 2 July 2010 in the field in Lelystad
Filled dots represent data used for valid flux determinations; open dots represent all available data.

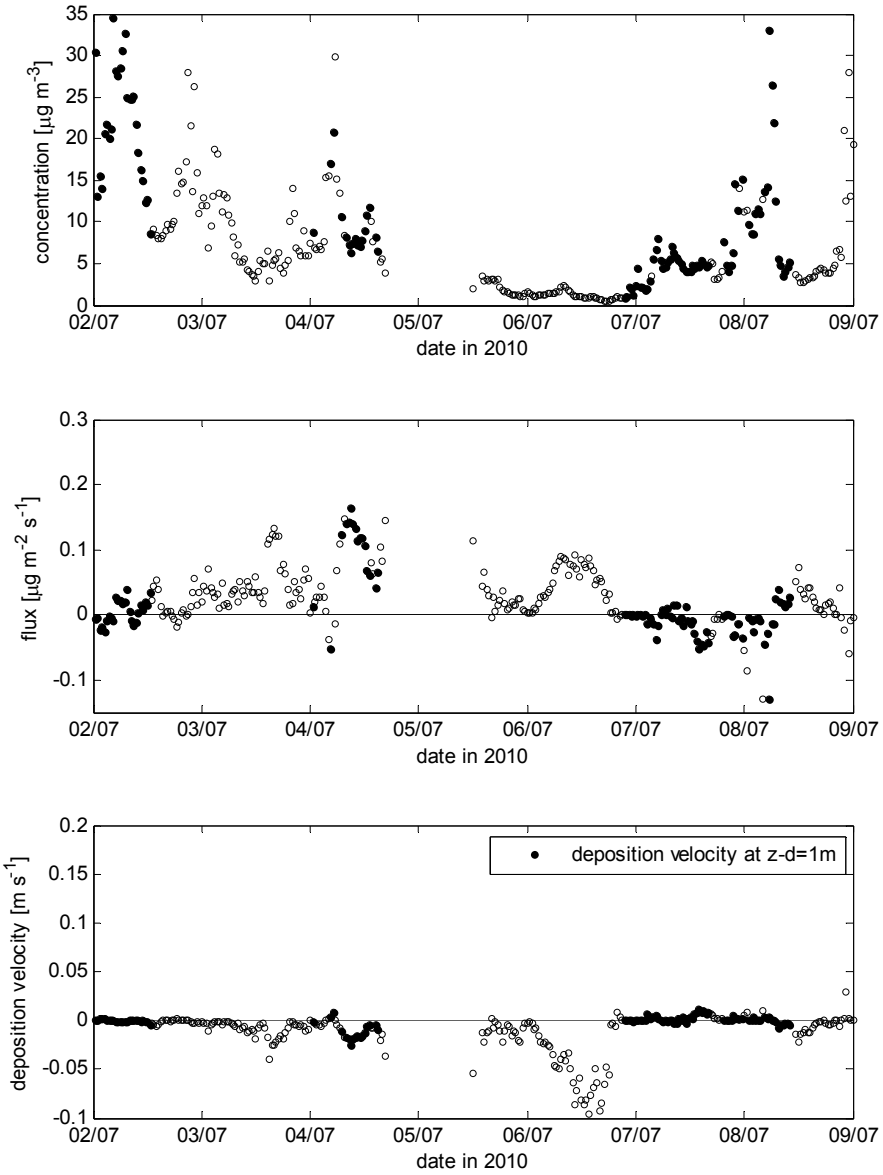

Figure 38. Same as Figure 36 for 2 to 9 July 2010

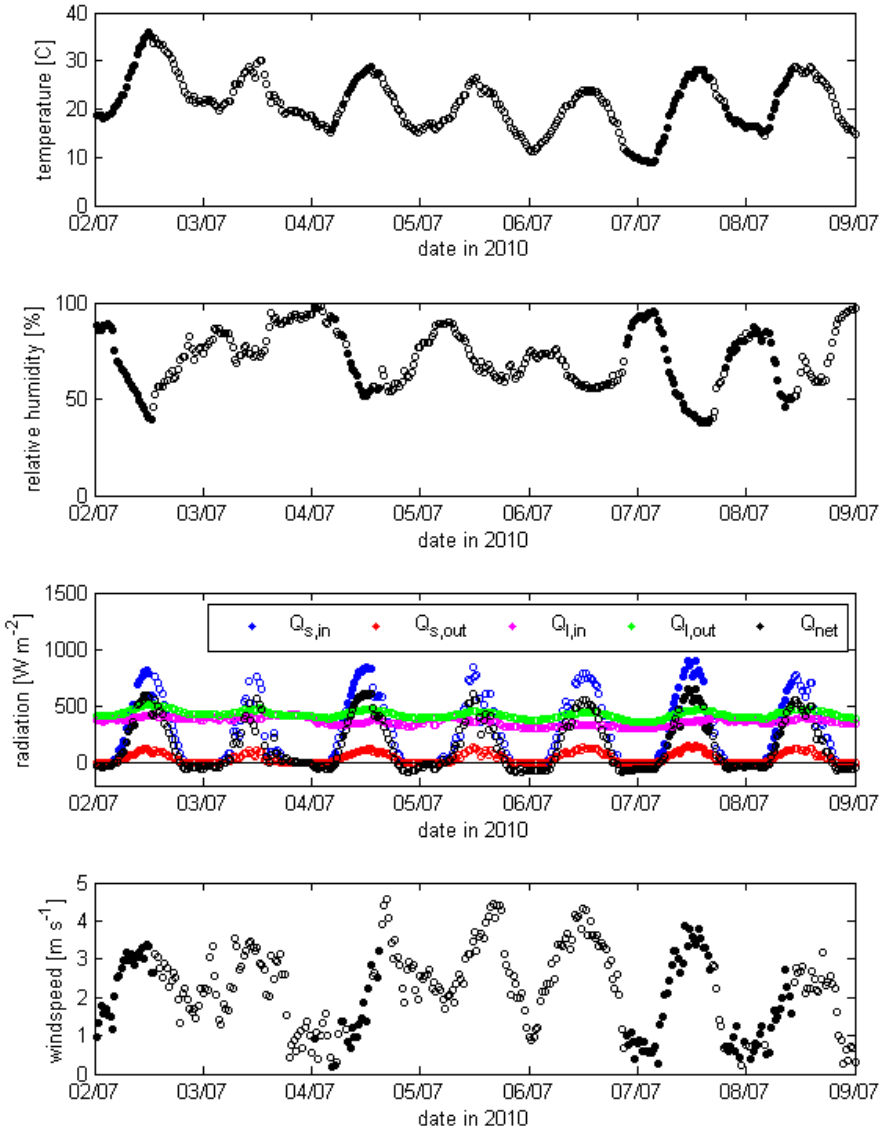

Figure 39. Same as Figure 37 for 2 to 9 July 2010

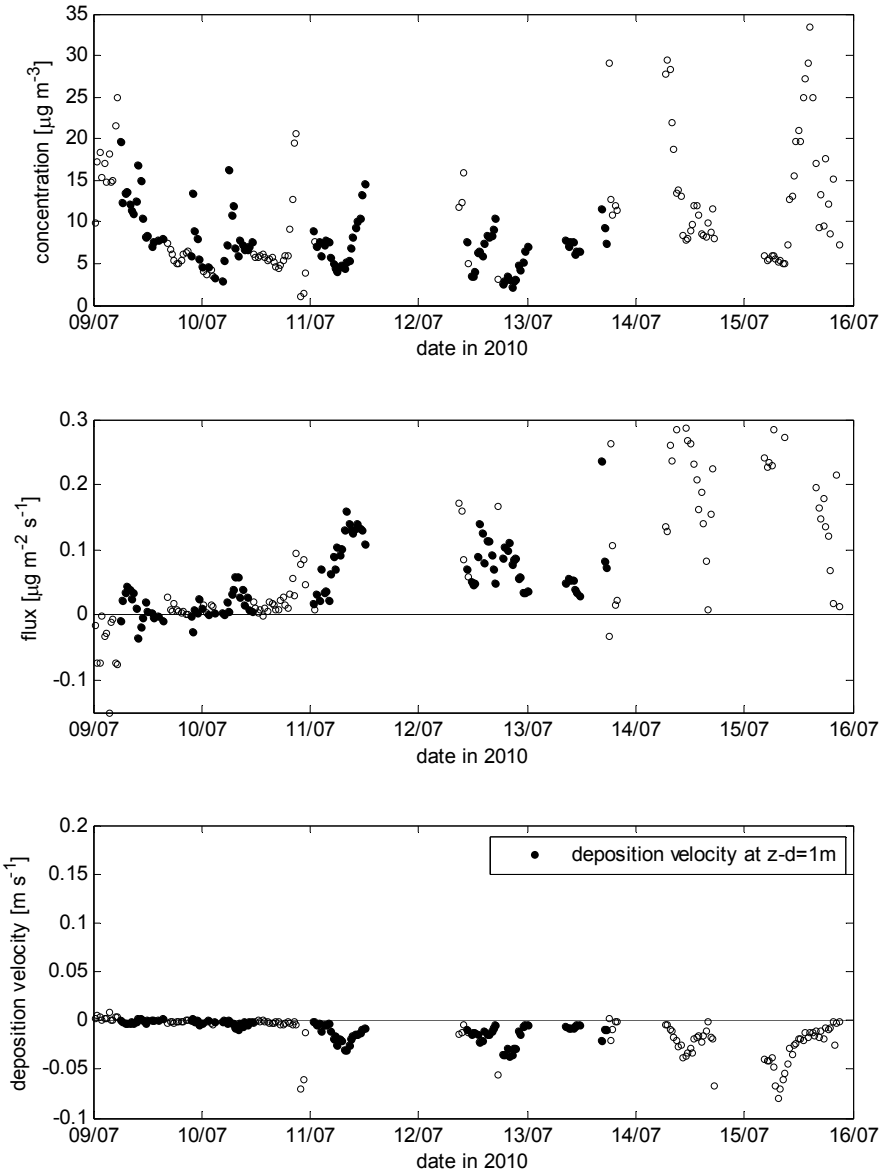

Figure 40. Same as Figure 36 for 9 to 16 July 2010

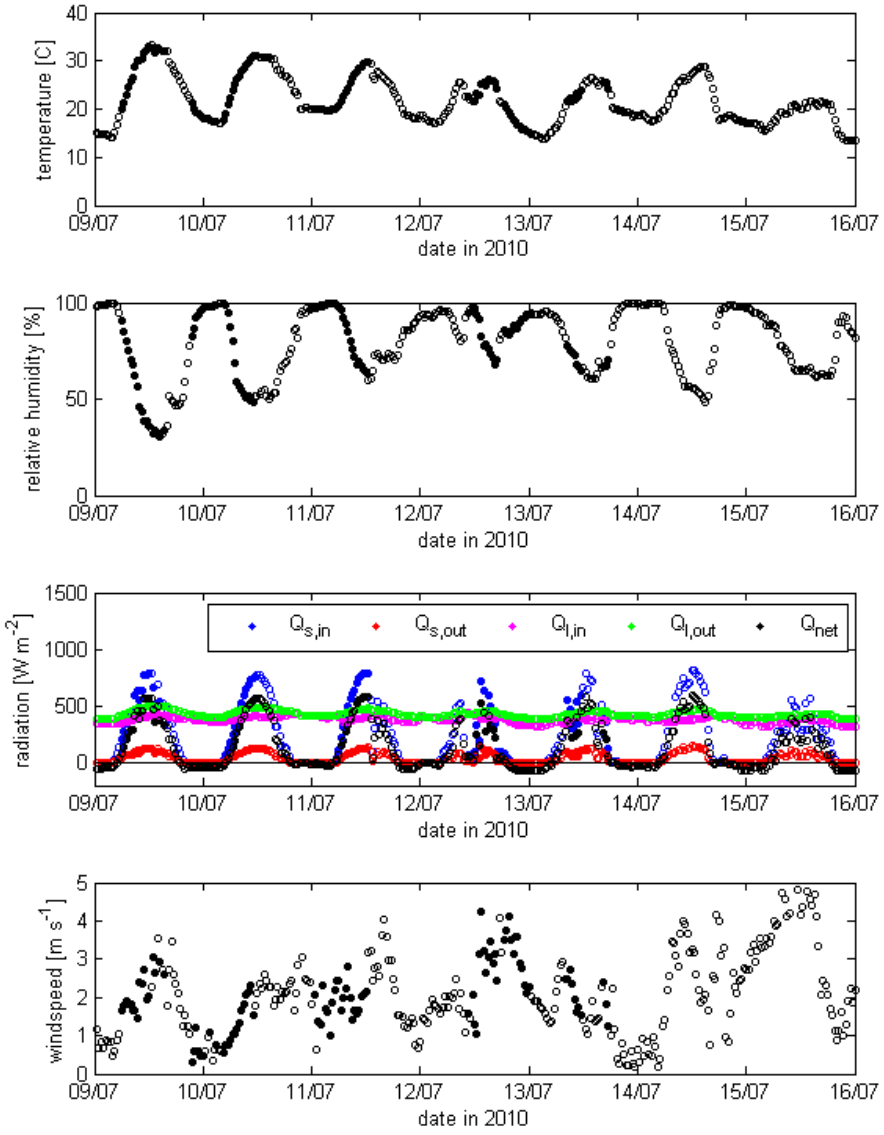

Figure 41. Same as Figure 37 for 9 to 16 July 2010

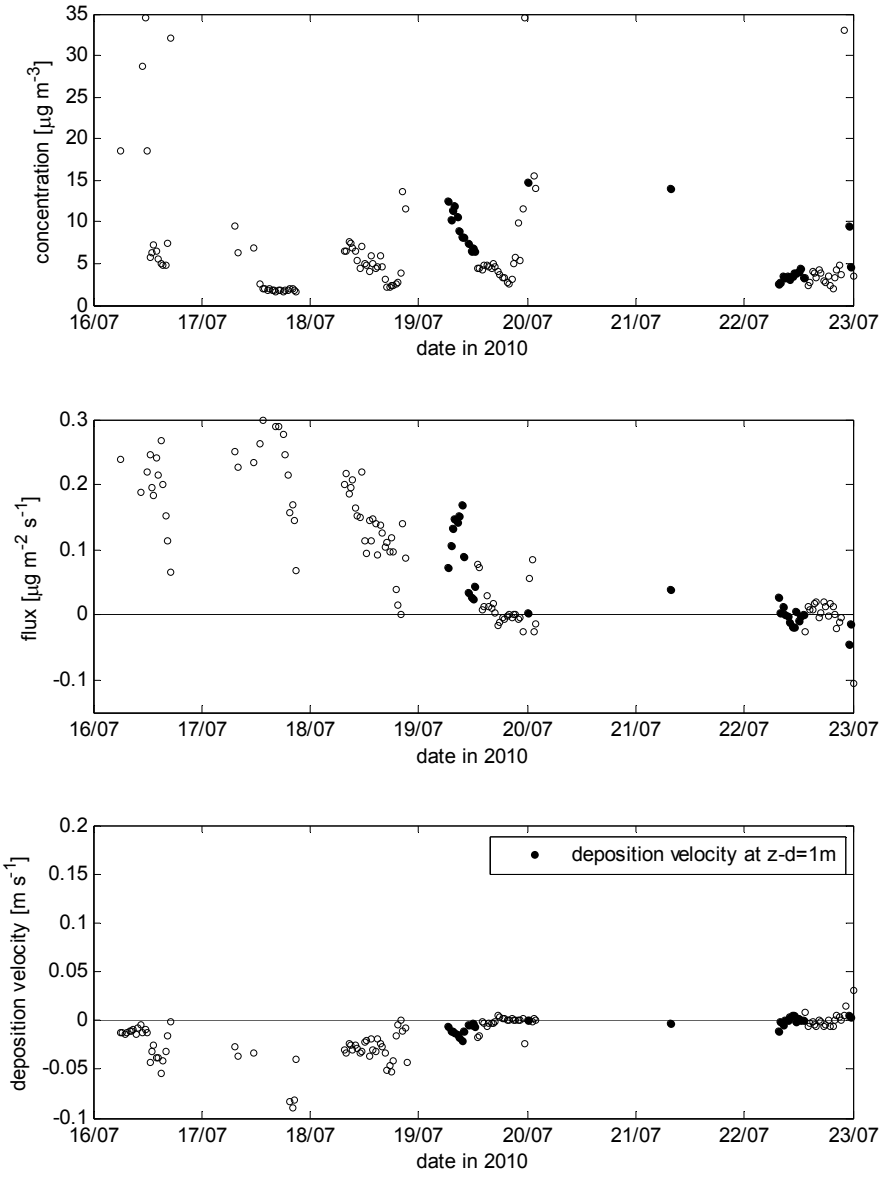

Figure 42. Same as Figure 36 for 16 to 23 July 2010

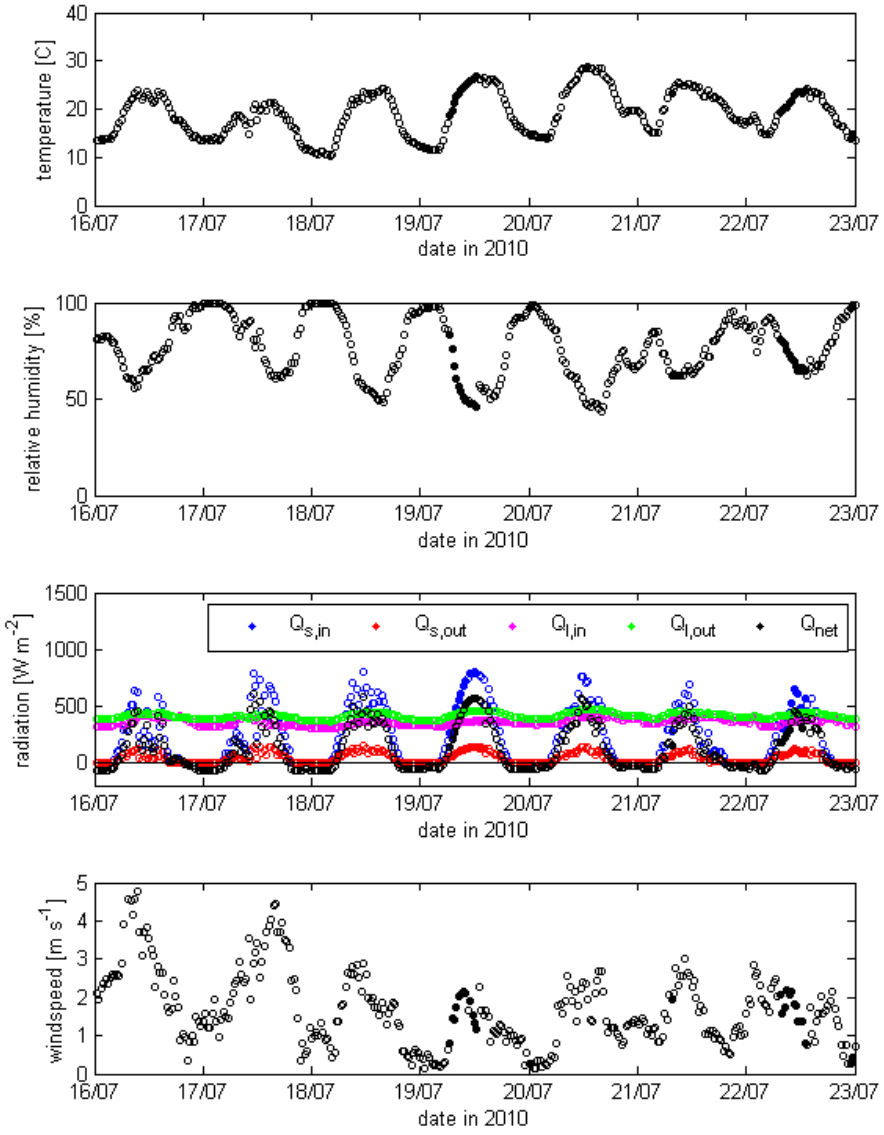

Figure 43. Same as Figure 37 for 16 to 23 July 2010

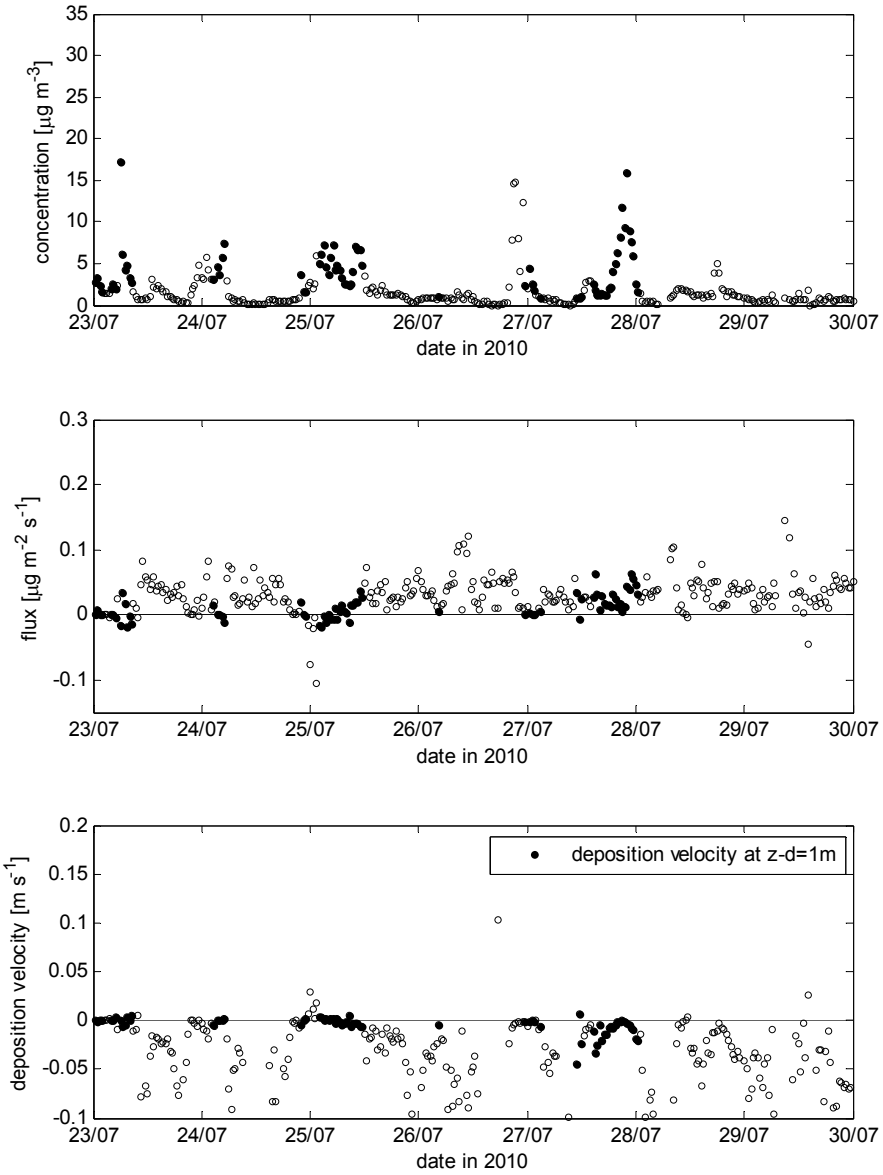

Figure 44. Same as Figure 36 for 23 to 30 July 2010

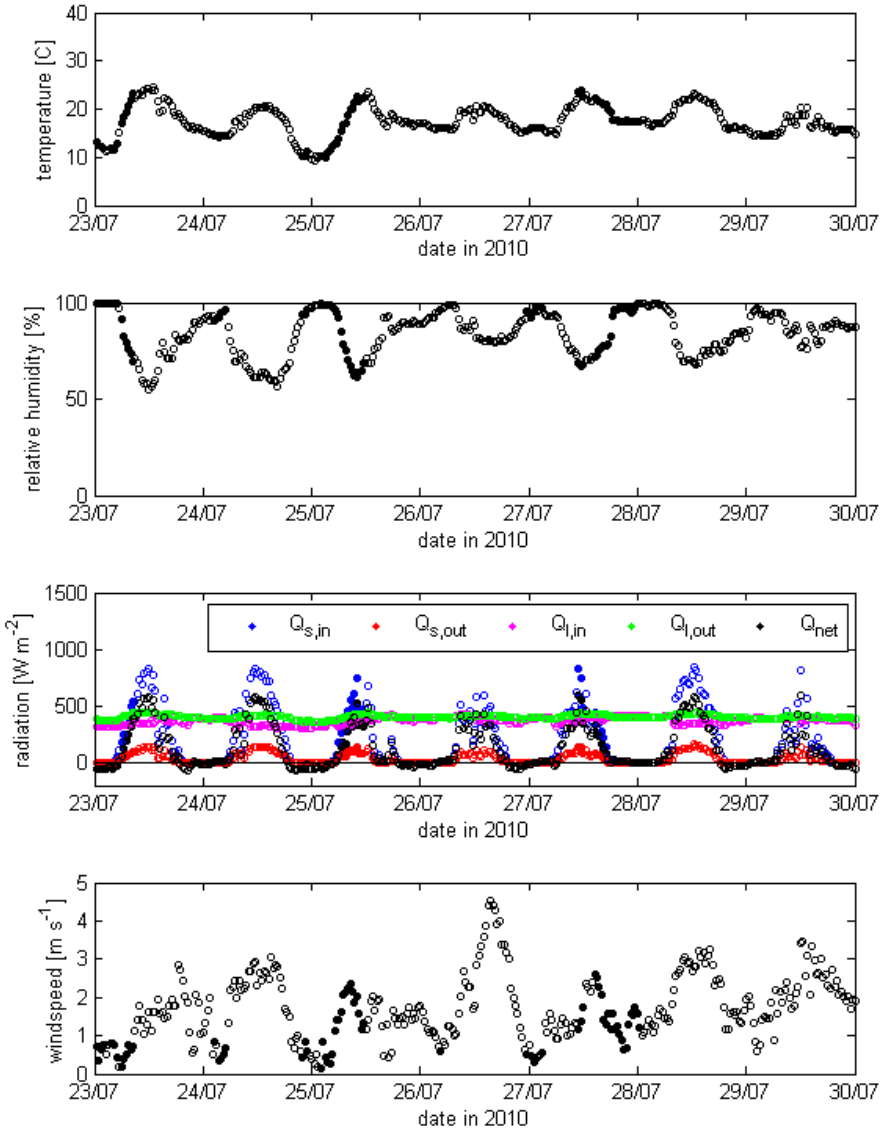

Figure 45. Same as Figure 37 for 23 to 30 July 2010

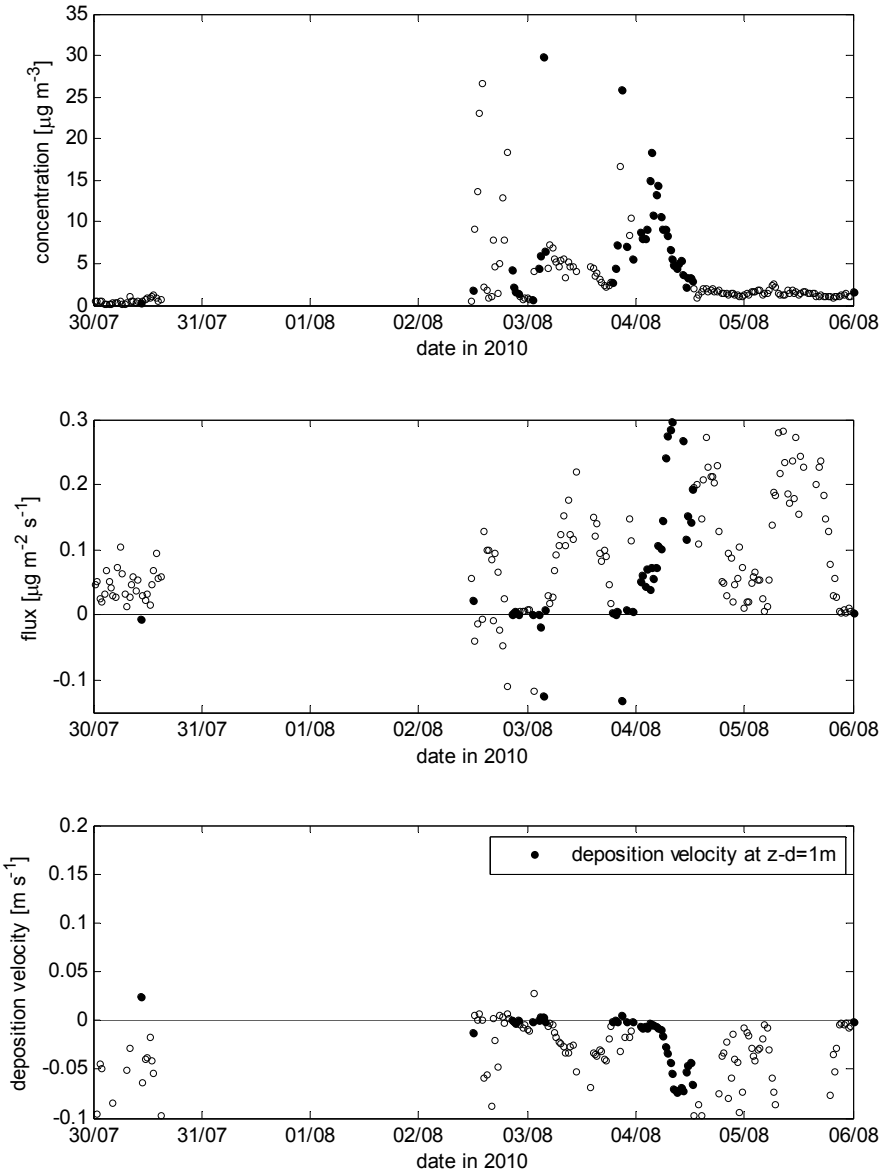

Figure 46. Same as Figure 36 for 30 July to 6 August 2010

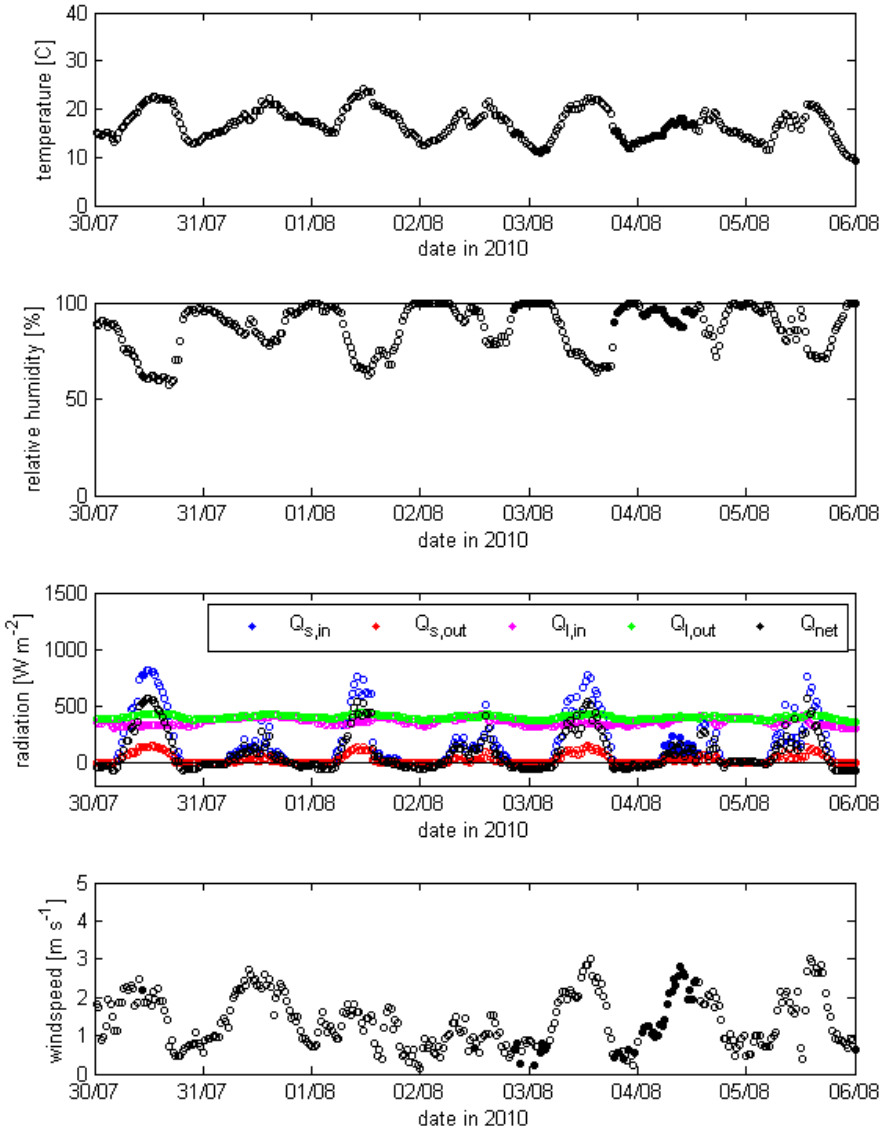

Figure 47. Same as Figure 37 for 30 July to 6 August 2010

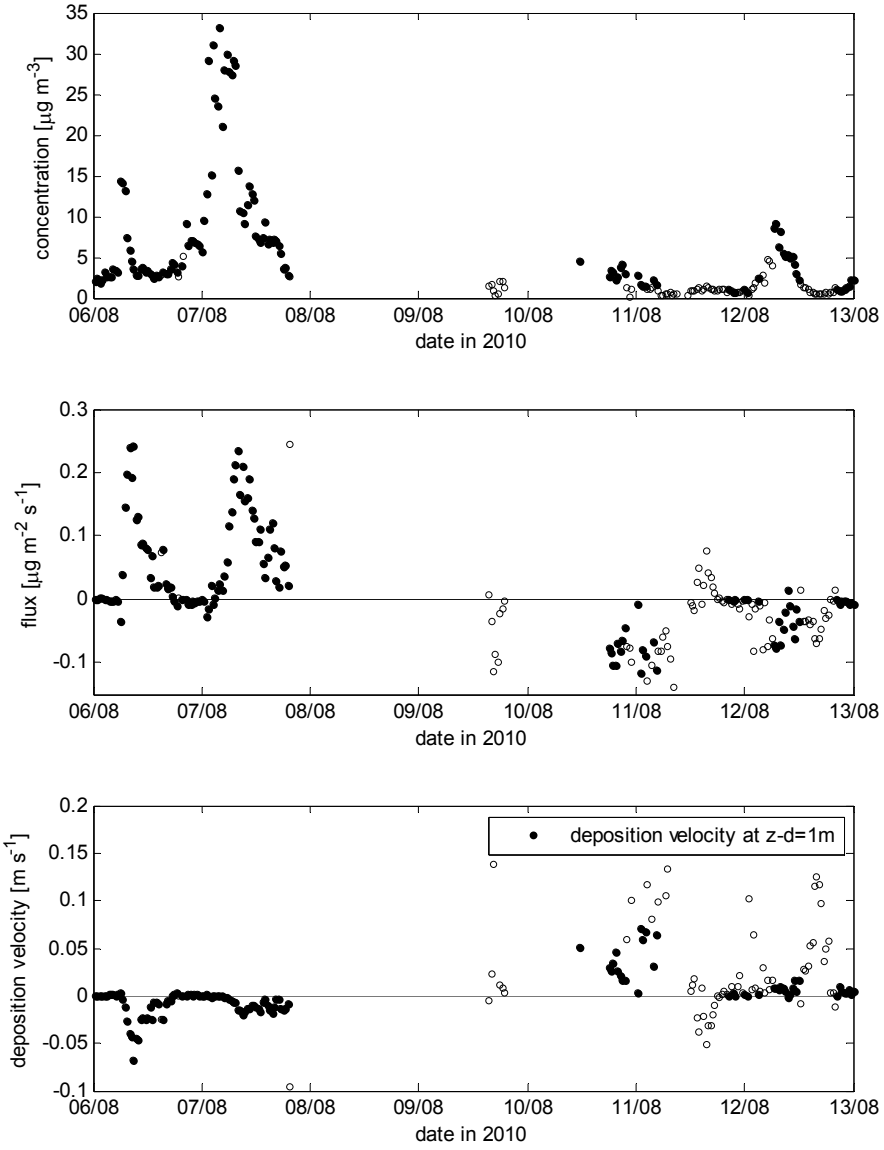

Figure 48. Same as Figure 36 for 6 to 13 August 2010

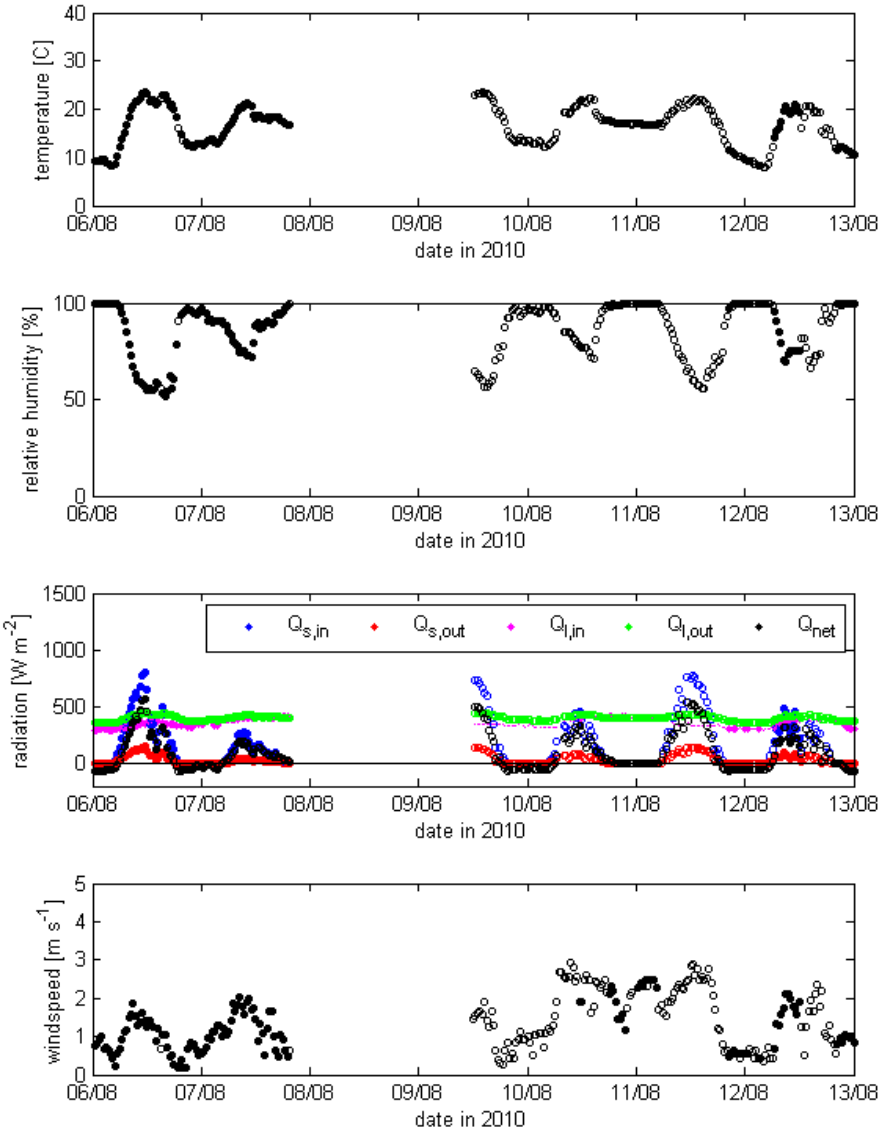

Figure 49. Same as Figure 37 for 6 to 13 August 2010

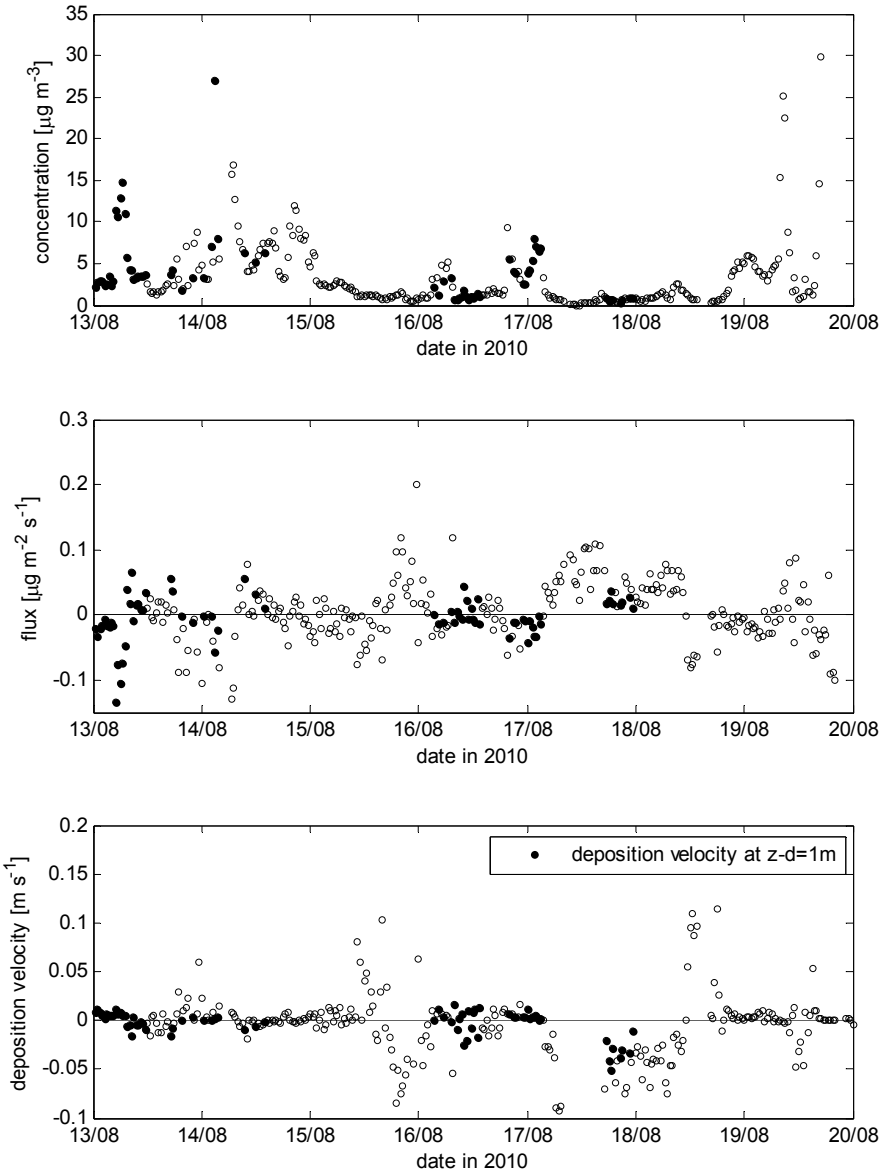

Figure 50. Same as Figure 36 for 13 to 20 August 2010

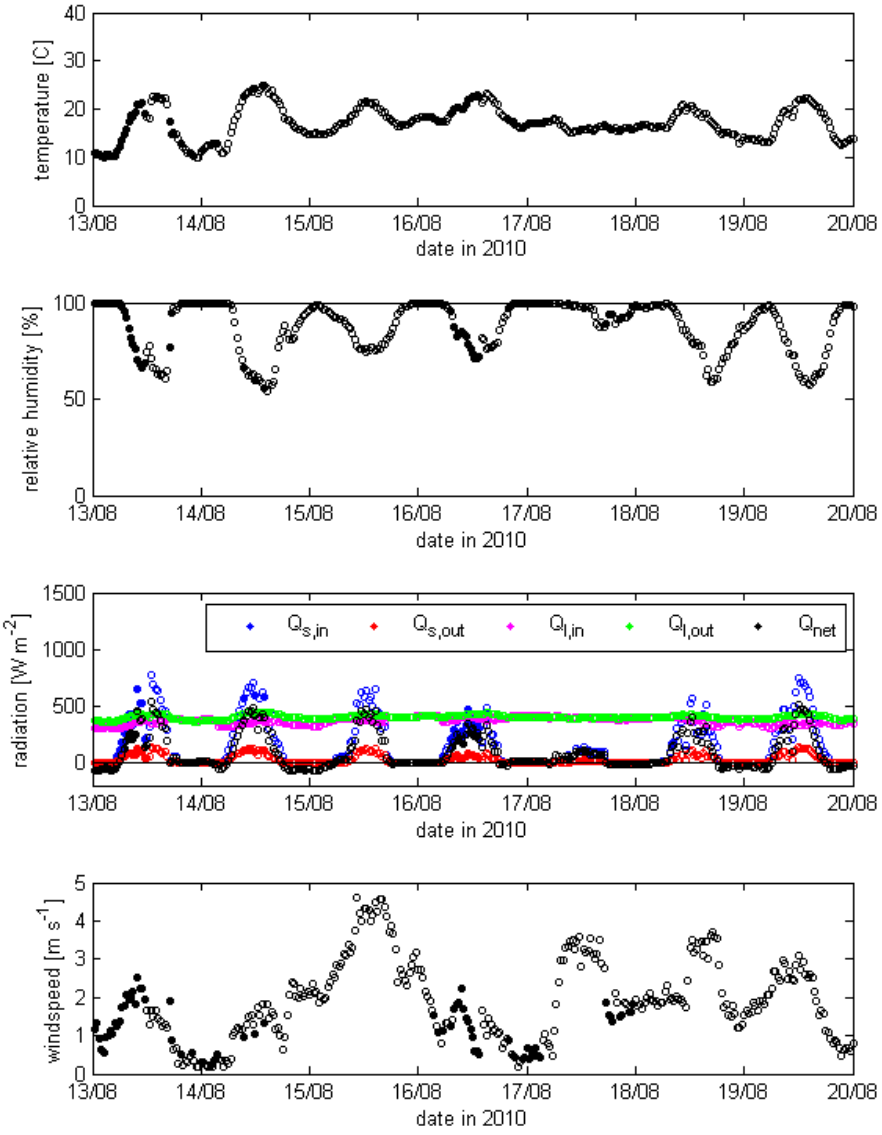

Figure 51. Same as Figure 37 for 13 to 20 August 2010

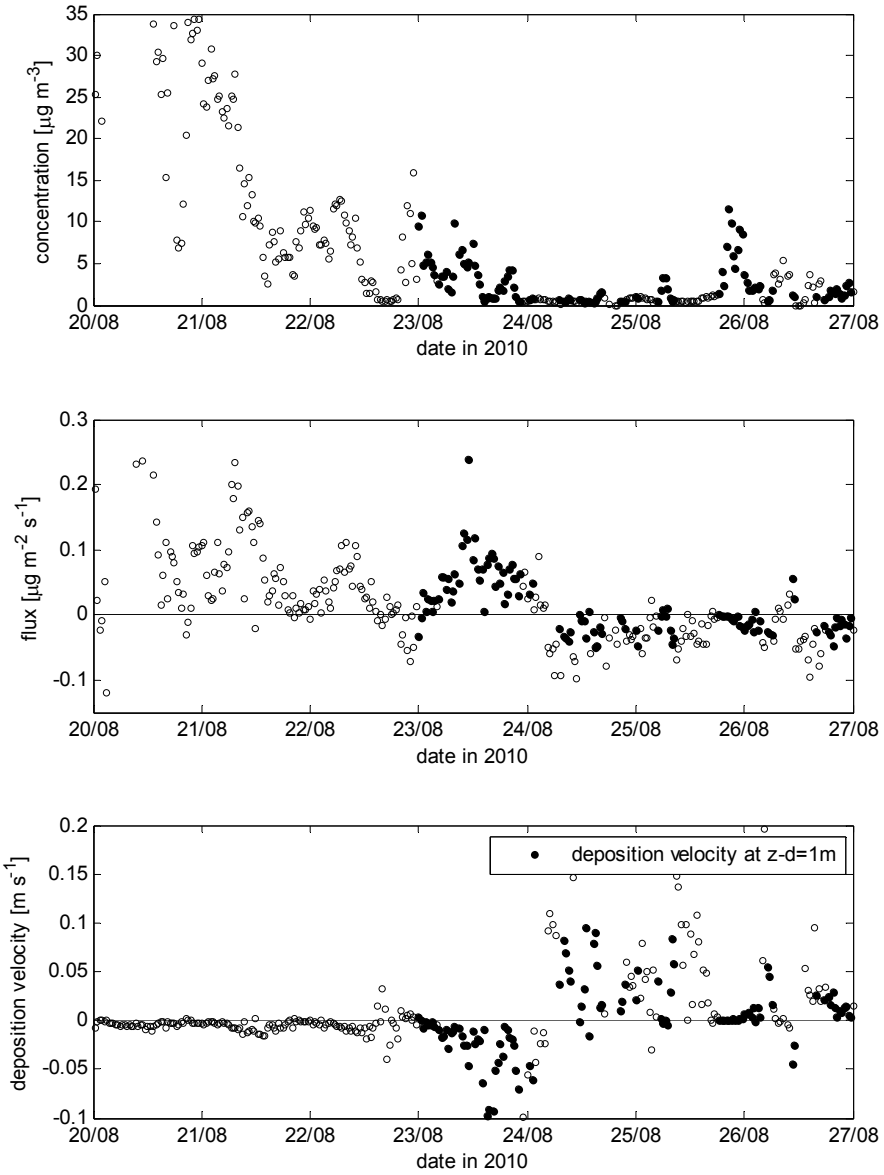

Figure 52. Same as Figure 36 for 20 to 27 August 2010

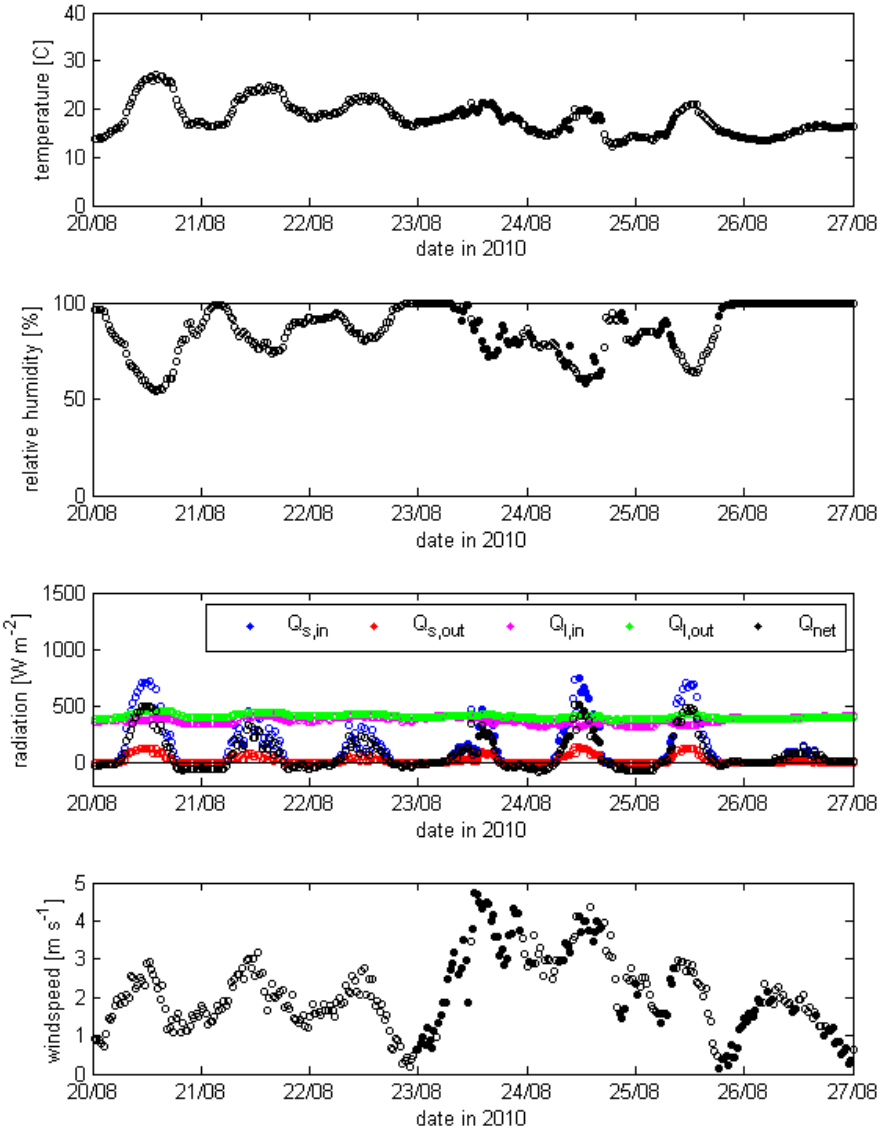

Figure 53. Same as Figure 37 for 20 to 27 August 2010

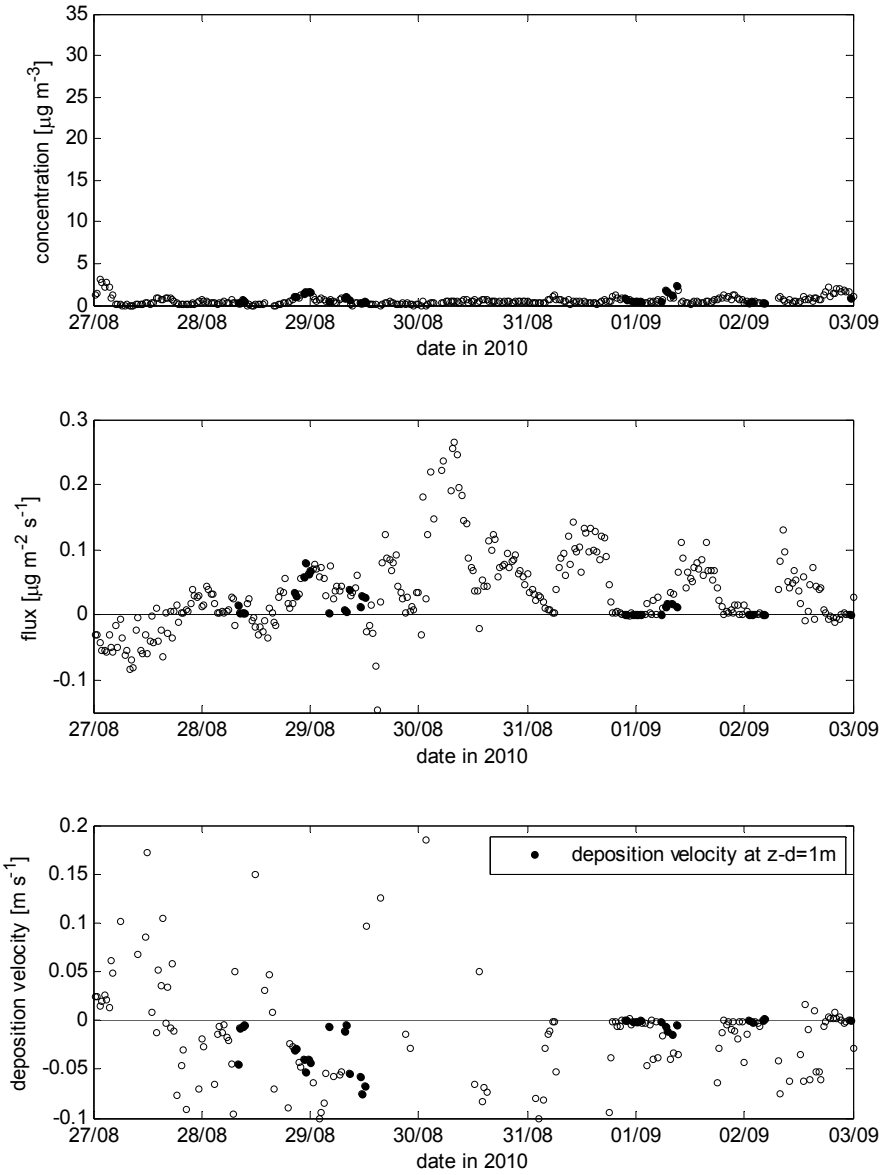

Figure 54. Same as Figure 36 for 27 August to 3 September 2010

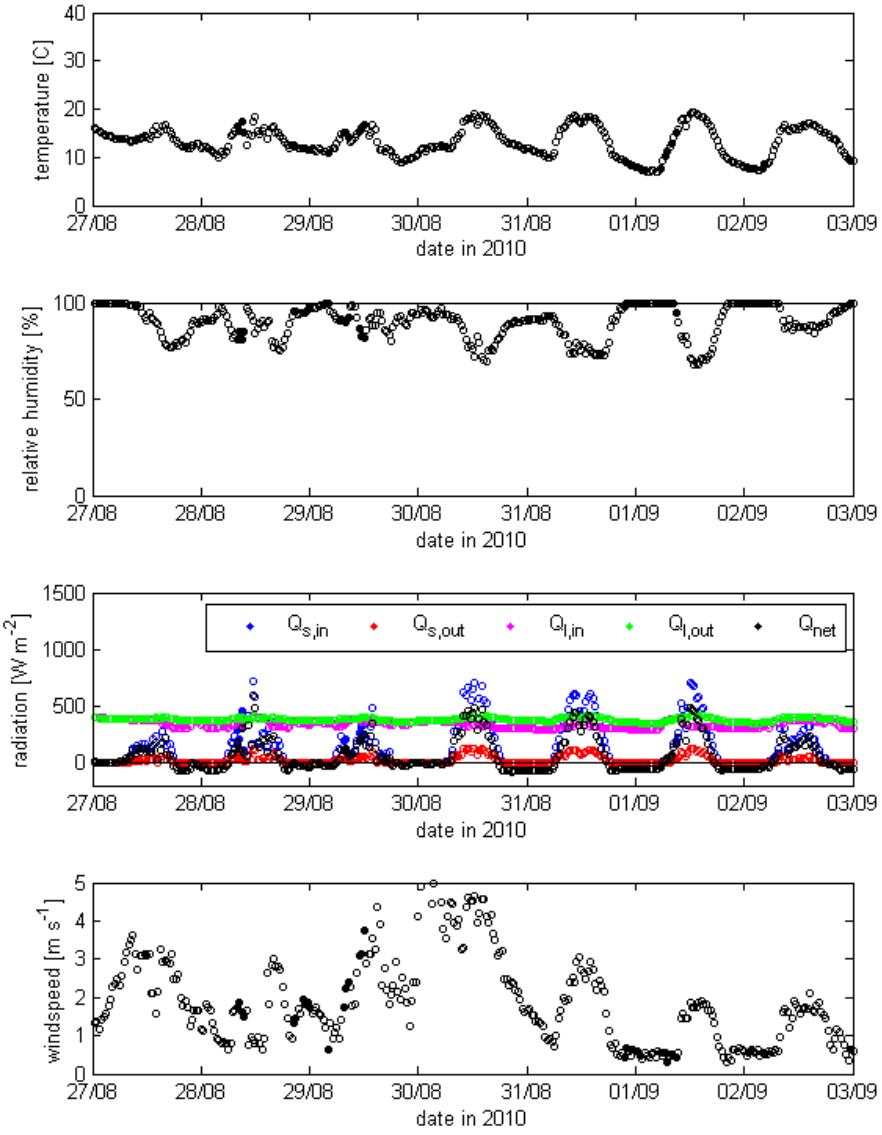

Figure 55. Same as Figure 37 for 27 August to 3 September 2010

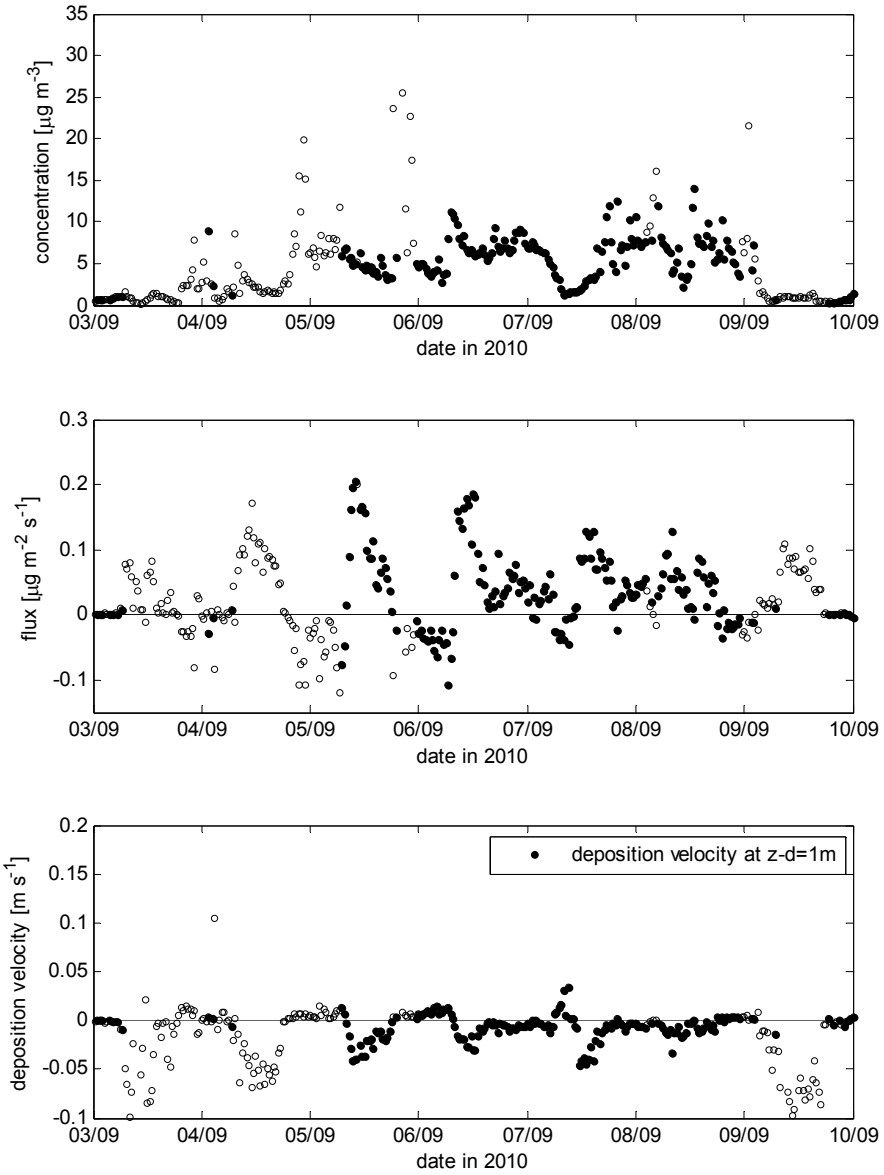

Figure 56. Same as Figure 36 for 3 to 10 September 2010

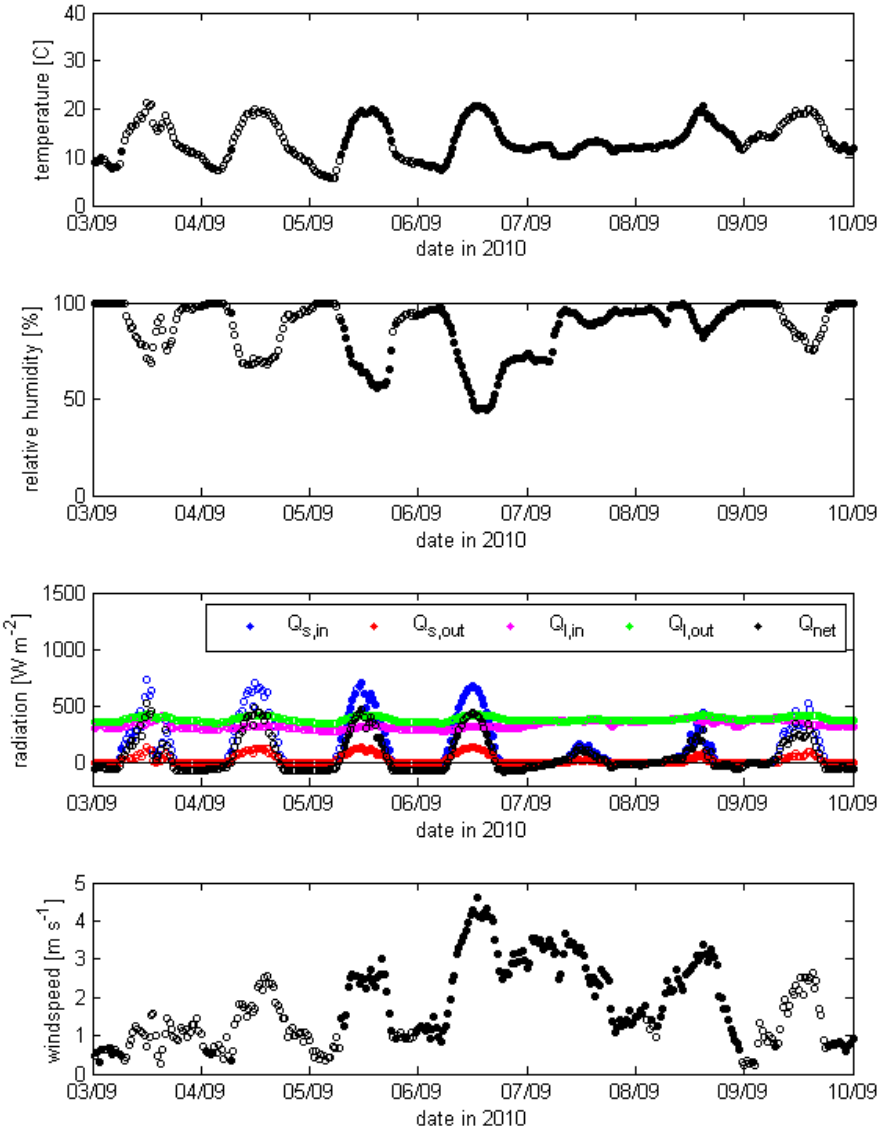

Figure 57. Same as Figure 37 for 3 to 10 September 2010

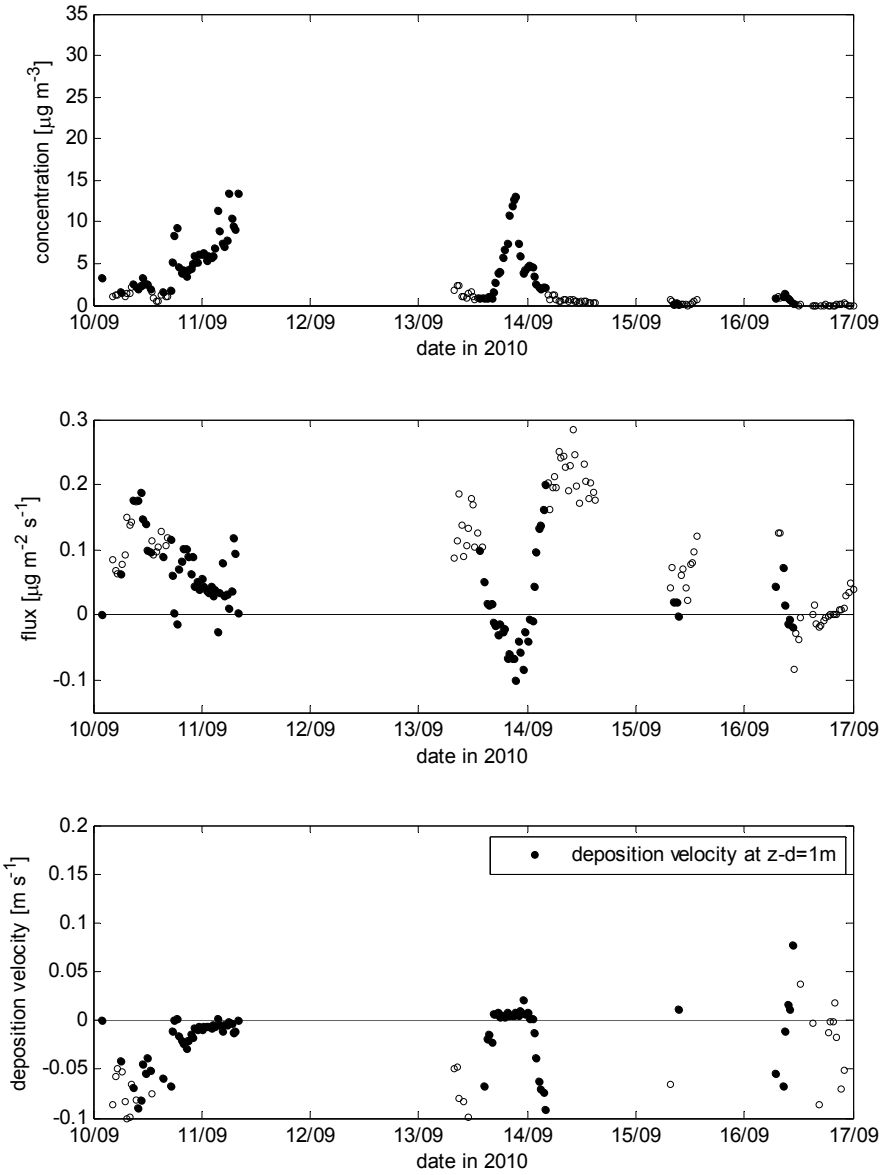

Figure 58. Same as Figure 36 for 10 to 17 September 2010

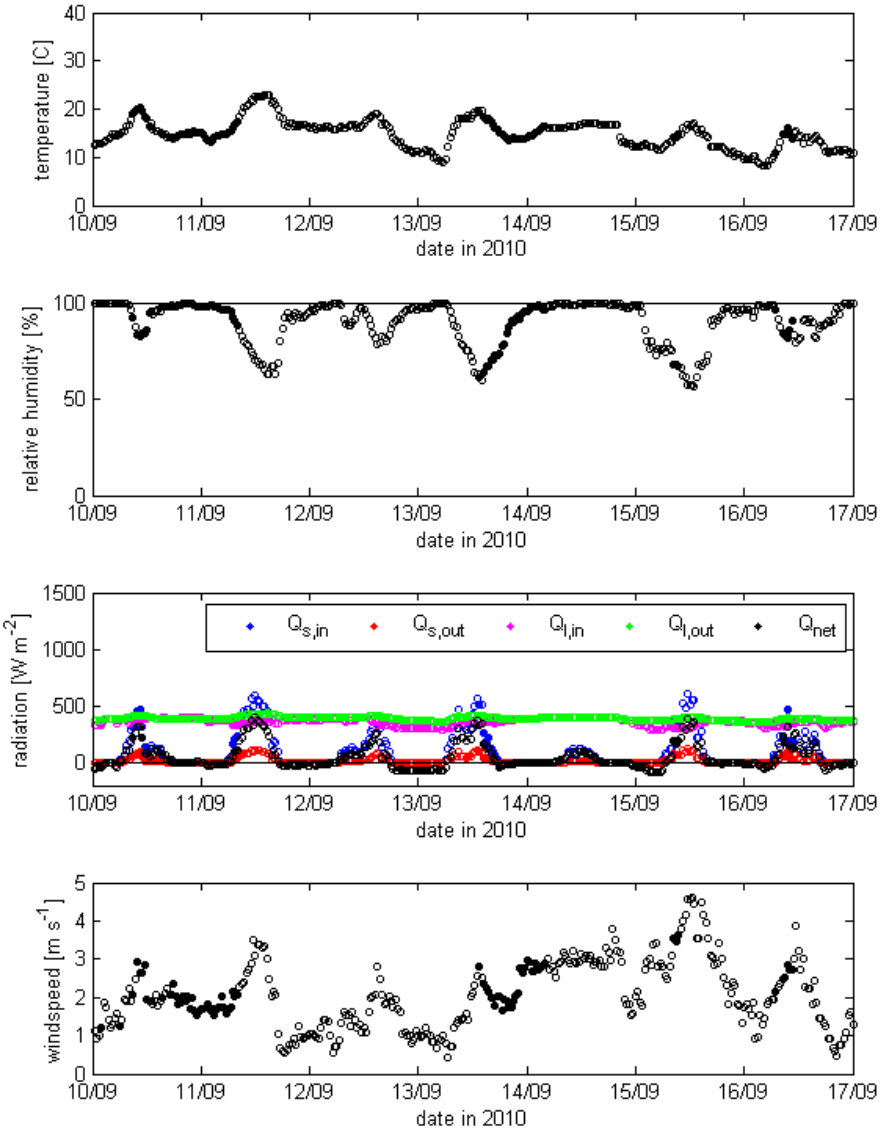

Figure 59. Same as Figure 37 for 10 to 17 September 2010

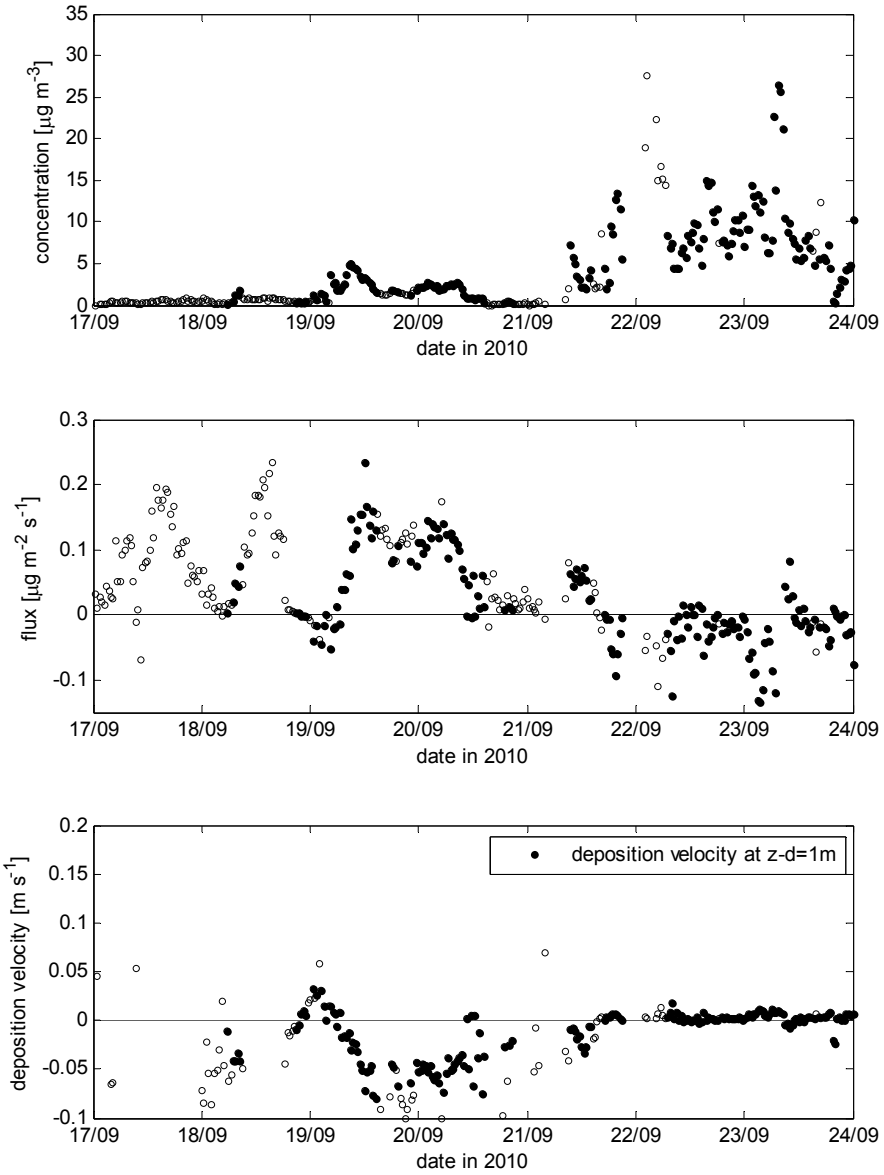

Figure 60. Same as Figure 36 for 17 to 24 September 2010

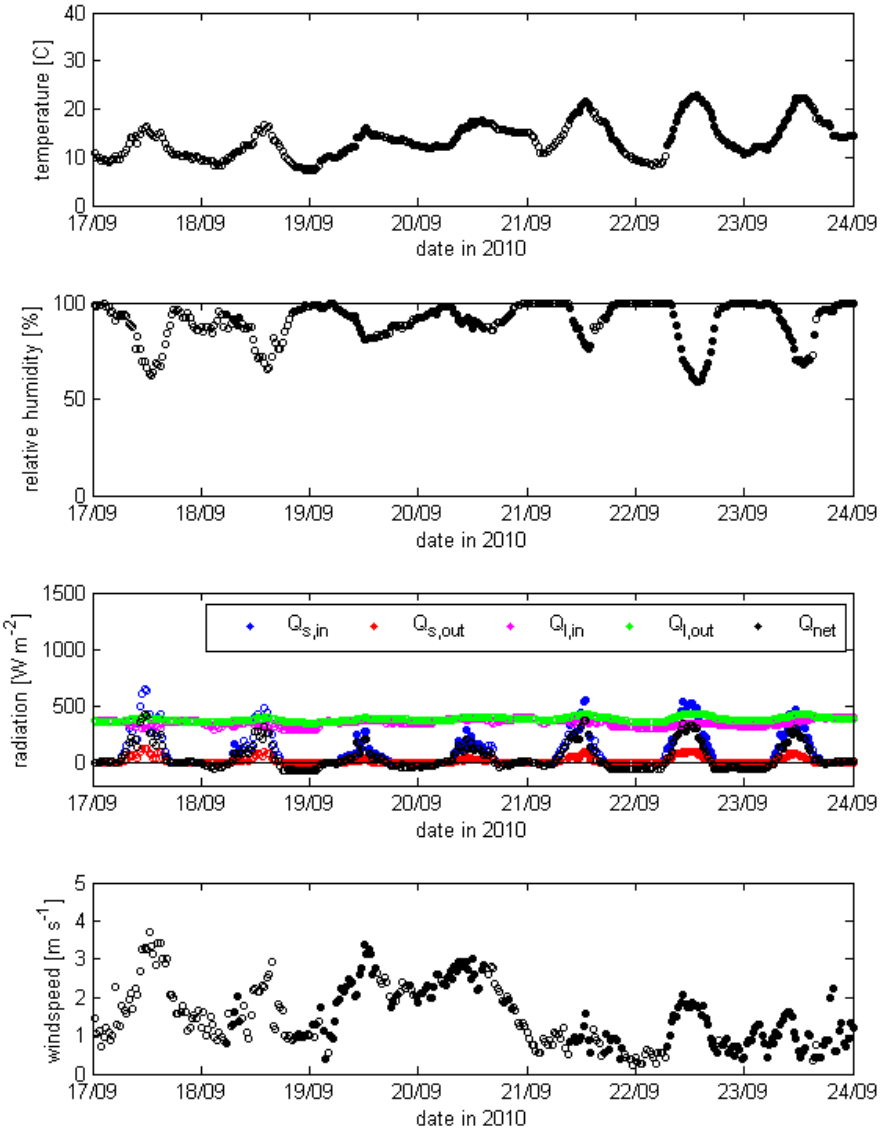

Figure 61. Same as Figure 37 for 17 to 24 September 2010

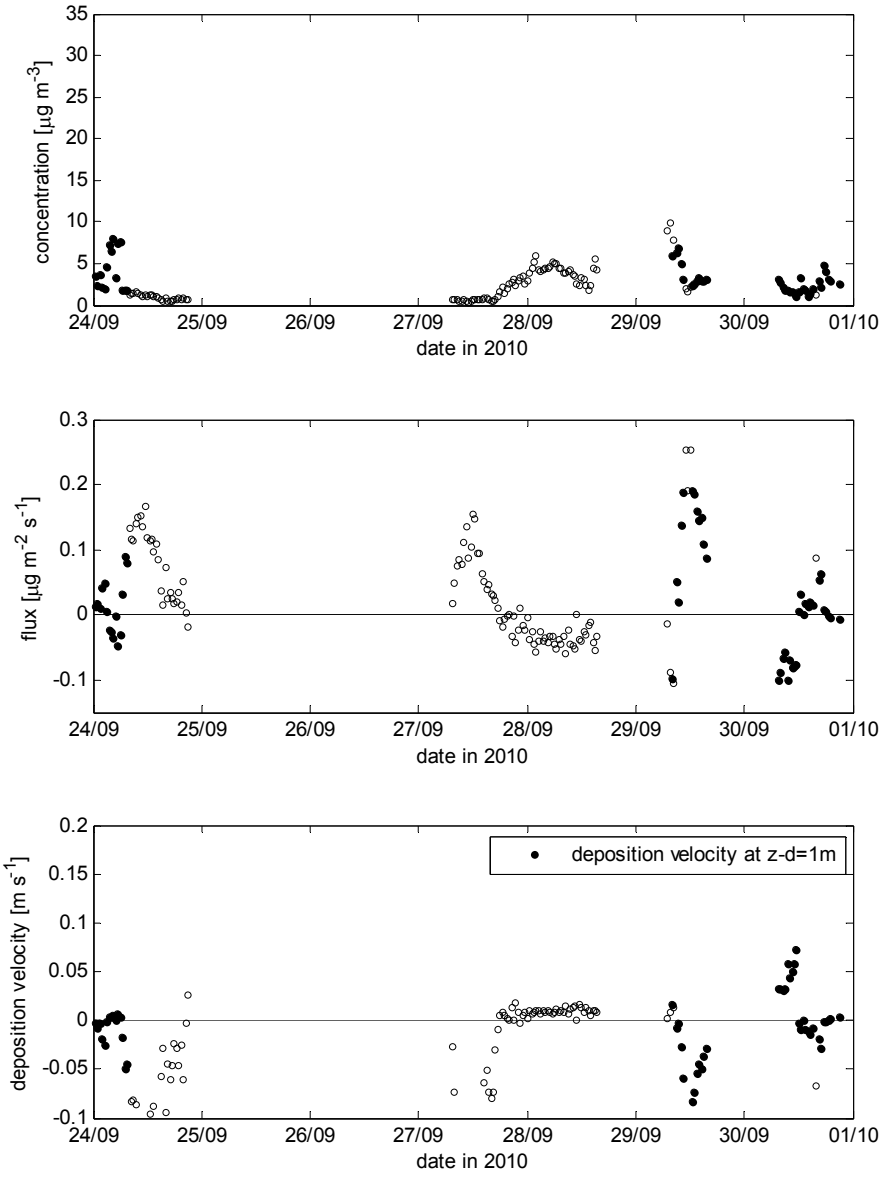

Figure 62. Same as Figure 36 for 24 September to 1 October 2010

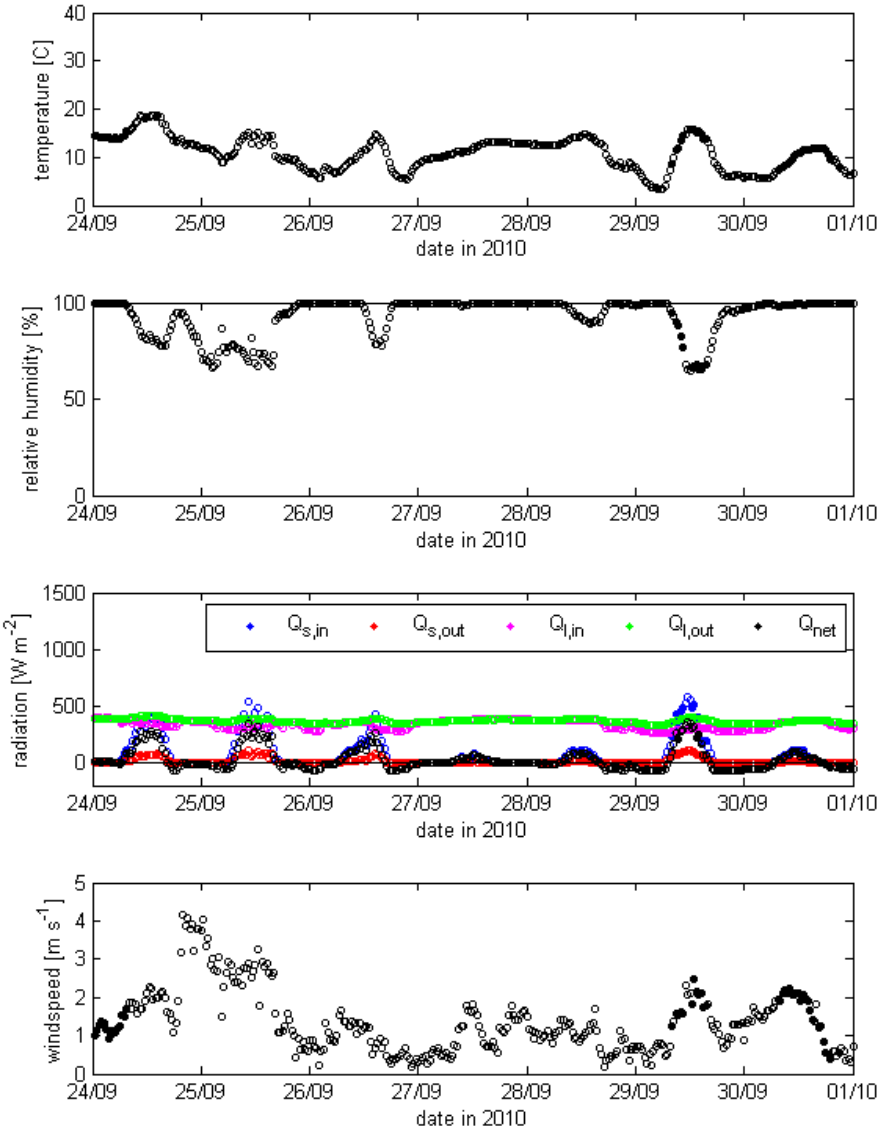

Figure 63. Same as Figure 37 for 24 September to 1 October 2010

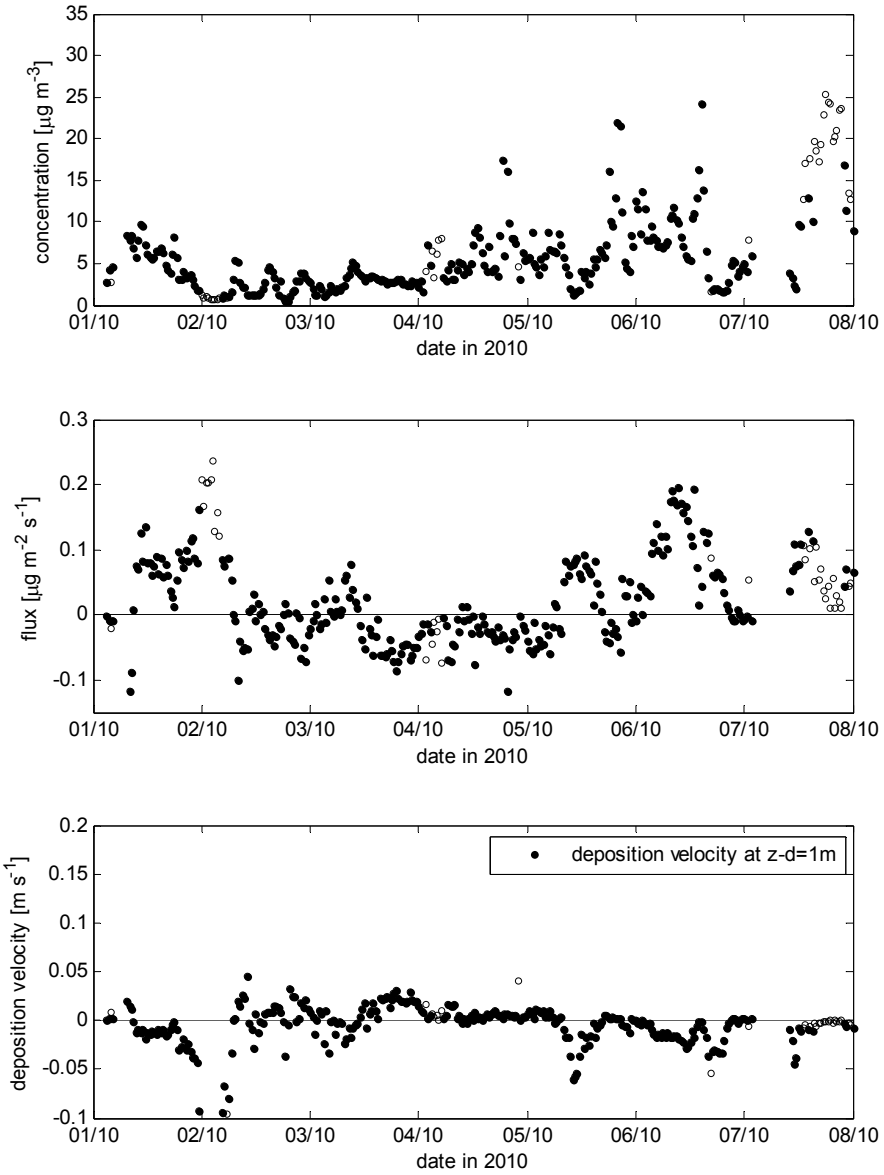

Figure 64. Same as Figure 36 for 1 to 8 October 2010

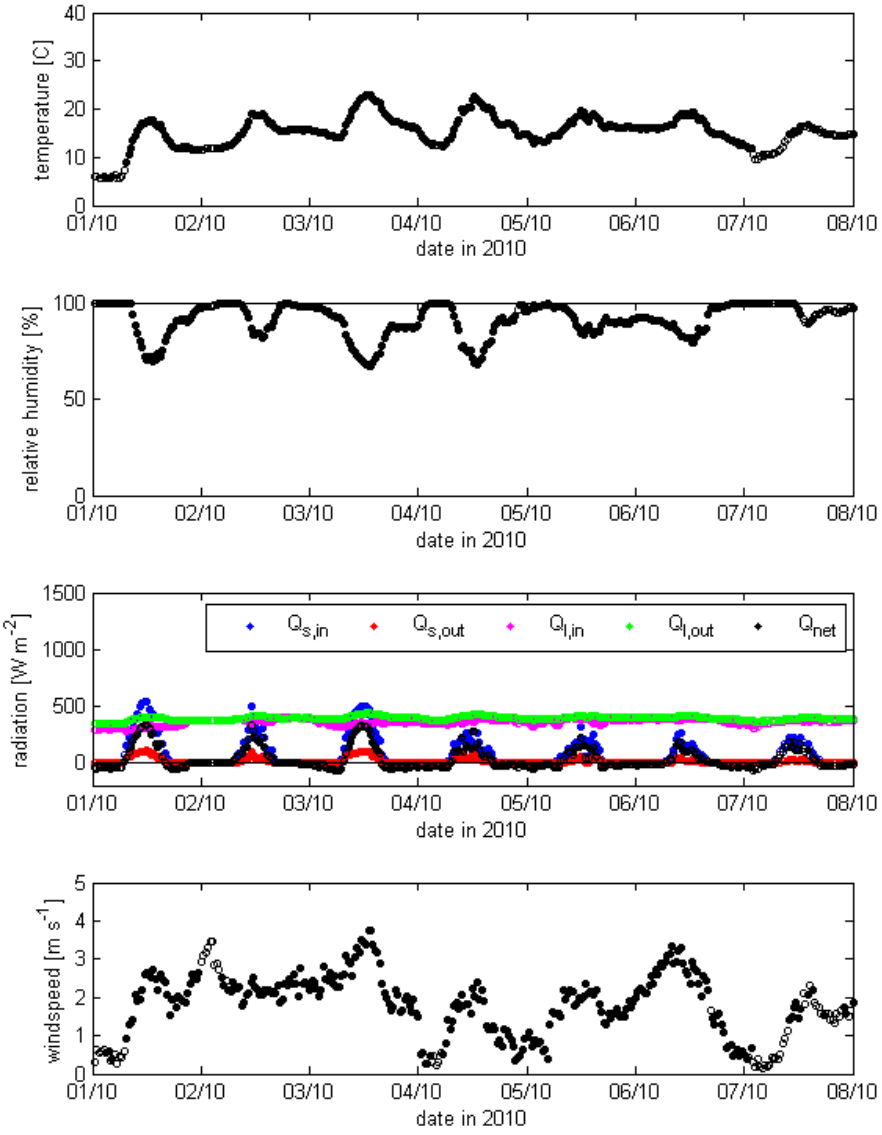

Figure 65. Same as Figure 37 for 1 to 8 October 2010

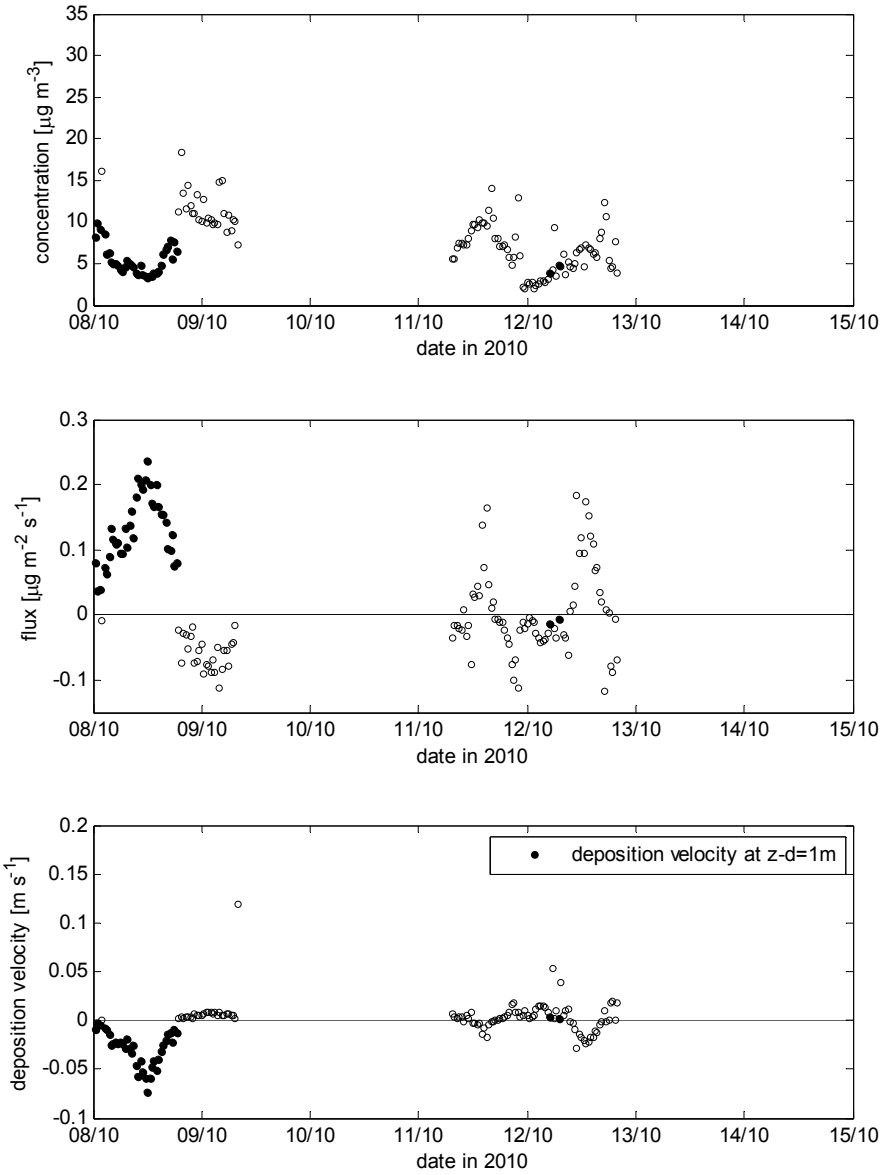

Figure 66. Same as Figure 36 for 8 to 14 October 2010

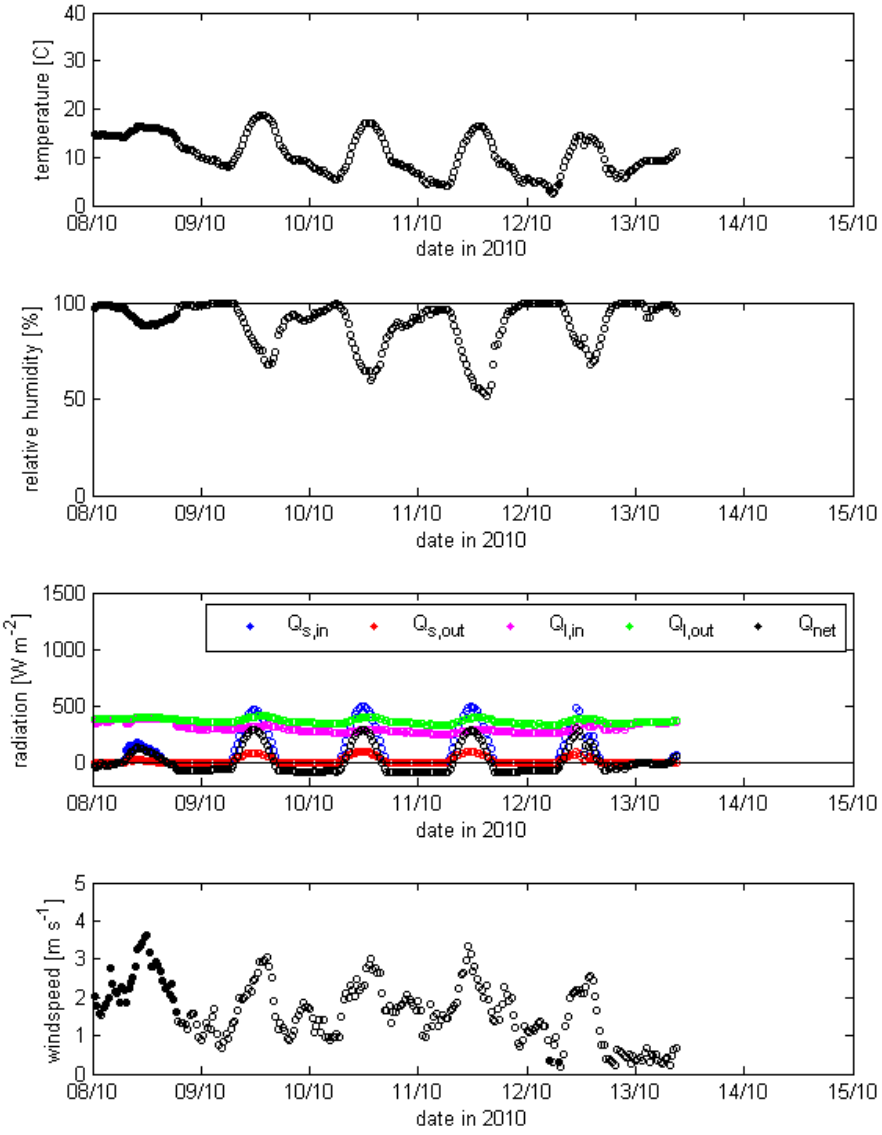

Figure 67. Same as Figure 37 for 8 to 14 October 2010

H. Volten | M. Haaima | D.P.J. Swart | M.C. van Zanten | W.A.J. van Pul

RIVM report 680180003/2012

This is a publication of:

National Institute for Public Health and the Environment

P.O. Box 1 | 3720 BA Bilthoven
The Netherlands
www.rivm.nl

March 2013

005084